Università degli Studi di Ferrara

DOTTORATO DI RICERCA IN
FARMACOLOGIA E ONCOLOGIA MOLECOLARE

CICLO XXVII

COORDINATORE Prof. Antonio Cuneo

Novel ligands and assays for nociceptin/orphanin FQ and classical opioid receptors

Settore Scientifico Disciplinare BIO/14

<table>
<tr><td>**Dottorando**</td><td>**Tutore**</td></tr>
<tr><td>Dott. Malfacini Davide</td><td>Prof. Calo' Girolamo</td></tr>
</table>

Anni 2012/2014

Abstract

The aim of the present study was twofold: pharmacologically characterize novel ligands and set-up and validate novel in vitro assays for nociceptin/orphanin FQ (N/OFQ) peptide (NOP) and classical opioid receptors. NOP and opioid receptors are 7TM receptors coupled with inhibitory G proteins; receptor activation leads to the inhibition of cAMP formation and calcium currents, and opening of potassium channels. Via these cellular inhibitory mechanisms, the N/OFQ – NOP receptor and classical opioid systems regulate a variety of biological functions both in the central nervous system and in the periphery.

The calcium mobilization assay has been and still is broadly used as primary screening for novel molecules in academic and industrial in vitro pharmacology laboratories. The use of chimeric G proteins allows to extend the calcium mobilization assay to virtually all types of G protein coupled receptors. This approach was previously used in our laboratories for characterizing NOP receptor ligands. In the frame of the present study, the calcium mobilization assay has been extended and validated for classical opioid receptors using a panel of standard opioid receptor agonists and antagonist. This test was used for investigating the pharmacological profile of novel opioid ligands including a series of morphine and oxymorphone analogues and novel cyclic endomorphin-2 derivatives. Calcium mobilization studies together with classical in vitro assays such as receptor binding, $[^{35}S]GTP\gamma S$ binding and bioassays with isolated organs were applied to novel NOP receptor ligands including i) 3 different series of spiroxatrine derivatives; ii) the antagonist NiK-21273; iii) $[X^5]N/OFQ(1-13)-NH_2$ derivatives; iv) three tetrabranched derivatives of N/OFQ generated with an innovative chemical approach named peptide welding technology.

Recent data demonstrated that biased agonists, i.e. receptor ligands able to select which signaling pathways become activated upon binding to the receptor, may display advantages over unbiased ligands. In particular, in the field of opioids, G-protein (vs arrestin) biased agonists for the mu receptor displayed an increased therapeutic index associated to reduced tolerance liability. No data are yet available about biased agonism in the NOP receptor field. Therefore a novel bioluminescence resonance energy transfer (BRET) based assay was set-up for the NOP receptor. This method that allows to study both NOP/G-protein and NOP/β-arrestin interactions has been validated using a large panel of NOP ligands encompassing full and partial agonist as well as antagonist activity. The comparison of data achieved investigating NOP/G-protein and NOP/β-

arrestin interaction allowed us to perform the very first study of biased agonism in the NOP receptor field.

In summary the studies performed in the frame of my PhD project extend our knowledge on the pharmacological profile of NOP and classical opioid receptors, provided to the scientific community novel compounds, pharmacologically characterized in detail, to be used as research tools and possibly as drug prototypes, and made available novel pharmacological assays useful for selecting fully innovative drugs such NOP receptor biased agonists.

Table of contents

1. Introduction

1.1 G-protein coupled receptors

G protein-coupled receptors (GPCRs) are the largest and most diverse group of membrane receptors in eukaryotes. GPCRs recognize a wide number of different extracellular stimuli, including photons, ions, small molecules, peptides and proteins, and transmit the resulting extracellular signals to elicit intracellular responses. With their common architecture of seven transmembrane (7TM) helices (Figure 1), GPCRs represent the largest protein family in the human proteome (> 800 human GPCRs). These receptors can be classified into major classes (i.e. secretin, adhesion, glutamate, frizzled/taste2, rhodopsin, and other 7TM receptors families) and further divided into subfamilies based on sequence similarities (e.g. opioid receptors belong to the SOG cluster of γ-group/rhodopsin family of GPCRs, (Fredriksson *et al.*, 2003)). Signal transmission occurs through the interaction between receptors and different intracellular proteins (e.g., heterotrimeric G-proteins, kinases, and arrestins (Rajagopal *et al.*, 2010)), which then activate downstream effectors and trigger cascades of cellular and physiological responses. GPCRs signaling have been related to numerous diseases, and these receptors are targeted by 30-40% of all drugs currently available (Wise *et al.*, 2002). Consequently, understanding the pharmacology of these receptors is of two-fold interest, for the basic science community interested to uncover the processes regulated by these receptors and their details at a molecular level, and for the applied science community devoted to discover more efficacious and better tolerated drugs.
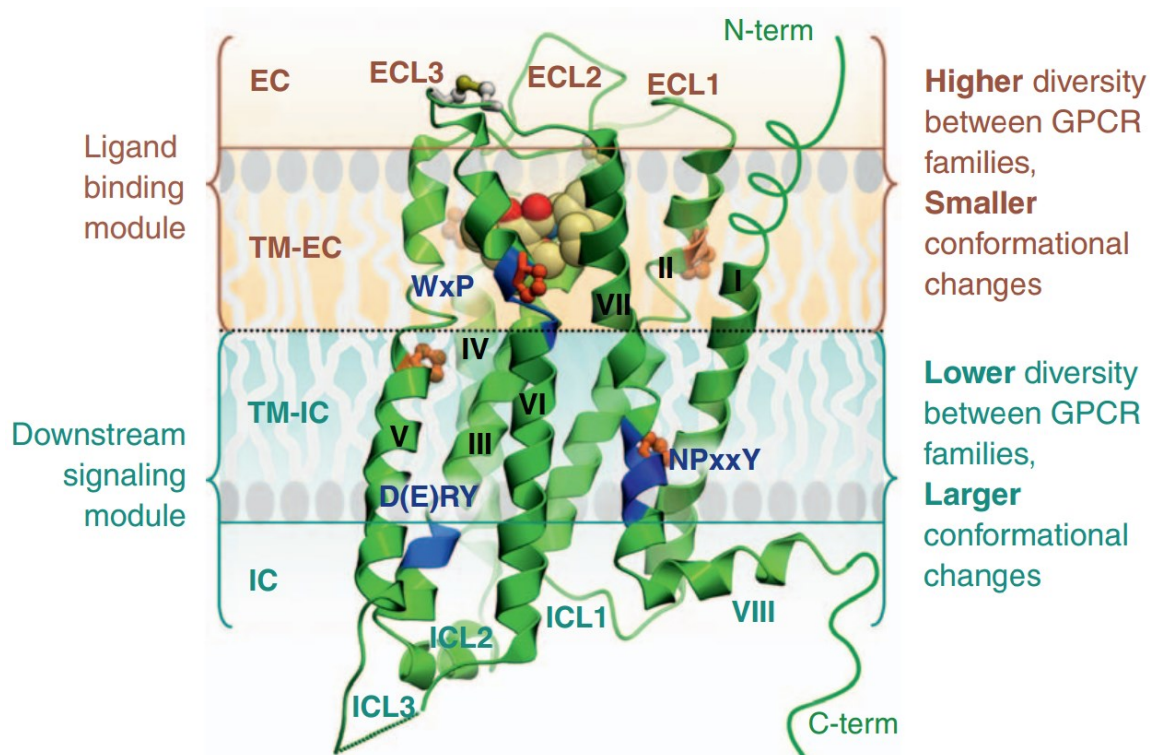
Figure 1. General architecture and modularity of GPCRs. N-terminal extracellular domains (top side), C-terminal intracellular domains (bottom side). Image taken from (Katritch *et al.*, 2012)

Structural data, ranging from NMR to X-ray 3D structures of active and inactive GPCRs, and site by site mutation analysis of GPCRs sequence/function, are now abundantly available; however the mechanisms by which drugs that bind GPCRs are able to evoke their effect through these receptors have not yet fully understood. It is possible to generalize the modes of GPCR activation processes in two models. In the classical model for GPCR activity, agonist binding to the GPCR causes the receptor to adopt a conformation that results in the activation of associated heterotrimeric G proteins. This activation involves the exchange of bound guanosine diphosphate (GDP) for guanosine-5'-triphosphate (GTP) by the Gα subunit of the G protein, leading to dissociation of the heterotrimeric protein complex into Gα and Gβγ subunits. This dissociation then promotes the production of and consequent signalling by second messenger systems, such as those involving cyclic AMP, diacylglycerol and calcium. Signalling by the activated conformation of the GPCR is terminated by phosphorylation of the cytoplasmic loops and tail of the GPCR, which is catalyzed predominantly by GPCR kinases (GRKs). This results in the binding of arrestins (i.e. β-arrestin 1 and 2) and consequent desensitization followed by

internalization into clathrin-coated pits (Lefkowitz & Shenoy, 2005). Thus, in the classical model, heterotrimeric G proteins mediate signal transduction and β-arrestins mediate receptor desensitization and internalization. Despite this simplification is widely accepted, it is now known that β-arrestins act not only as regulators of GPCR desensitization, but also as adaptor proteins that carry the GPCR signaling through multiple mediators such as mitogen-activated protein kinases, proto-oncogene tyrosine-protein kinase SRC, nuclear factor-κB and phosphoinositide 3-kinase. Moreover, biochemical data suggest that the signaling mediated by β-arrestins has distinct functional and physiological consequences from that mediated by G proteins (Lefkowitz & Shenoy, 2005; Rajagopal *et al.*, 2010) (Figure 2).
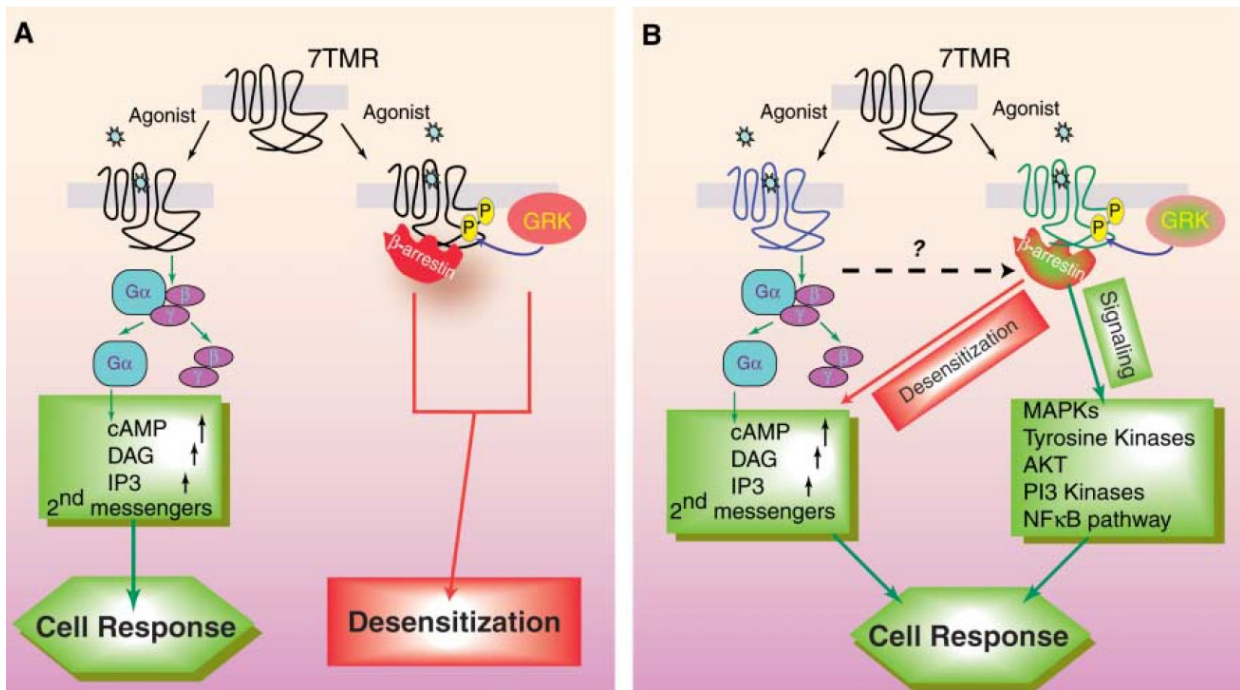
Figure 2. Signal transduction by seven transmembrane receptors. (A) Classical paradigm. The active form of the receptor (R*) stimulates heterotrimeric G proteins and is rapidly phosphorylated by G protein–coupled receptor kinases (GRKs), which leads to β-arrestin recruitment. The receptor is thereby desensitized, and the signaling is stalled. (B) New paradigm. β-arrestins not only mediate desensitization of G protein–signaling but also act as signal transducers themselves. Image taken from (Lefkowitz & Shenoy, 2005).

The biological role of arrestins within the classical opioid receptor field was demonstrated in vivo using mice lacking the β-arrestin 2 gene that displayed a remarkable potentiation and prolongation of the analgesic effect of morphine (Bohn *et al.*, 1999) and reduced tolerance liability (Bohn *et al.*, 2002) compared to their wild type littermates. It is also known that some

GPCR ligands may act as biased agonists i.e. ligands able to bind a single receptor and differentially activate some of its pathways over others, for example G-protein over arrestin or vice versa. Based on these findings it has been proposed that opioid receptor biased agonists able to promote receptor/G-protein better than receptor/arrestin interaction may display in vivo higher efficacy and/or better tolerability (Violin *et al.*, 2014).

1.2. N/OFQ - NOP system

Nociceptin/Orphanin FQ (N/OFQ) is a neuropeptide of 17 amino-acids (FGGFTGARKSARKLANQ) that binds with high affinity the N/OFQ peptide (NOP) receptor (Meunier *et al.*, 1995; Reinscheid *et al.*, 1996). N/OFQ is cleaved from a peptide precursor preproN/OFQ (ppN/OFQ). This precursor is composed by 176 amino acids in humans, 181 in rats, and 187 in mice, sharing an high degree of conservation. Moreover, the ppN/OFQ gene both in term of structural similarity and of organizational characteristics resembles those of the opioid peptide precursors, in particular preproenkephalin and preprodynorphin, suggesting a common ancestor for these peptide precursors (Mollereau *et al.*, 1996). It is worth mentioning that N/OFQ is the first ligand that was discovered by reversed pharmacology. Before molecular biology techniques became common, firstly, ligands had been discovered and, then, their receptors found by classical pharmacology approaches. Nowadays, most GPCRs are identified on the basis of their DNA sequences and thus are initially unmatched to known natural ligands and classified as orphan GPCRs. For discovering the endogenous ligand of NOP receptor, the orphan receptor was cloned by homology cloning and transfected in mammalian cells; tissue extracts were prepared from the brain, purified, and fractionated following a number of rounds of fractionation. The extracts were then subsequently tested for their ability to modify cAMP levels in cells expressing the NOP receptor, N/OFQ was then isolated and characterized (Meunier *et al.*, 1995; Reinscheid *et al.*, 1996).

NOP is a G-protein coupled receptor (GPCR) whose activation leads to the inhibition of both cAMP levels and calcium channels, and to the stimulation of potassium currents; these cellular effects are due to the activation of pertussis toxin (PTX)-sensitive G-proteins ($G_{i/o}$) (Lambert, 2008). Like many other GPCRs it is known that the NOP receptor may interact (and signal) not

only with G-proteins but also with other proteins, such as GRKs and arrestins (Soergel *et al.*, 2014).

NOP receptor shares high degree of structural similarities with opioid receptors. Furthermore, N/OFQ sequence is similar to that of dynorphin A, an endogenous opioid peptide. Despite such similarities, N/OFQ does not bind opioid receptors and NOP does not interact with opioid neuropeptides. Thus, the NOP receptor was defined as opioid-related rather than opioid (Alexander *et al.*, 2013). Recently, the crystal structure of the human NOP receptor was solved in complex with the antagonist compound-24 (C-24) (Thompson *et al.*, 2012) revealing some substantial differences in the binding pockets of NOP and classical opioid receptors (Filizola & Devi, 2013; Thompson *et al.*, 2012) (Figure 3).
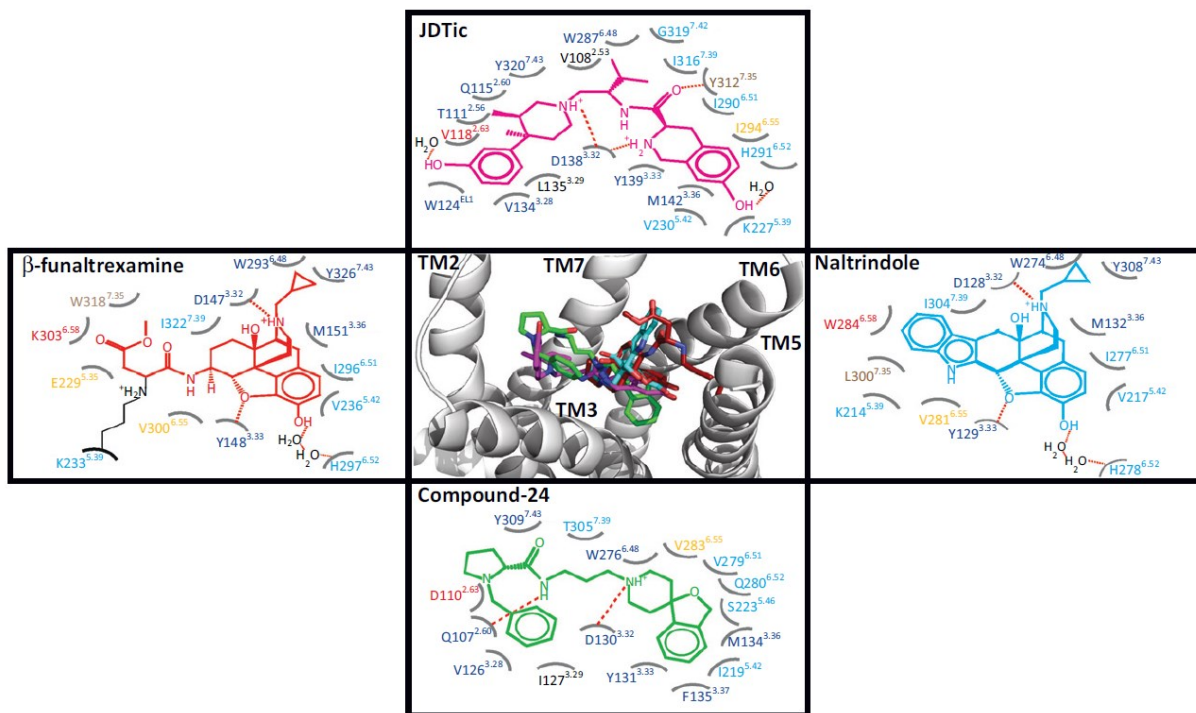
Figure 3. Overlay of the crystallized opioid ligands in a representative opioid receptor crystal structure along with schema of their interaction modes in each crystal structure. The central panel shows an overlay of β-funaltrexamine (red), naltrindole (cyan), JDTic (magenta), and compound 24 (green) in the MOP receptor crystal structure, which is partially shown in a grey cartoon representation. Interaction schema for β-funaltrexamine, naltrindole, JDTic, and compound 24 in the mu opioid (MOP), delta opioid (DOP), kappa opioid (KOP), and NOP receptor crystal structures are shown in the left, right, upper, and lower panels, respectively. Identical residues in all four receptors are shown in blue. Identical resides in MOP, DOP, and KOP but unique to NOP are shown in cyan. Divergent residues in all four opioid receptors are shown in red. Divergent residues in MOP, DOP, and KOP but not NOP are shown in brown. Unique residues to either MOP, DOP, or KOP are shown in orange. Image taken from (Filizola & Devi, 2013).

The N/OFQ-NOP system has been deeply investigated by academic and industrial researchers leading to the discovery of a variety of selective NOP receptor ligands (Calo & Guerrini, 2013; Mustazza & Bastanzio, 2011). Using such compounds the role of this system in physiology and pathology has been, at least partially, elucidated. N/OFQ and the NOP receptor are involved in the regulation of different biological functions at both central and peripheral levels including pain, mood and anxiety, food intake, learning and memory, locomotion, cough and micturition reflexes, cardiovascular homeostasis, intestinal motility and immune responses (Lambert, 2008) (Figure 4).
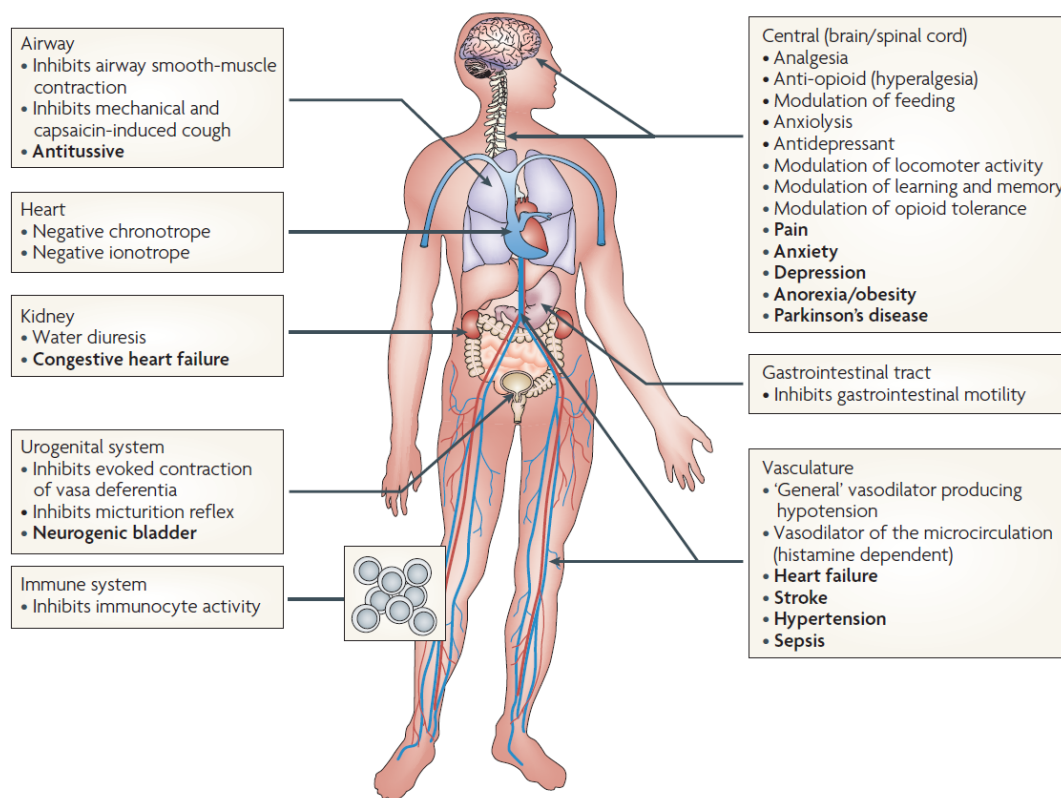
Figure 4. Pleiotropic effects of nociceptin/orphanin FQ (N/OFQ) on major organ systems. Potential clinical indications are noted in bold. Image taken from (Lambert, 2008).

The role of N/OFQ in pain regulation has been clear since the earliest studies performed in rodents. The administration of N/OFQ has been shown to cause hyperalgesia, allodynia and analgesia. N/OFQ is able to increase pain sensitivity in mice and rats when administered supraspinally (Meunier *et al.*, 1995; Reinscheid *et al.*, 1995). Such hyperalgesic effects of N/OFQ was only seen after intracerebroventricular (i.c.v.), rather than after intrathecal (i.t.) administration. It has been demonstrated that most prominent role of N/OFQ in supraspinal pain

modulation is a "functional opioid antagonism" directed against many different opioid receptor agonists (Mogil & Pasternak, 2001). The anti-opioid role of N/OFQ has been corroborated by results obtained in vary assays/conditions, firstly N/OFQ counteracts the analgesic effects of endogenous opioids (Tian *et al.*, 1997), of morphine (Bertorelli *et al.*, 1999; Calo *et al.*, 1998; Grisel *et al.*, 1996; Zhu *et al.*, 1997), and of a panel of selective opioid receptor agonists (King *et al.*, 1998). These anti-opioid effects of N/OFQ are subjected to tolerance liability (Lutfy *et al.*, 1999).

Since NOP and classical opioid receptors largely share similar transduction mechanisms, it is probably that their opposite effects on pain threshold are due to distinct localisations of these endogenous agonists and respective receptors on the neuronal networks involved in pain transmission at the supraspinal level. A cellular model explaining the anti-opioidergic action of supraspinal N/OFQ focalizes on brain stem, in particular of the nucleus raphe magnus (NRM), the major site of supraspinal N/OFQ effects on pain processing. In this brain region, different type of neurons, named ON and OFF cells, can be distinguished. ON cells firing occurs immediately before the nociceptive reaction, while OFF cells are inhibited by the GABA release due to ON cells firing. When OFF cells are activated, these cells induce a spinal antinociceptive effect via descending tracts. MOP opioids inhibit ON cells and thereby cause a subsequent disinhibition of the antinociceptive OFF cells. By contrast, N/OFQ inhibits nearly all cell types in the RVM. Via a direct inhibition of OFF cells, N/OFQ counteracts the disinhibitory effects of MOP agonists on these cells and thereby reverses opioid-induced supraspinal analgesia. The same mechanism may also account for the apparent hyperalgesic effect of N/OFQ, providing a cellular basis for the reversal of stress-induced analgesia by N/OFQ. These studies demonstrate that the net effects of N/OFQ on nociception at supraspinal sites strongly depend on the activation state (resting versus sensitized) of pain controlling neuronal circuits, see for a review (Zeilhofer & Calo, 2003).

N/OFQ was shown to block morphine-induced place preference (Ciccocioppo *et al.*, 2000) an effect that was later extended to other drugs of abuse influencing the dopaminergic mesocorticolimbic pathway, such as alcohol, amphetamine and cocaine (Zaveri, 2011). One

mechanism whereby N/OFQ attenuates reward elicited by drugs of abuse is by directly inhibiting NOP expressing dopaminergic mesocorticolimbic neurons (Murphy *et al.*, 1996).

The peptide N/OFQ is involved in learning and memory, being able to inhibit long-term potentiation in rat hippocampal slices (Yu *et al.*, 1997). These observations received strong support from the observation that knockout mice for NOP receptor not only displayed greater learning ability and have better memory than wild type animals, but also showed increased long-term potentiation in the hippocampal CA1 region (Manabe *et al.*, 1998). However systematic studies on the possible cognitive enhancing properties of selective NOP antagonists have not yet been performed.

NOP antagonists are able to elicit antidepressant like effects in the forced swimming test in mice (Redrobe *et al.*, 2002). This finding was later confirmed and extended in other studies with other antagonists. Clinical studies suggest that N/OFQ levels are increased in depressed patients. Mechanisms of action involved in the antidepressant effects of NOP antagonists are still unknown. However, it has been reported that N/OFQ is able to inhibit noradrenaline and serotonin release from the cerebral cortex as well as neuronal firing in the dorsal raphe and locus coeruleus. Assuming that chronic stress/despair conditions stimulate the release of N/OFQ, the peptide may reduce monoaminergic signaling acting both at presynaptic and postsynaptic sites. By preventing such effects of N/OFQ, NOP antagonists may restore normal levels of noradrenaline and serotonin at their respective synaptic clefts. Thus, NOP receptor antagonists, by acting at different levels and with different mechanisms, may achieve a similar endpoint to that of classical antidepressants, i.e., an increase in cortical synaptic concentrations of monoamines (Gavioli & Calo, 2013). Furthermore, N/OFQ also affects the brain response to stress and anxiety; indeed one of the most intensively studied actions of N/OFQ is its ability to counteract stress related behaviors and promote anxiolytic like effects. The mechanisms by which N/OFQ exerts its anxiolytic effects are not fully understood but there is evidence for the involvement of GABA A receptor signaling. However CRFergic and serotonergic pathways might be also implicated.

The endogenous peptide N/OFQ has been demonstrated to inhibit the spontaneous locomotor activity, this effect is evident both in mice and rats, this inhibitory effect of N/OFQ is abolished

in the presence of NOP antagonists and NOP knock out mice. Despite these findings, the N/OFQ-NOP receptor system does not tonically control spontaneous locomotion since NOP antagonists do not modify per se this behavior and knockout animals do not show phenotypes a this level. Worth of mention, intranigral injection of the selective NOP antagonist of peptide nature UFP-101, dose-dependently improved rat performance in the drag and rotarod tests (Marti *et al.*, 2004), in addition the NOP knockout mice outperformed wild type animals in the same assays. These results suggest that endogenous N/OFQ may indeed exert an inhibitory influence over motor activity that becomes relevant during exercise. Other findings obtained in models of Parkinson's disease suggest that NOP receptor blockade may represent a new strategy for treating hypokinetic disorders and proposed NOP receptor antagonists as drugs for treating Parkinson. Clinical evaluations on cerebrospinal fluids from parkinsonian patients showed 3.5 fold higher levels of N/OFQ compared to that of healthy subjects.

N/OFQ-NOP receptor system is also involved in food intake control, in fact it has been shown that supraspinal N/OFQ (1–10 nmol) administration increases food intake in satiated rats. This effect is mimicked by a variety of NOP synthetic agonists. Moreover the involvement of the NOP receptor in this action has been confirmed in receptor antagonists and knockout studies.

The value of the N/OFQ-NOP receptor system as target for the development of innovative drugs has been demonstrated in several studies, for instance NOP receptor agonists might be used as novel analgesics particularly for neuropathic pain, as anxiolytic agents, as novel agents to treat drug dependence, and for the treatment of cough and urinary incontinence. On the other hand, NOP receptor antagonists can be worthy of development for treating, major depression and Parkinson's disease and possibly some inflammatory diseases (Lambert, 2008).

1.3. Classical opioid receptor system

The history of classical opioid receptors is longer than that of the NOP receptor. Beckett and Casy in 1954 proposed the existence of receptors for opiate drugs (Beckett & Casy, 1954) based on their studies of structure activity relationships for antinociceptive activity in a series of

synthetic opiates. These receptors are called opioid since the discovery of endogenous peptides with effects similar to those of opiate drugs. Portoghese and colleagues (1965) through structure activity relationship studies, proposed that more than one opioid receptor type or that multiple modes of interaction of ligands with opioid receptors were possible. Endogenous opioid systems play a critical role in modulating a large number of sensory, motivational, emotional, and cognitive functions. As inhibitory neuropeptide transmitters, they fine-tune neurotransmission across a wide range of neuronal circuits, setting thresholds or upper limits. Earliest direct demonstrations of opioid receptors binding sites were obtained by receptor binding studies with radiolabelled naloxone and etorphine molecules (Pert & Snyder, 1973; Simon *et al.*, 1973; Terenius, 1973). The first definitive evidence that these receptors did not form a homogeneous population was presented in 1976 (Martin *et al.*, 1976). The proposed receptor forms were named after the prototypic drugs used in these studies, i.e. the mu, for morphine receptor and the kappa, for ketocyclazocine receptor. Pharmacological analysis of opioid peptide effects in guinea-pig ileum and mouse vas deferens led to the discovery of a third opioid receptor named the delta, for deferens receptor (Lord *et al.*, 1977). The three opioid receptors, MOP, DOP, and KOP have been cloned and the recombinant receptors shown to have binding and functional characteristics consistent with their endogenous counterparts (Evans *et al.*, 1992; Kieffer, 1995; Kieffer *et al.*, 1992; Satoh & Minami, 1995).

As far as endogenous opioid peptides are concerned, three families of opioid peptides have been identified: enkephalins, endorphins, and dynorphins. Each family derives from a distinct precursor protein, prepro-opiomelanocortin (POMC), prepro-enkephalin, and prepro-dynorphin, respectively. These precursors are encoded by distinct genes and are subjected to complex cleavages and posttranslational modifications resulting in the synthesis of multiple active peptides. The opioid peptides share a common amino terminal sequence of Tyr-Gly-Gly-Phe (followed by Leu or Met), the opioid message domain. This motif is followed by carboxy terminal extensions yielding peptides ranging from 5 to 31 residues. β-endorphin (which derives from cleavage of POMC) is also processed into nonopioid peptides such as adrenocorticotropic hormone, melanocyte stimulating hormone, and β-lipotropin. Proenkephalin contains multiple copies of met-enkephalin, as well as a single copy of leu-enkephalin. Prodynorphin contains three peptides of differing lengths that all begin with the leu-enkephalin sequence: dynorphin A,

dynorphin B, and neoendorphin (Brunton *et al.*, 2011). A comparison of peptide sequences is shown in Table 1.

Other important opioid peptides are endomorphin 1 (EM-1) that was identified in 1997 in the bovine brain (Zadina *et al.*, 1997) and endomorphin-2 (EM-2) found together with EM-1 in the human brain cortex (Hackler *et al.*, 1997). The sequences of these peptides are Tyr-Pro-Trp-Phe-NH_2 and Tyr-Pro-Phe-Phe-NH_2, for EM-1 and EM-2, respectively (Table 1). EM-1 and EM-2 peptides showed high affinity for the mu opioid receptor with K_i values being 1.1 and 1.3 nM, respectively (Hackler *et al.*, 1997), and more than 4000 fold selectivity for mu over the other opioid receptors. Radioimmunological and immunocytochemical analysis revealed that endomorphins are distributed throughout the human, bovine, and rodent central nervous system. EM-1 is widely distributed in the brain and upper brainstem being particularly abundant in the nucleus accumbens, the cortex, the amygdala, the thalamus, the hypothalamus, the striatum, and the dorsal root ganglia. In contrast, EM-2 is more prevalent in the spinal cord and lower brainstem, hypothalamus, the nucleus of the solitary tract, less abundant EM-2 distribution is in the nucleus accumbens, the stubstantia nigra, the nucleus raphe magnus, the ventral tegmental area, pontine nuclei and the amigdala. However, endomorphins precursors or processing pathways still remains unidentified. The effects elicited by exogenous administration of EM-1 and EM-2 are similar to that of other mu selective opioid peptides, for the physiological role played by these peptides see the review (Fichna *et al.*, 2007).

Opioid receptors are coupled, via G_i proteins, to the inhibition of adenylyl cyclase activity, the activation of potassium currents, and the suppression of voltage gated calcium currents; this is typical of both opioid and NOP receptors. These receptors are then coupled to an array of second-messenger systems, e.g. MAP kinases and phospholipase C mediated cascades. Systems as GRKs and β-arrestins are also involved in the opioid receptors regulation and cascade. Prolonged exposure to opioids results in adaptations at multiple levels within these signaling cascades that may relate to effects such as tolerance, sensitization, and withdrawal (Brunton *et al.*, 2011). It has been demonstrated that the β-arrestin 2 gene plays a pivotal role in morphine induced analgesia, knockout mice for β-arrestin 2 resulted in the potentiation and prolongation of the analgesic effect of morphine and reduced liability compared to their wild type littermates (Bohn *et al.*, 2002; Bohn *et al.*, 1999).

Table 1. Amino acid sequence of opioid peptides.

Peptide	amino acidic sequence
Enkephalins	YGGFM
	YGGFL
Dynorphins	YGGFLRRIRPKLKWDNQ
	YGGFLRRQFVVT
	YGGFLRKYPK
Endorphin	YGGFMTSEKSQTPLVTLKNAIIKNAYKKGE
Endomorphin 1	YPWF
Endomorphin 2	YPFF
N/OFQ	FGGFTGARKSARKLANQ

1.4. NOP and OP ligands

The discovery of selective receptor ligands played a fundamental role for identifying the biological roles played by NOP and OP receptors systems. Opioid receptors are bound by a plethora of different synthetic ligands in terms of pharmacological activity. Radiolabelled compounds have allowed the definition of ligand binding characteristics for the three receptor subtype and the determination of anatomical distribution of the receptors using autoradiographic techniques showing receptor specific anatomical distribution in brain, spinal cord, and the periphery.

Naloxone is a universal opioid antagonist, while CTOP, naltrindole, and nor-binaltorphimine (nor-BNI) are selective antagonists for the MOP, DOP, and KOP receptors, respectively. Synthetic selective agonists are DAMGO, DPDPE, and U-69,593 for MOP, DOP, and KOP, respectively.

As far as selective NOP receptor ligands, N/OFQ(1-13)-NH$_2$ (Guerrini *et al.*, 1997), UFP-112 (Rizzi *et al.*, 2007), [Arg^{14}Lys^{15}]N/OFQ (Okada *et al.*, 2000), Ro 65-6570 (Wichmann *et al.*, 1999), and SCH 221510 (Varty *et al.*, 2008) are selective full agonists, while [Phe$^1\psi$(CH$_2$-NH)Gly^2]N/OFQ(1-13)-NH$_2$ ([F/G]N/OFQ(1-13)-NH$_2$) (Calo *et al.*, 1998), UFP-113 (Arduin *et al.*, 2007), Ac-RYYRIK-NH$_2$ (Dooley *et al.*, 1997) are described in literature as partial agonists,

and [Nphe^1]N/OFQ(1-13)-NH$_2$ (Calo *et al.*, 2000b), UFP-101 (Calo *et al.*, 2002), J-113397 (Kawamoto *et al.*, 1999), SB-612111 (Zaratin *et al.*, 2004), C-24 (Goto *et al.*, 2006) as selective antagonists for the NOP receptor.

Opioid therapeutics are of common use for the treatment of pain, e.g. morphine, buprenorphine, methadone, fentanyl, tapentadol, etc. Although the widespread use of opiates, opioid analgesics share typical disadvantages such as constipation, respiratory depression, tolerance liability, and drug abuse. Much efforts have been spent for developing more effective and well tolerated drugs, this research is still ongoing and innovative drug candidates are now being discovered in research laboratories, examples of these compounds under clinical evaluation are: i) cebranopadol, a mixed NOP/opioid receptor agonist by Grünenthal, candidate for chronic, severe and neuropathic pain (Linz *et al.*, 2014; Schunk *et al.*, 2014); ii) TRV130 by Trevena Inc, candidate for treating postoperative pain, it is a MOP receptor agonist able to promote G-protein signaling but not to recruit β-arrestins, TRV130 is more effective than morphine with less side effects (Hackler *et al.*, 1997; Soergel *et al.*, 2014).

1.5. In vitro pharmacological assays for inhibitory-G protein-coupled receptors

An assay is a well-defined analytical method that contains the measurement procedure and how the measurement should be interpreted to obtain the properties of a system or object. Assays are very important tools in the pharmaceutical industry and in the medical diagnostics industry. The characterization of a substance requires the determination of its physiochemical properties by physiochemical assays and the determination of its biological activities by bioassays. The physiochemical properties of a drug substances include its chemical composition, chemical structure, solubility, particle size, crystal property, purity, etc.. through physical and chemical techniques, such as high-performance liquid chromatography (HPLC), mass spectrum, nuclear magnetic resonance (NMR), X-ray crystallography, amino acid sequencing, and so forth. In contrast, the biological activity of a substance by definition is the effect of the substance on a biological test system. Thus, the biological activity of a substance cannot be measured by

13

studying the drug substance alone, it requires a biological test system. The biological test system can be biochemical, such as the activity of an enzyme or the ability to bind to a predefined protein; cell based, such as isolated primary cells or transformed cell lines; tissue or organ based; and animal based (Wu, 2010).

Figure 5. Tissue chambers for isolated tissues assays (left panel), FLIPR instrumentation (right panel).

Historically, in vitro studies for assessing the pharmacological profile of new molecules were performed by using in vitro bioassays on isolated tissues, at least until '70. Such techniques maintain the advantage of studying the receptor in a physiological environment constituted by the tissue/organ. Bioassays on isolated tissues are functional assays and have the ability to estimate both the potency and the efficacy of new ligands. On the other hand bioassay techniques are difficult and time consuming, and can only be employed for studying receptors expressed by the experimental animals. This method is still playing an important role in the characterization of novel opioid ligands, and concurred at the characterization of the major part of available NOP receptor ligands and drugs (Figure 5, left panel).

Conversely, another in vitro approach, which for many years has been the most widely used method to screen new molecules, is the receptor binding. This approach involves the use of cell membranes, both isolated from native tissues and from cells expressing recombinant receptors, and the use of labeled ligands. Ligands are often labeled with a radioactive isotope (usually ^{3}H or ^{125}I) that allows to measure through the specific radioactivity the amount of molecule that bound the receptors, less commonly are linked to moieties of fluorescence properties. These type of measurements led to the determination of the onset of interaction and dissociation, the affinity, and the receptor levels into the membrane preparation. The disadvantage of this method is that

14

does not allow to evaluate the efficacy of a compound, this type of information can be obtained only using functional assays. An assay used to measure the potency and efficacy of a ligand to an active Gi receptor is the stimulation of the [^{35}S]GTPγS binding in activated G proteins. This technique is widely used, but requires a purification of the components of the membranes, the use of radioisotopes and lack of amplification of the signal. Another technique for the measurement of the signal of G proteins is the measurement of stimulation or, in the case of Gi, inhibition of the forskolin induced accumulation of cAMP, this latter method suffers from vary limitations, e.g. the inhibition rarely exceeds 60% of the stimulation, and also, this assay is high expensive both in term of costs and time.

The modern drug-discovery processes, based on the use of big library of compounds have required the development of High Throughput Screening (HTS) methods. These methods allow the rapid determination of the effects of a large number of new ligands. The development of a panel of calcium-sensitive fluorescent dyes and proteins revolutionized the ability to visualize calcium as important second messenger and its complex signaling characteristics. In fact, the major part of the HTS methods are capable to measure fluorescence and the most used is the measurement of fluorescence in response to mobilization of intracellular calcium. The classic tool dedicated to this activity is the Fluorimetric Imaging Plate Reader (FLIPR, Molecular Devices) (Figure 5, right panel) able to screen new compounds in microplates 96/384 wells seeded with transfected cells. In these methods radioactive substances are not needed and it is possible to test several compounds simultaneously. This approach is costly and it is not suitable to test ligands for those receptors not coupled to calcium signaling.

Others methods for studying G$_i$ coupled GPCRs that are also based on fluorescence measurements employ dyes sensitive to perturbation of cell membrane potential (e.g. (Knapman & Connor, 2015)), recently other methods based on Förster/Fluorescence Resonance Energy Transfer (FRET), or Bioluminescence Resonance Energy Transfer (BRET) are increasing their support to pharmacological assays because genetic engineering is getting fairly common and using these type of "proximity" assays it is possible to test a wide spectrum of receptor/effector or receptor/receptor interactions (Salahpour *et al.*, 2012). Other methods named "label free" are able to follow GPCR activation by an "holistic" point of view without the needing to use any type of radioactive or dye compound, e.g. measuring changes in impedance of cells and the dynamic mass redistributions following receptor activation (Grundmann & Kostenis, 2015; Ke *et al.*,

2015), nowadays the high costs of instruments and particularly consumables for these type of experiments limit the use of these assay to industrial laboratories.

1.5.1. Chimeric G proteins and calcium mobilization assay

The use of calcium mobilization assays was limited to G_q coupled receptors whose activation stimulates phospholipase C-β, which catalyzes the cleavage of membrane-bound phosphatidylinositol 4,5-biphosphate into the second messengers inositol (1,4,5) trisphosphate (IP_3) and diacylglycerol. IP_3 acts on IP_3 receptors in the endoplasmic reticulum membrane to elicit calcium release from the reticulum.

The introduction of chimeric G proteins capable to force receptors to signal toward the mobilization of calcium enabled to applay this assay to virtually all GPCR. Several biochemical studies showed that within the Gα structure there are sequences capable of regulating the selectivity of interaction of G proteins and GPCRs. In particular, the C-terminal region of Gα plays a key role in determining the specificity of Gα/GPCR interaction. Furthermore, the replacement of at least three amino acid residues at the $Gα_q$ C-terminal (G_q proteins are coupled to calcium signaling) with the corresponding residues of $Gα_i$ generated a chimeric G protein able to cause a switch in the coupling of several G_i coupled GPCR to the calcium signaling, e.g. $α_2$ adrenergic receptors, adenosine A_1 and D_2 dopaminergic receptor, the substitution of five amino acids was demonstrated being the most efficient ($Gα_{qi5}$) (Conklin *et al.*, 1993). The seminal results by Conklin were then extended to an higher number of GPCRs and also used for the process of GPCR deorphanization (Kostenis *et al.*, 2005b). Subsequent studies have clarified that other regions of G proteins are important to determine the specificity of Gα/GPCR interactions. In particular, the G66 residue of the linker region I is involved in this process, it has been shown that by point mutating the glycine residue into an aspartic, the $Gα_{qG66D}$ protein is less selective when tested for the interaction with GPCRs, allowing GPCRs normally coupled to $Gα_i$ or $Gα_s$ to stimulate calcium mobilization. The proposed mechanism for this increase in promiscuity of the G protein/GPCR coupling event is the following i) the mutational replacement of glycine by other amino acids reduces the conformational freedom of a linker region and might thus yield a Gα in an inactive state with a slightly opened nucleotide binding cleft, ii) this in turn might lower

the activation energy for a GPCR to induce nucleotide exchange on Gα, enabling GPCRs from all coupling classes to facilitate the Gα-activation event (Kostenis *et al.*, 2005b). This mutation cooperatively interacts with the replacement of the 5 residues at the C terminal ($Gα_{qi5}$ and $Gα_{qs5}$) in reducing the receptor/effector specificity. This has been demonstrated for a large number of receptors by performing experiments in which potency and/or maximal effects of reference agonists were always higher in cells expressing the double mutated protein ($Gα_{qG66Di5}$) compared to cell lines expressing either one of the single mutated proteins or native G proteins (Kostenis *et al.*, 2005a) (Figure 6).
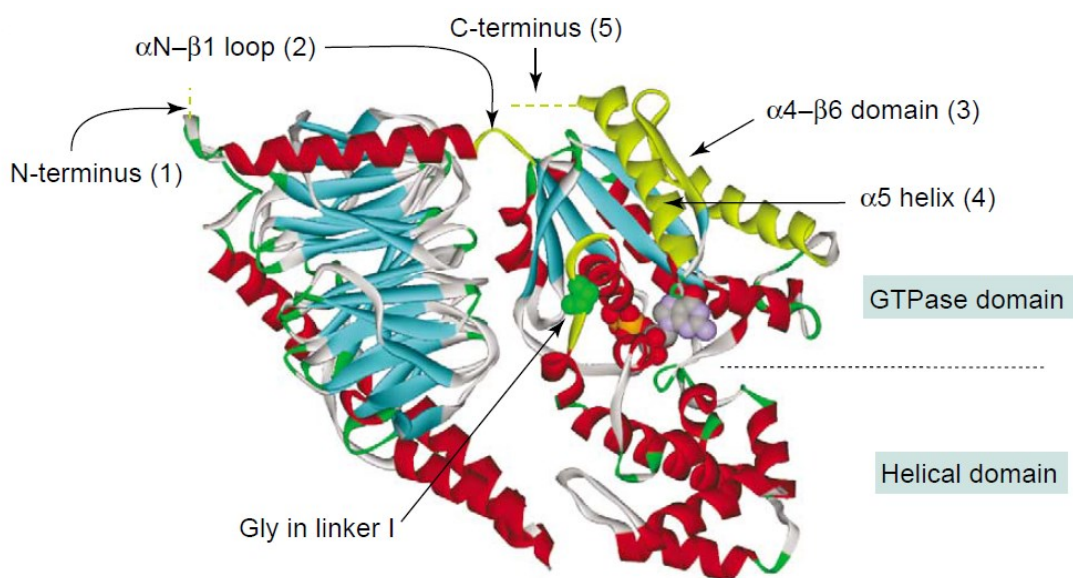

Figure 6. Structure of a heterotrimeric G protein. A highly conserved glycine residue in the linker I region that connects the GTPase domain with the helical domain is highlighted in green. The guanine nucleotide GDP is buried in a cleft between the helical domain and the GTPase domain of the Gα subunit (Kostenis *et al.*, 2005b).

In our laboratories the calcium mobilization assay with chimeric G proteins was successfully setup and validated for the NOP receptor using a large panel of ligands of different activity and applying classical pharmacological criteria (Camarda *et al.*, 2009). This study demonstrated that the overall pharmacological profile of the human NOP receptor evaluated with the calcium mobilization assay, is not affected by the application of chimeric G protein technology.

This study also underlined some limitations of the calcium mobilization assay.. Similar to other assays that measure second messengers, the high level of amplification generated a high

efficiency of the stimulus/response coupling. Under these experimental conditions ligand efficacy is overestimated and for instance partial agonists may display similar maximal effects as full agonists.. Moreover the rapid and transient nature of the calcium peak (i.e. rapid calcium release and subsequent ions sequestration) may produce two different artifacts: for agonist ligands, a possible underestimation of potencies for slow interacting ligands; for antagonist ligands, the evaluation of the type of antagonism (competitive vs non competitive) can be difficult due to hemi equilibrium condition that is typical of this assay. For a review see (Charlton & Vauquelin, 2010).

1.5.2. Bioluminescence Resonance Energy Transfer pharmacological assays

Green Fluorescent Proteins (GFP) and other recombinant modified peptides are useful tools for investigating the network of macromolecular interactions occurring in living cells. These proteins, together with an increasing number of chemical fluorescent probes are designed for arranging a wide spectrum of subcellular, cellular, tissue, and organ occurring phenomena. Protein biochemists have extensively adopted techniques based on Resonance Energy Transfer (RET) between a donor/acceptor couple of chromophores linked to different proteins to investigate molecular interactions. Fluorescence RET (FRET) is one of the most common methods applied both at cell biology and at in vitro GPCR pharmacology. Examples of this use in pharmacology are: protein biosensors for measuring cAMP (Mathiesen *et al.*, 2013), calcium levels (Roelse *et al.*, 2013), and also methods for studying GPCRs oligomerization (Ciruela *et al.*, 2014). Without entering in details the application of Homogenous Time-Resolved FRET (HTRF), that is based on the long lasting fluorescent emission of lanthanide metals, enhances the quality of FRET measurements by diminishing the background noise that is very common when studying fluorescence in cells (Norskov-Lauritsen *et al.*, 2014). TR-FRET was successfully applied to monitoring those mechanisms in which low background levels is a fundamental requirement, such as receptor binding (Emami-Nemini *et al.*, 2013) and receptor/effector interactions (Ayoub *et al.*, 2010). Bioluminescence RET (BRET) is a recently introduced variation that exploits energy transfer occurring between a luciferase-bound donor, able to produce light by metabolizing a chemical substrate (e.g. luciferine, coelenterazine), and a compatible fluorescent

protein acceptor. BRET has two advantages over conventional FRET. First, it does not require incident light, which can damage subcellular structures. Second, it may lead to assays with a better signal-to-noise ratio, because endogenous luminescence is negligible when compared to autofluorescence, at least in mammalian cells (Pfleger & Eidne, 2006) (Figure 8). For these reasons BRET was successfully applied both to monitor second messenger levels with biosensors (e.g. cAMP, IP_3, calcium) but also to evaluate the proximity of proteins and peptides (e.g. GPCR to different types of G proteins and/or arrestins), see for a review (Salahpour *et al.*, 2012).
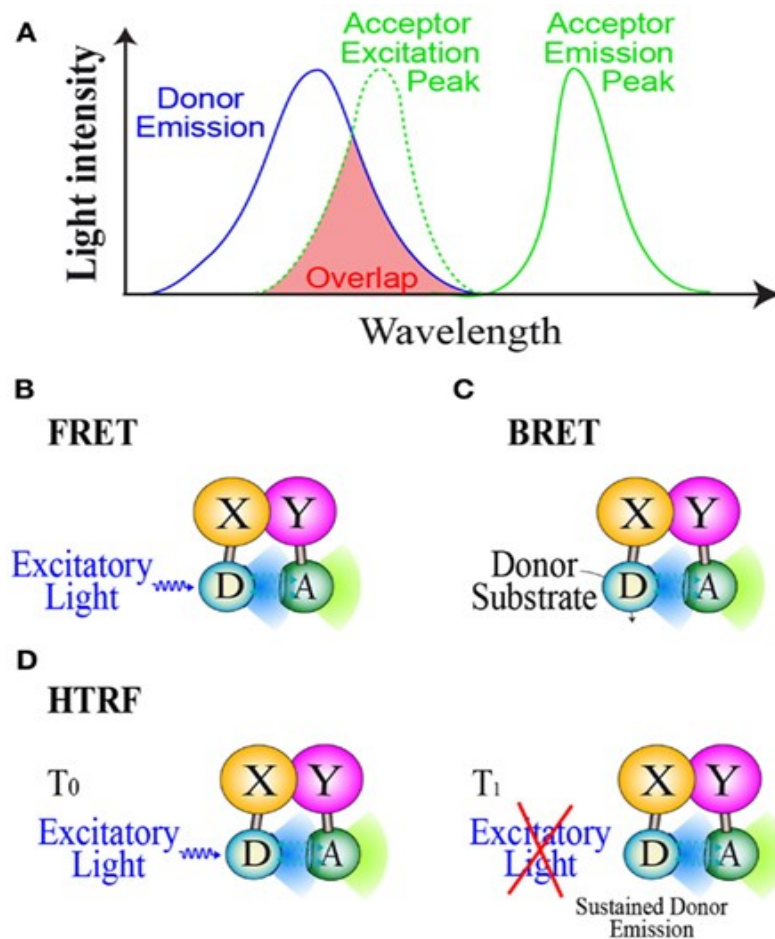
Figure 8. Light emission spectra of Donor/Acceptor couple (panel A). FRET, BRET, and HTRF mechanisms are summarized in B, C, and D panels.

In the present study we setup and validate a BRET-based assay useful for investigating ligand induced NOP/G-protein and NOP/β-arrestin 2 interactions. Methodological setup and validation of linked donor and acceptor couple have been previously made for demonstrating that complementation-induced BRET allows detection of the GPCR/β-arrestin interaction with high

signal-to-noise ratio, good dynamic range and rapid response (Molinari *et al.*, 2008). This assay was then pharmacologically validated for MOP and DOP opioid receptors (Molinari *et al.*, 2010), and for the β2-adrenergic receptor (Casella *et al.*, 2011).

1.6. Aim of the Study

The aims of the present study were to set-up and validate two assays, the calcium mobilization assay for performing pharmacological studies at classical opioid receptors and a BRET-based assay for characterizing novel ligands by studying NOP/G-protein and NOP/β-arrestin 2 interactions . This study was also aimed to evaluate, using different in vitro pharmacological methods, the pharmacological profile of novel ligands at classical opioid and NOP receptors. In particular we investigated compounds generated in the frame of SAR studies of morphine and oxymorphone derivatives, and of endomorphin-2 cyclic pentapeptide derivatives. Similarly SAR studies were performed with both non peptide (spiroxatrine derivatives) and peptide (nociceptin/orphanin FQ(1-13)-NH$_2$ derivatives modified in position 5). Finally innovative ligands were characterized pharmacologically in details such as the NOP antagonist NiK-21273 and N/OFQ tetrabranched derivatives .

2. Material and Methods

2.1. Receptor binding and stimulation of [^{35}S]GTPγS binding

CHO cells stably expressing human classical opioid receptors (MOP, KOP, and DOP receptors) were maintained in Nutrient F12 containing 10% FBS; CHO cells expressing human NOP receptors were maintained in DMEM/Nutrient F12 (50/50) with 5% FBS; all media were further supplemented with penicillin (100 IU/mL), streptomycin (100 μg/mL) and fungizone (2.5 μg/mL). Stock cultures additionally contained geneticin (G418) (200 μg/mL) for CHO$_{MOP}$, CHO$_{DOP}$, and CHO$_{KOP}$, or G418 (200 μg/mL) and hygromycin B (200 μg/mL) for CHO$_{NOP}$ cells. For assessing receptor binding, CHO$_{NOP}$ membranes (40 μg) were incubated in 0.5 mL of buffer consisting of Tris (50 mM), BSA (0.5%), ~0.8 nM [^{3}H]UFP-101 and increasing concentrations (1 pM - 10 μM) of ligands. Non-specific binding was determined in the presence of 1 μM N/OFQ. CHO$_{MOP}$, CHO$_{DOP}$, and CHO$_{KOP}$ membranes were used at a concentration of 50 μg and incubated in 0.5 mL buffer consisting of Tris (50 mM), BSA (0.5%), ~0.8 nM [^{3}H]-diprenorphine and a range of concentrations of ligands. Non-specific binding was determined in the presence of 10 μM naloxone. For both displacement assays, reactions were incubated at room temperature for 1 h and terminated by vacuum filtration through polyethylenimine (0.5%)-soaked Whatman GF/B filters (Fisher Scientific, Loughborough, UK), using a Brandel harvester. Radioactivity was determined following an 8 h extraction of filters in ScintiSafe Gel using liquid scintillation spectroscopy.

For studying the stimulation of [^{35}S]GTPуS binding, 40 μg of membranes taken from CHO$_{NOP}$ cells were incubated in 0.5 mL buffer containing Tris (50 mM), EGTA (0.2 mM), MgCl2 (1 mM), NaCl (100 mM), BSA (0.1%), bacitracin (0.15 mM), GDP (100 mM) and ~150 pM [^{35}S]GTPуS. NOP ligands were included in varying concentrations, and non-specific binding was determined in the presence of 10 μM GTPγS. Reactions were incubated for 1 h at 30°C with gentle shaking and terminated by vacuum filtration through dry Whatman GF/B filters. Radioactivity was determined following an 8 h extraction of filters in ScintiSafe Gel using liquid scintillation spectroscopy.

2.2. Calcium mobilization assay

Cell lines permanently co-expressing the NOP, MOP, or KOP receptors and the C-terminally modified $G\alpha_{qi5}$, and cells co-expressing DOP and $G\alpha_{qG66Di5}$ were all prepared by infecting the CHO_{NOP}, CHO_{MOP}, CHO_{DOP}, and CHO_{KOP} lines with a recombinant retrovirus expressing the chimeric α subunit and the hygromycin resistance gene. Polyclonal cell lines were generated using the pantropic retroviral expression system from BD-Clontech, as described previously (Molinari et al. 2008). Stable lines were selected under hygromycin B (100 μg/ml) and geneticin (600 μg/ml active drug) for 2–3 weeks after the infection. These cell lines were maintained in Dulbecco Minimum Essential Medium (DMEM) and Ham F-12 (1:1), 2 mM L-glutamine, 200 μg/ml geneticin, 100 μg/ml hygromicin B and cultured at 37°C in 5% CO_2 humidified air.

Cells were seeded at a density of 50,000 cells/well into 96-well black, clear bottom plates. After 24 h incubation, the cells were loaded with medium supplemented with 2.5 mM probenecid, 3 μM of the calcium sensitive fluorescent dye Fluo-4 AM and 0.01% pluronic acid, for 30 min at 37°C. Afterwards, the loading solution was aspirated and 100 μl/well of assay buffer: Hank's balanced salt solution (HBSS) supplemented with 20 mM HEPES, 2.5 mM probenecid, and 500 μM Brilliant Black (Aldrich) was added. Concentrated solutions of ligands were made in distilled water (1 mM, peptide ligands) or dimethyl sulfoxide (10 mM, non-peptide ligands) and kept at −20°C. Serial dilutions were made in HBSS/HEPES (20 mM) buffer containing 0.02% BSA. Cell plate and compound plate are placed into the automatized fluorescence reader FlexStation II (Molecular Device, Union City, CA, US), and fluorescence changes were measured at 37°C. Online additions were carried out in a volume of 50 μl/well. Antagonists were incubated 15 min before the addition of the agonist. Maximum change in fluorescence, expressed in percent of baseline fluorescence, was used to determine agonist response.

2.3. BRET assay

Plasmids - Human NOP Rluc-tagged fusion proteins were made by replacing stop codons with a sequence encoding a 10-mer linker peptide (GPGIPPARAT) and cloned into pRluc-N1 (PerkinElmer, Waltham, MA, USA). NOP-Rluc inserts were then transferred into the retroviral expression vector pQIXN (Clontech, Los Baños, Philippines). Bovine $G\beta_1$ N-terminal-tagged

with RGFP (Prolume, Pinetop, USA) was built by linking the RGFP sequence without its stop codon to Ser^2 of $G\beta_1$ through a 21-mer linker peptide (EEQKLISEEDLGILDGGSGSG) and cloned into the retroviral expression vector pQIXH. The N terminus of human β-arrestin 2 after removal of the start codon was tethered to the C terminus of RGFP through a 13-mer linker peptide (EEQKLISEEDLRT) and sub-cloned in pQIXH (Molinari *et al.*, 2010).

Cell and Membrane Preparation - Human Embryonic Kidney (HEK293) cells were grown in Dulbecco's modified Eagle's medium, supplemented with 10% (v/v) fetal calf serum, 100 units/ml penicillin G, and 100 ng/ml streptomycin sulfate, in a humidified atmosphere of 5% CO_2 at 37 °C. Cell lines permanently co-expressing the different pairs of fusion proteins, i.e. NOP-RLuc/$G\beta_1$-RGFP and NOP-RLuc/β-arrestin 2-RGFP, were prepared using the pantropic retroviral expression system by Clontech as described previously (Molinari *et al.*, 2008). For G-protein experiments enriched plasma membrane aliquots from transfected cells were prepared by differential centrifugation; cells were detached with PBS / EDTA solution (1 mM, pH 7.4 NaOH) then, after 5 min 500 g centrifugation, Dounce-homogenized (30 strokes) in cold homogenization buffer (TRIS 5 mM, EGTA 1 mM, DTT 1 mM, pH 7.4 HCl) in presence of sucrose (0.32 M). Three following centrifugations were performed at 1000 g (4°C) and supernatants kept. Two 25,000 g (4°C) subsequent centrifugations (the second in the absence of sucrose) were performed for separating enriched membranes that after discarding the supernatant were kept in ultrapure water at -80°C (Vachon *et al.*, 1987). The protein concentration in membranes was determined using the QPRO - BCA kit (Cyanagen Srl, Bologna, IT) and the spectrophotometer Beckman DU 520 (Brea, CA, USA).

Compound interaction with luciferase activity - For assessing whether compounds affect luciferase activity all the ligands were assayed at 1 and 10 μM employing cell membranes obtained from HEK293 expressing the human NOP-RLuc and β-arrestin 2-RGFP. 5 μM of coelenterazine were added together with membranes 15 min before readings and compounds 5 min before readings. Data were expressed as mean CPS values in 4 readings (~ 60 s delayed) using the 460(25) filter with the microplate luminometer Victor 2030 (PerkinElmer, Waltham, MA, USA).

Receptor levels - The levels of NOP fusion proteins expressed in transfected cells were determined by measuring RLuc luminescence activity. Dilutions of cell membranes (0.1 - 4 μg) made in duplicate were counted in the Victor 2030 (PerkinElmer, Waltham, MA, USA) luminometer to detect RLuc emission; 5 μM coelenterazine was automatically injected to each

sample, and, after a delay of 2 s, total light emission was counted at 0.5 s intervals for 5 s. Integrated photon counts were plotted as a function of membrane protein concentration and the linear regression of the data has been analyzed.

Receptor-transducer interaction - In whole cells luminescence was recorded in 96-well sterile poly-D-lysine-coated white opaque microplates, while in membranes it was recorded in 96-well untreated white opaque microplates (PerkinElmer, Waltham, MA, USA). For the determination of NOP/β-arrestin 2 interactions, cells co-expressing NOP-Rluc and β-arrestin 2-RGFP were plated 24 h before the experiment (100,000 cells / well). The cells were prepared for the experiment substituting the medium with Dulbecco's phosphate buffered saline (DPBS) with 0.5 mM $MgCl_2$ and 0.9 mM $CaCl_2$. For the determination of NOP/G-protein interaction, membranes (3 μg of protein) prepared from cells co-expressing NOP-Rluc and $G\beta_1$-RGFP were added to wells in DPBS. Coelenterazine at a final concentration of 5 μM was always injected 10 minutes prior reading the cell plate. The receptor / G-protein interaction was measured in cell membranes to exclude the involvement of other cellular processes (i.e. arrestin recruitment, internalization*).* Next, different concentrations of ligands in 20 μL of PBS - BSA 0.01 % (Bovine Serum Albumin, Sigma Chemical Co. (Poole, UK)) were added and incubated for an additional 5 min before reading luminescence. Signals were collected using a Victor 2030 luminometer (PerkinElmer, Waltham, MA, USA), emissions were selected using a 460(25) and a 510(10) bandpass filters for Rluc and RGFP, respectively. All the experiments were performed at room temperature. All the experiments were performed at room temperature.

Kinetic evaluations – The effects of 100 nM N/OFQ were evaluated after 5, 10, and 15 min of incubation in cell membranes (NOP/RLuc and Gβ1/RGFP) and living cells (NOP/RLuc and β-arrestin 2/RGFP).

Assessment of antagonist potency - Compounds that do not display agonist activity were further evaluated as antagonists. Three types of experiments were performed i) concentration-response curves to N/OFQ in absence and in presence of a fixed concentration of antagonist, ii) concentration-response curves to N/OFQ in absence and in presence of increasing concentrations of SB-612111 (Schild analysis), iii) inhibition-response curves to SB-612111 against a fixed concentration of N/OFQ approximately corresponding to its EC_{80}.

In pilot experiments performed in cell membranes, 15 min pre-incubation with SB-612111 100 nM, C-24 10 nM, and UFP-101 1 μM were challenged against N/OFQ by measuring BRET ratio 5 min after agonist injection. Concentration response curves to N/OFQ were rightward shifted in

the presence of all antagonists, the agonist maximal effect in presence of UFP-101 was not significantly different than control while in the presence of SB-612111 or C-24 the agonist maximal effect was strongly depressed. These experiments were then repeated by increasing to 15 min the time between agonist injection and the measure of BRET ratio. Under these experimental conditions all antagonists produced a rightward shift of the concentration response curve to N/OFQ without modifying agonist maximal effect. Therefore this protocol was adopted for all subsequent antagonist experiments.

2.4. Electrically Stimulated mouse Vas Deferens

Experimental procedures - Mouse vas deferens (mVD) tissues were taken from Male CD-1 mice (Harlan, San Pietro in Natisone, Udine, Italy) which were handled according to guidelines published in the European Communities Council directives (86/609/EEC), National regulation (D.L 116/92). They were housed in 425 x 266 x 155 mm cages (Techniplast, Milan, Italy), fifteen animals/cage, under standard conditions (22ºC, 55 % humidity, 12-h light/dark cycle, light on at 7:00 am) with food and water available ad libitum.

On the day of the experiments the animals were killed by a lethal injection of urethane. From the mouse the prostatic portion of the vas deferens was isolated, and prepared according to (Hughes *et al.*, 1975). The tissues were suspended in 5 ml organ baths containing heated Krebs solution, composition in mM: NaCl 118.5, KCl 4.7, KH_2PO_4 1.2, $NaHCO_3$ 25, glucose 10 and $CaCl_2$ 2.5. The solution was oxygenated with 95% O_2 and 5% CO_2 (pH 7.4) and the temperature set at 33 °C.

Tissues were continuously stimulated through two platinum ring electrodes with supramaximal voltage rectangular pulses of 1 ms duration and 0.05 Hz frequency, with an applied resting tension of 0.3 g. The electrically evoked contractions (twitches) were measured isotonically with a strain gauge transducer (Basile 7006; Ugo Basile s.r.l., Varese, Italy). Following an equilibration period of 60 min, the contractions induced by electrical field stimulation were stable. At this time, cumulative concentration-response curves were performed by sub sequentially addition of increasing concentrations of the ligand to the same buffer, stabilization of each concentration-mediated effect was allowed prior the injection of the following higher

concentration. Antagonists were evaluated against the concentration-response curve to the agonist following 15 min of pre-incubation.

Instruments - For bioassays two chamber-glass bathes for isolated organs were utilized. The outer chamber contains water heated at 33, while the inner chamber contains 5 ml of oxygenated Krebs solution. One end of the tissue is fixed to the bottom side of the inner chamber and the other end is linked to a force transducer by a surgery thread. The role of the transducer is to convert the mechanical signal in electrical signal, then amplified and recorded with a PC-based acquisition system Power Lab 4/25 (model ML845, ADInstruments, USA).

2.5. Data analysis and terminology

All data are expressed as the mean ± standard error of the mean (SEM) of n experiments. For potency values 95% confidence limits were indicated. Data have been statistically analyzed with one way ANOVA followed by the Dunnett's test for multiple comparisons; p values less than 0.05 were considered to be significant.

Receptor binding data are expressed as % displacement. Stimulation of $[^{35}S]GTP\gamma S$ binding data are expressed as stimulation factor that is the ratio between specific agonist stimulated $[^{35}S]GTP\gamma S$ binding and basal specific binding. In calcium mobilization experiments, maximum change in fluorescence, expressed as percent over the baseline fluorescence, was used to determine agonist response. BRET data are computed as stimulated BRET ratio units, i.e. the ratio between CPS from RGFP and RLuc in the presence of ligands, followed by baseline subtraction, i.e. the BRET value in the absence of ligand. Maximal agonist effects (E_{max}) were expressed as fraction of the N/OFQ E_{max} which was determined in every assay plate and reported in the graphs as E / E_{max}. BRET ratio are obtained between CPS measured for the RGFP and RLuc light emitted using 460(25) and 510(10) filters (PerkinElmer, Waltham, MA, USA), respectively. Electrically stimulated tissues data are expressed as % of the control twitch induced by electrical field stimulation.

Affinity values are showed as pK_i calculated using the Cheng-Prusoff equation:

$pK_i = \log\{IC_{50} / (1 + [L]/KD)\}$

Where IC_{50} is the concentration of antagonist that produces 50% inhibition of the agonist response, [L] is the concentration of free radioligand, and K_D is the dissociation constant of the radioligand for the receptor.

Agonist potencies are given as pEC_{50} i.e. the negative logarithm to base 10 of the molar concentration of an agonist that produces 50% of the maximal effect of that agonist. Maximal effects elicited by the agonists are expressed as intrinsic activity α using N/OFQ as standard full agonist. Concentration-response curves to agonists were fitted to the classical four-parameter logistic nonlinear regression model:

Effect = Baseline + (E_{max} - Baseline) / (1+10^(($LogEC_{50}$ – Log[compound]) HillSlope))

Curves fitting were performed using PRISM 5.0 (GraphPad Software In., San Diego, USA).

EC_{50} is the concentration of agonist producing a 50% maximal response and n is the Hill coefficient of the concentration-response curve to the agonist.

Antagonist potencies were derived in functional experiments in inhibition response experiments as pK_B, which was calculated as the negative logarithm to base 10 of the K_B from the following equation:

$K_B = IC_{50} / ([2 + ([A] / EC_{50})^n]^{1/n} – 1)$,

where IC_{50} is the concentration of antagonist that produces 50% inhibition of the agonist response, [A] is the concentration of agonist, EC_{50} is the concentration of agonist producing a 50% maximal response and n is the slope coefficient of the concentration-response curve to the agonist (Kenakin, 2014). When antagonists were assayed at a single concentration against the concentration-response curve to the agonist their pK_B was derived with the following equation:

$pK_B = log(CR - 1) - log[A]$

where CR is the ratio between agonist potency (expressed as EC_{50}) in the presence and absence of antagonist and [A] is the molar concentration of antagonist. The type of antagonism exerted by antagonists was assayed by using the classical Schild analysis. The Schild plot was analyzed by linear regression to derive the pA_2 value of the antagonist.

To quantify the differences of agonist efficacies for G protein and arrestin interactions the Bias factors were calculated by choosing the endogenous NOP ligand N/OFQ as standard unbiased ligand. For this analysis, the E_{max} and EC_{50} of the agonist were derived using a 3-parameters logistic model with unitary slope values. In fact, although several agonist curves displayed slope values different from 1, on refitting the curves with the parameter fixed to unity did not produce a

28

statistically significant reduction of the goodness of fit (extra-sum of squares principle (DeLean *et al.*, 1978)). Under such conditions, the relative ratio $(E_{max}/EC_{50})_{lig}$ / $(E_{max}/EC_{50})_{N/OFQ}$ is equivalent to the relative $(\tau/K)_{lig}/(\tau/K)_{N/OFQ}$ ratio as defined by the operational model (Black & Leff, 1983; Griffin *et al.*, 2007), and represents the ratio of both intrinsic efficacy (i.e., ε as defined in (Furchgott, 1966)) and binding affinity of the ligands with respect to the reference agonist (Kenakin & Beek, 1982; Onaran *et al.*, 2014). By taking ratios of these values between G protein and arrestin can cancel the common K and yield the ratio of ligand intrinsic efficacy across the two transduction proteins. Thus, the following formula was used for calculating agonist bias factors in log_{10} units:

$$\text{Bias factor} = \log \frac{[(Emax/EC50)lig \, / \, (Emax/EC50)N/OFQ]_{G-protein}}{[(Emax/EC50)lig \, / \, (Emax/EC50)N/OFQ]_{\beta-arr}}$$

29

3. Results

3.1. Novel assays

3.1.1. Pharmacological studies on classical opioid receptors coupled with calcium signaling via chimeric G proteins.

In order to extent the use of the calcium mobilization assay performed on cells expressing chimeric G proteins from the NOP receptor (Camarda *et al.*, 2009) to classical opioid receptors, a panel of standard opioid ligands has been assessed. The results obtained with these compounds were compared to those described in literature with classical assays for G_i coupled receptors. The overall aim of these series of experiments was to set up and validate experimental conditions in order to use this assay for the pharmacological characterization of novel opioid receptor ligands.

MOP receptor - Concentration-response curves to dermorphin and endomorphin-1 (EM-1) were performed in CHO cells stably co-expressing the human MOP receptor and the $G\alpha_{qi5}$ chimeric G protein. Dermorphin and EM-1 exhibited similar maximal effects ($E_{max} \approx 200$ % over the basal) and pEC_{50} values (8.19 (8.11-8.27) and 8.00 (7.92-8.09), respectively (Figure 9).
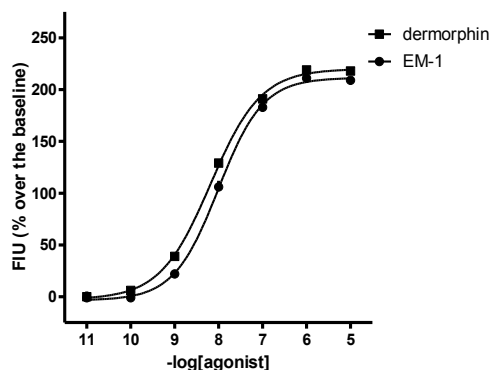

Figure 9. Concentration-response curve to dermorphin and EM-1 in calcium mobilization experiments performed on CHO$_{MOP}$ cells stably expressing the $G\alpha_{qi5}$ protein. Agonist effects were expressed as % over the baseline. Data are the mean of 4 separate experiments performed in duplicate.

In a parallel experiments, DPDPE did not stimulate calcium mobilization up to 1 µM while dynorphin A produced a stimulatory effect only at micromolar concentrations (Table 2).

In a separated series of experiments a fixed concentration of dermorphin (30 nM) was challenged against increasing concentrations (10 pM - 10 µM) of naloxone and selective opioid receptor antagonists. Naloxone and CTOP were able to concentration dependently inhibits the stimulatory effect of dermorphin giving pIC_{50} values of 7.47 and 6.63, respectively (Figure 10); from these data pK_B values of 8.45 (8.11-8.79) and 7.91 (7.36-8.46), were calculated. Parallel experiments were performed with naltrindole and nor-binaltorphimine (nor-BNI); both compounds mimicked the inhibitory effect of naloxone and CTOP with pK_B values of 8.24 (7.95-8.53) and 7.44 (7.07-7.80)
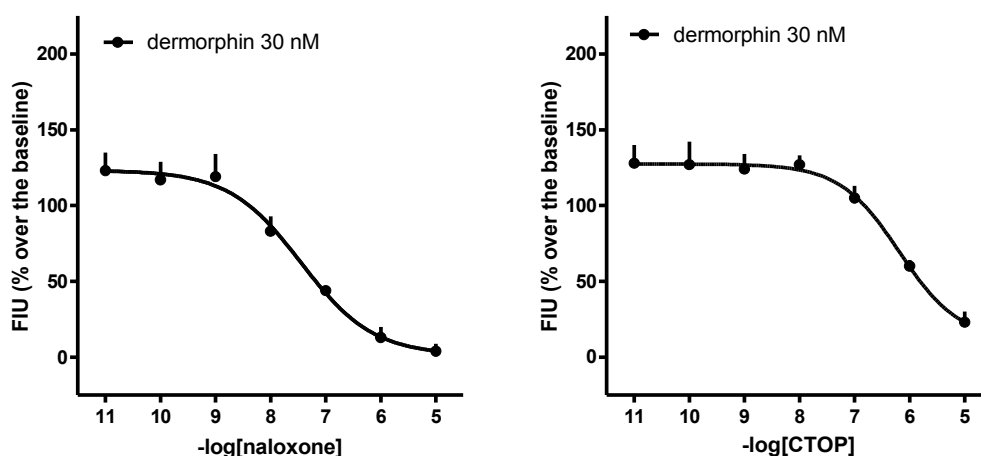

Figure 10. Inhibition-response curves obtained by challenging 30 nM dermorphin with increasing concentrations of naloxone (left panel) and CTOP (right panel) in the calcium mobilization assay performed in CHO_{MOP} cells stably expressing the $G\alpha_{qi5}$ protein. Data are the mean ± sem of 4 separate experiments performed in duplicate.

In order to evaluate the nature of the antagonism exerted by naloxone the classical Schild analysis was performed. The concentration-response curve to EM-1 was evaluated in absence and in presence of increasing concentrations of naloxone (10 nM - 1 µM). As shown in the left panel of Figure 11, the antagonist was able to rightward shift the concentration-response curve to the agonist in a concentration dependent and parallel manner without significantly affecting agonist maximal effect. The corresponding Schild plot (Figure 11, right panel) was linear with a slope not significantly different from unity (1.02 ± 0.1). A pA_2 value of 8.27 was derived from these data.
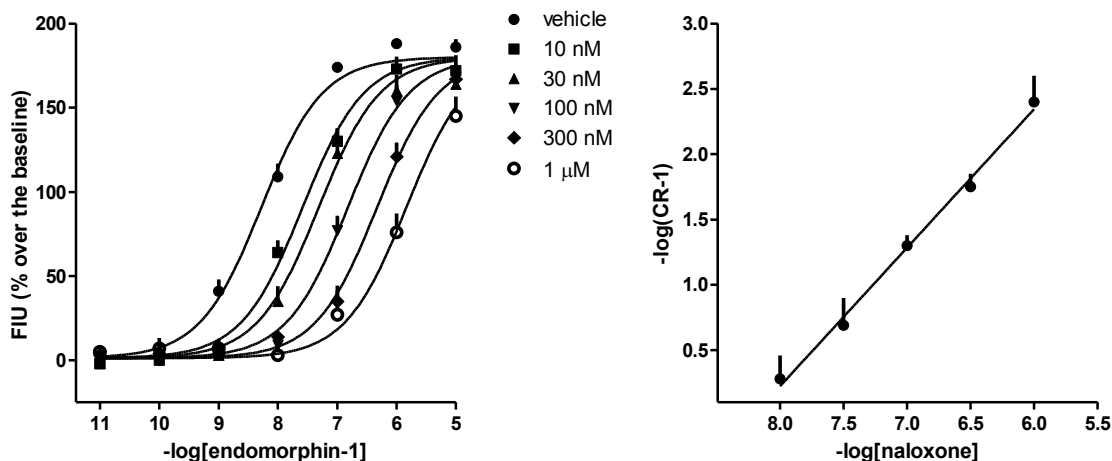
Figure 11. Concentration-response curve to EM-1 obtained in the absence (vehicle) and in presence of increasing concentrations of naloxone (left panel). The corresponding Schild plot is shown in the right panel. Data are the mean of 4 separate experiments performed in duplicate.

DOP receptor - The synthetic peptide DPDPE concentration dependently stimulated the calcium mobilization in CHO cells stably expressing the human DOP receptor and the $G\alpha_{qi5}$ chimeric protein, reaching the maximal effect of 76 ± 2 % over the basal and a potency (pEC_{50}) value of 8.89 (8.16 - 9.63) (Table 2). The signal to noise ratio measured with CHO_{DOP} cells expressing the $G\alpha_{qi5}$ chimeric protein was low and possibly not sufficient for performing antagonist type experiments. Thus, CHO_{DOP} cells were transfected with the $G\alpha_{qG66Di5}$ chimeric G protein that is reported in literature to be more efficient than $G\alpha_{qi5}$ in forcing G_i receptors to couple with the calcium signaling (see introduction chapter). The effects of adenosine triphosphate (ATP) and DPDPE were then tested and compared in CHO_{DOP} expressing either $G\alpha_{qi5}$ or $G\alpha_{qG66Di5}$. ATP, which interact with natively expressed G_q coupled purinergic receptors, was able to stimulate calcium mobilization generating superimposable concentration-response curves in the two cell lines (Figure 12). DPDPE displayed similar high potency in the two cell line while its maximal effects were significantly higher in $G\alpha_{qG66Di5}$ than in $G\alpha_{qi5}$ cells (146 $\pm$ 23% and 70 $\pm$ 10% over the basal, respectively) (Figure 12). Based on these results all the subsequent experiments were performed with CHO_{DOP} expressing the $G\alpha_{qG66Di5}$ chimeric protein.
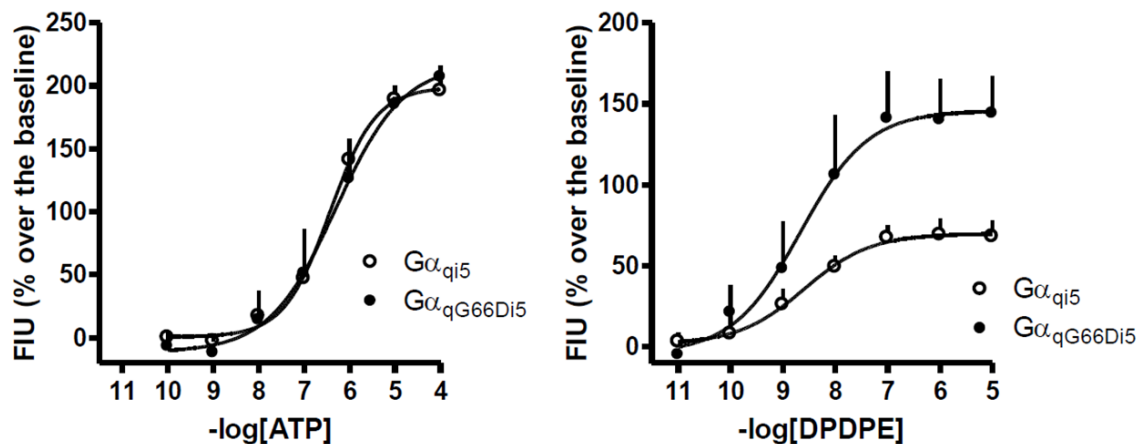
Figure 12. Concentration-response curve to ATP (left panel) and DPDPE (right panel) in calcium mobilization experiments performed on CHO_{DOP} cells stably expressing either the $G\alpha_{qi}5$ or the $G\alpha_{qG66Di5}$ chimeric G proteins. Agonist effects were expressed as % over the baseline. Data are the mean of 4 separate experiments performed in duplicate.

Dermorphin and dynorphin A were also able to elicit similar maximal effects to that of DPDPE with potency values of 6.43 and 7.73, respectively.

In a parallel series of experiments, a fixed concentration of DPDPE (30 nM) was challenged against increasing concentrations (10 pM - 10 μM) of naloxone and naltrindole. Naloxone and naltrindole were able to concentration dependently inhibits the stimulatory effect of DPDPE giving pIC_{50} values of 5.15 (4.88 - 5.42) and 9.14 (6.71 - 11.57), respectively (Figure 13). From these data the following pK_B values 6.08 (5.56 - 6.60) and 10.18 (9.35 - 11.01), were calculated for naloxone and naltrindole, respectively.
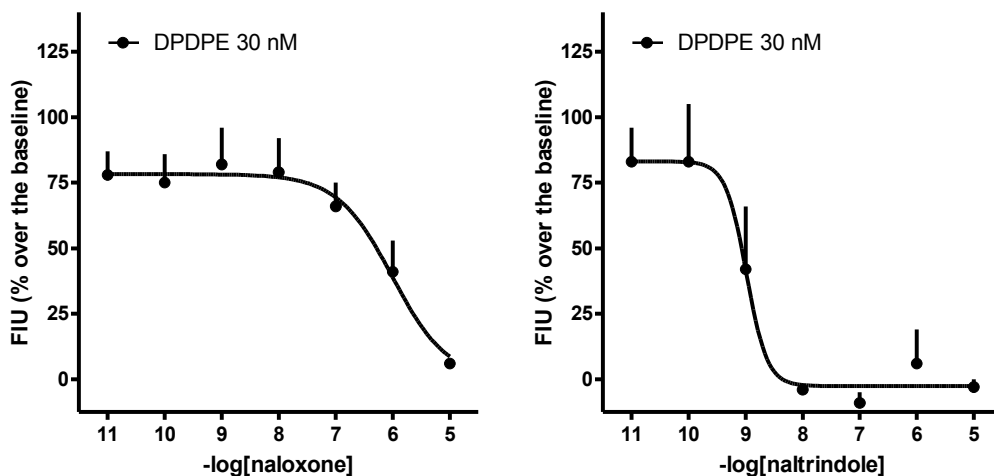
Figure 13. Inhibition-response curves obtained by challenging 30 nM DPDPE with increasing concentrations of naloxone (left panel) and naltrindole (right panel) in the calcium mobilization assay performed in CHO_{DOP} cells stably expressing the $G\alpha_{qG66Di5}$ protein. Data are the mean ± sem of 4 separate experiments performed in duplicate.

KOP receptor - The endogenous peptide dynorphin A stimulated the calcium mobilization in CHO_{KOP} expressing the $G\alpha_{qi5}$ chimeric protein in a concentration dependent manner with a pEC_{50} value of 9.05 (8.90 - 9.20) and maximal effect 225 ± 16 % (Figure 14) (Table 2).
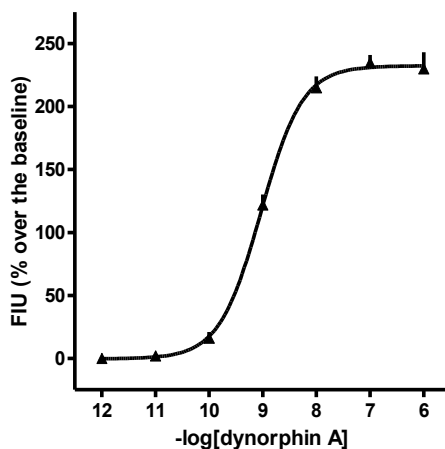

Figure 14. Concentration-response curve to dynorphin A in calcium mobilization experiments performed on CHO_{KOP} cells stably expressing the $G\alpha_{qi5}$ protein. Agonist effects were expressed as % over the baseline. Data are the mean of 4 separate experiments performed in duplicate.

Naloxone and nor-BNI were tested as antagonist in inhibition-response experiments against a fixed concentration of dynorphin A (30 nM) showing pIC_{50} values of 6.10 (5.74 - 6.46) and 8.23 (8.12 - 8.34), respectively. The calculated pK_B values are 7.59 (7.47 - 7.71) and 9.53 (8.78 - 10.28), for naloxone and nor-BNI respectively (Figure 15).
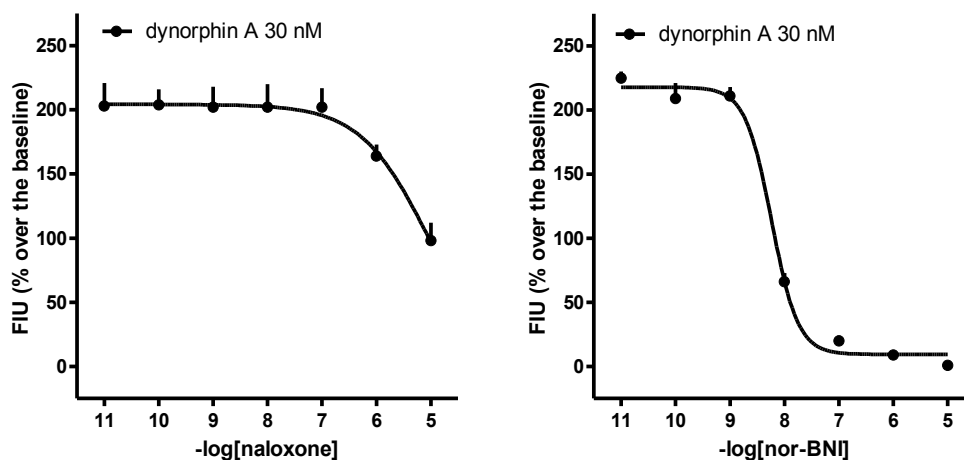

Figure 15. Inhibition-response curves obtained by challenging 30 nM dynorphin A with increasing concentrations of naloxone (left panel) and nor-BNI (right panel) in the calcium mobilization assay performed in CHO_{KOP} cells stably expressing the $G\alpha_{qi5}$ protein. Data are the mean ± sem of 4 separate experiments performed in duplicate.

In order to evaluate the nature of the antagonism exerted by nor-BNI, the classic Schild analysis was performed. The concentration-response curve to dynorphin A was evaluated in absence and in presence of increasing concentrations of nor-BNI (1 nM - 100 nM). As shown in the figure (Figure 16, left panel), dynorphin A potency and maximal effects were 9.31 (8.96 – 9.67) and 165 ± 12 % over the basal; the antagonist was able to rightward shift the concentration-response curve of the agonist in a parallel manner with a decrease of its maximal effect. The corresponding plot (Figure 16, right panel) was linear with a slope value corresponding to 0.9 ± 0.1 and a pA_2 value of 9.33 was found, the pA_2 value obtained from linear regression at low agonist response (E_{max} 50% over the basal) was very similar to that from the Schild analysis (~ 3 fold higher, graph not shown). This value is also similar to that obtained in inhibition-response experiments (9.53).
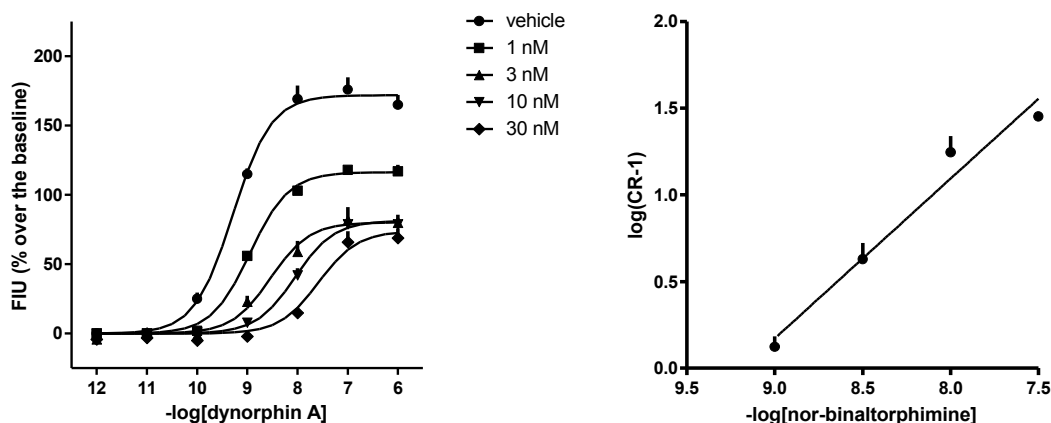
Figure 16. Concentration-response curve to dynorphin A obtained in the absence (vehicle) and in presence of increasing concentrations of naloxone (left panel). The corresponding Schild plot is shown in the right panel. Data are the mean of 4 separate experiments performed in duplicate.

Agonist potencies and maximal effects are summarized for each opioid receptor in Table 2, while antagonist potencies are summarized as summarized in Table 3.

Table 2. Effects and potencies of standard opioid receptor agonists and ATP in CHO cells expressing either the human MOP, KOP, or DOP receptors, and $G\alpha_{qi5}$ chimeric protein in the calcium mobilization assay

	MOP / $G\alpha_{qi5}$		KOP / $G\alpha_{qi5}$		DOP / $G\alpha_{qi5}$	
	pEC_{50}	E_{max}	pEC_{50}	E_{max}	pEC_{50}	E_{max}
ATP	6.18	$270 \pm 42\%$	5.91	$252 \pm 20\%$	5.80	$176 \pm 17\%$
dermorphin	8.19	$218 \pm 1\%$	Inactive		6.43	$78 \pm 3\%$
dynorphin A	6.37	$192 \pm 17\%$	9.05	$225 \pm 16\%$	7.73	$75 \pm 4\%$
DPDPE	inactive		Inactive		8.89	$76 \pm 2\%$

Data in table are mean of at least 3 separate experiments performed in duplicate
Inactive means the compound was found inactive up to 1 μM.

Table 3. Potencies (pK$_B$) of standard opioid receptor antagonists in CHO cells expressing either the human MOP, KOP, or DOP receptors, and chimeric proteins in the calcium mobilization assay

	MOP/Gα$_{qi5}$	KOP/Gα$_{qi5}$	DOP/Gα$_{qG66Di5}$
naloxone	8.34	6.93	6.14
CTOP	7.70	inactive	inactive
nor-BNI	7.58	10.22	8.62
naltrindole	8.24	7.42	9.54

Data in table are mean of at least 3 separate experiments performed in duplicate.
Inactive means the compound was found inactive up to 1 μM.

With these experiments we investigated the possible impact of the use of chimeric G proteins on the pharmacological profile of MOP, DOP, and KOP opioid receptors. Cells co-expressing the human recombinant receptors and chimeric G proteins were used for measuring the calcium mobilization due to the stimulation evoked by a panel of standard opioid receptors agonists. Moreover, the effects of selective and non-selective antagonists for these receptors have been measured. Finally, it has been investigated the type of antagonism exerted by naloxone on the MOP receptor, and nor-BNI on the KOP receptor. The obtained results in which we applied the classical pharmacology criteria for receptor characterization and classification, namely rank order of potency of agonists and values of potency of selective and competitive antagonist, demonstrated that the aberrant signaling evoked by chimeric G proteins does not cause significant modifications on the pharmacological profile of the opioid receptors.

CHO cells expressing the human recombinant receptors MOP, KOP and DOP have been stably transfected with the chimeric G protein Gα$_{qi5}$ (Conklin *et al.*, 1993). Previous studies demonstrated that this protein is able to force the coupling of many GPCRs natively coupled to inhibitory Gα protein to the PLC/IP$_3$/Ca^{2+} pathway. This was confirmed in our laboratories for the NOP receptor with a large panel of ligands encompassing agonists with different efficacy and antagonists of both peptide and non-peptide nature (Camarda *et al.*, 2009).

The three cellular clones co-expressing the opioid receptors and the Gα$_{qi5}$ protein were able to evoke similar high calcium mobilization levels when stimulated with ATP, that activates endogenously expressed G$_q$ coupling purinergic receptors. Similar results were obtained in wild

type CHO, and in CHO transfected with only $G\alpha_{qi5}$ or the opioid receptors (data not shown). These experiments demonstrated that i) ATP stimulates the calcium mobilization independently from both the $G\alpha_{qi5}$ protein and the opioid receptors, ii) the maximal calcium mobilization levels achievable in the three cellular clones is comparable.

A series of agonists acting at the opioid receptors has been evaluated. Small differences found in terms of affinity/potency (receptor binding > calcium mobilization > bioassay) of agonists may be easily discussed both in terms of accessibility of the receptor in the different preparations (membranes > cells > tissues) and in terms of efficiency of the stimulus/response coupling (recombinant > native).

Dermorphin acts as a potent (pEC_{50} 8.21) and selective (approximately 100 fold) MOP agonist, similar values of potency were found in the guinea pig ileum (e.g. 8.7 (Guerrini *et al.*, 1998)) and also in line with binding affinity values (pKi 9.5, (Raynor *et al.*, 1994)). Dynorphin A acts as a universal opioid agonist showing the highest potency value at the KOP receptor (pEC_{50} 9.05). In fact this peptide is considered a KOP preferential agonist. Finally, the synthetic peptide DPDPE acts as a selective DOP agonist showing high potency (pEC_{50} 8.89). This value of potency is similar to literature data, i.e. in the electrically stimulated mouse vas deferens its pEC_{50} value is 8.07 (Dietis *et al.*, 2012). In addition N/OFQ (data not shown) was completely inactive at the classical opioid receptors confirming its pharmacological profile of NOP receptor selective agonist (Calo *et al.*, 2000c).

The present experiments demonstrated the following rank order of potencies for standard opioid agonists.

MOP receptor: dermorphin = EM-1 > dynorphin A >> DPDPE;

DOP receptor: DPDPE > dynorphin A > dermorphin;

KOP receptor: dynorphin A >>> dermorphin = DPDPE.

These rank orders are in line with the data from the literature (Raynor *et al.*, 1994; Toll *et al.*, 1998).

As far as signal to noise ratios (S/N) are concerned, the stimulation of calcium mobilization was good enough for both agonism and antagonism studies in $G\alpha_{qi5}$ expressing CHO_{KOP} and CHO_{MOP} cells (S/N ranging from 2 to 3), while in CHO_{DOP} cells the effects measurable were very low (S/N < 2). Basic fundamentals of assay development have taught that for those assays in which maximal effects are below 200% of the basal value, the study of antagonist properties of ligands

become very difficult if not impossible. For this reason CHO_{DOP} cells were transfected using a more efficient chimeric G protein, in which a substitution of the Gly66 residue in the α_q subunit of G protein with an Asp residue, together with the α_{qi5} substitution, synergistically facilitate the forced coupling.. Further evidences of this enhancement have been described in the present study, DPDPE concentration dependently stimulates the calcium mobilization in CHO_{DOP} cells expressing the double engineered chimeric protein ($G\alpha_{qG66Di5}$) showing higher maximal effects than those obtained in CHO_{DOP} cells expressing the $G\alpha_{qi5}$ protein. For this reason, antagonism type experiments have been performed in CHO_{DOP} cells expressing the $G\alpha_{qG66Di5}$ protein.

In a separate series of experiments inhibition-response experiments were performed for a series of standard antagonists for classical opioid receptors, the universal antagonist naloxone and the selective antagonist CTOP (MOP), naltrindole (DOP), and nor-BNI (KOP). Naloxone behaves as antagonist over the three classical opioid receptors acting as universal antagonist. It is worth of mention that it is considered opioid mediated each naloxone sensitive biological action. The highest value of potency for naloxone has been measured on MOP (8.05), followed by KOP (7.59), and DOP (6.08). This rank order of selectivity is in line with published data, moreover these pK_B values are similar to the binding affinity values at human recombinant receptors (MOP 9.03, KOP 8.63, and DOP 7.77) (Raynor *et al.*, 1994), and also similar to antagonist potencies in bioassay studies (MOP 8.8, KOP 8.0, DOP 7.5) (Calo *et al.*, 1997). CTOP, naltrindole, and nor-BNI exhibited high potency for the human MOP (7.56), DOP (10.18), and KOP (9.53), respectively. Again these values are in line with those from literature (CTOP 9.74, naltrindole 10.69, and nor-BNI 10.56) (Raynor *et al.*, 1994).

Besides potency and selectivity of action, the type of antagonism exerted, competitive or non-competitive, is another important property of receptor antagonists. For evaluating this property, concentration-response curves to agonists were assessed in absence and in presence of increasing concentrations of antagonists. A competitive antagonist rightward shifts the concentration-response curve to the agonist in a parallel and concentration dependent manner, without affecting the maximal effect elicited by the agonist. This is a typical surmountable behavior, if the Schild analysis of the curves produces a straight line with slope value not significantly different from 1, these antagonists are of competitive nature, and the potency (pA_2) obtained as the abscissae intercept of the line is close to that derived in inhibition-response experiments (pK_B). On the contrary, a non-competitive antagonist shows an insurmountable behavior by decreasing the

maximal effect of the agonist even after prolonged agonist incubation times. An intermediate condition is the one of slow dissociating competitive antagonists, these compounds similarly to non competitive ligands produce a depression of the agonist maximal, the real antagonist nature is evident only after prolonged exposures to the agonist, when equilibrium conditions occur.

This type of experiment has been performed for naloxone and nor-BNI, for MOP and KOP receptors respectively. Naloxone rightward shifted the concentration-response curve to the agonist (EM-1) in a parallel and concentration dependent manner, without affecting its maximal effect, the Schild analysis confirmed the competitive nature of naloxone (slope ~ 1, pA$_2$ 8.27), close values of antagonist potency obtained by Schild analysis and by inhibition response experiments also confirmed the competitive nature of naloxone. This is in line with those obtained in classical bioassay experiments, namely a surmountable behavior of naloxone against morphine in the electrically stimulated guinea pig ileum (pA$_2$ 8.56 (Tallarida *et al.*, 1982)).

Similarly to naloxone, for evaluating the nature of the antagonism exerted by nor-BNI, the classic Schild analysis was applied. Nor-BNI produced a rightward shift of the concentration-response curve to dynorphin A in a parallel manner, producing however a decrease of its maximal effect. The pA$_2$ value obtained from the Schild analysis was 9.33 (slope ~ 1), that is very similar to what derived in inhibition-response experiments (pK$_B$ 9.53) and to the literature data (recombinant rat receptor, pK$_i$ 9.59 (Meng *et al.*, 1993)). Nor-BNI is described in the literature as a competitive antagonist, the insurmountable behavior found in the present experiments might be possibly due to assay artifacts. According to Charlton and Vauquelin, insurmountability will also be observed when pre-formed antagonist receptor complexes are reversible but dissociate so slowly that only part of the receptors can be liberated and, hence, occupied/stimulated by the subsequently added agonist before the response is measured. This situation will readjust with time until ultimately, both the agonist/ and the antagonist/receptor interactions reach equilibrium. Therefore, the insurmountability of slow dissociating antagonists is only apparent and can theoretically be overcome by measuring the response after a sufficient time lapse. Yet, this is not possible with calcium response measurements and, because of the much shorter delay between these measurements and the agonist administration when compared with other experimental paradigms (e.g. bioassays or GTPγS binding), quite fast dissociating competitive antagonists may display insurmountable behavior (Charlton & Vauquelin, 2010). According to what suggested by these authors the antagonist potency value was also calculated by computing concentration ratios at low agonist response (i.e. 50% over the basal, approximately the EC$_{20}$ of the agonist in the

absence of antagonist), the antagonist potency obtained was very similar to that from the Schild analysis. Moreover, the calculation of antagonist potency at low agonist response is quite robust in the presence of high levels of stimulus/coupling efficiency (e.g. high levels of receptors and/or G proteins).

Collectively, the rank order of agonists potency obtained for the MOP, DOP, and KOP receptors, indicate that the use of chimeric proteins for measuring the calcium mobilization and studying these receptors do not sustantially affect the pharmacological profile of classical opioid receptors. The use of the double mutated chimeric G-protein ($G\alpha_{qG66Di5}$) enhanced our ability to test both agonist and antagonist ligands at the DOP receptor. The values of potency obtained for competitive and selective antagonists at classical opioid receptors were similar to that already published in literature, confirming the ability of this method to accurately investigate the antagonist properties of ligands. The results obtained by studying the nature of antagonists suggest that this assay might produce misleading results for those antagonists characterized by slower kinetics of dissociation. This type of studies, calcium mobilization assay using chimeric G proteins, have been performed by independent groups on several GPCR, including the opioid field (Zhang *et al.*, 2012), and it has been validated by our group for the NOP receptor (Camarda *et al.*, 2009).

Taken together our results extended the application of this assay to the study of opioid receptors and confirmed the validity of calcium mobilization as a useful primary screening assay.

3.1.2. Pharmacological profile of nociceptin/orphanin FQ receptors interacting with G-proteins and β-arrestins 2

Functional selectivity or biased agonism is emerging as an important and therapeutically relevant pharmacological concept in the field of G protein coupled receptors including opioids. To evaluate the relevance of this phenomenon in the NOP receptor, we used a BRET technology to measure the interactions of the NOP receptor with either G proteins or β-arrestin 2 in the absence and in presence of increasing concentration of ligands.

Ligands effect on luciferase activity - NOP receptor ligands used in this study were tested for their effects over RLuc activity in cell membranes. At 1 µM the compounds did not modify RLuc activity . Similar results were obtained by testing the compounds at 10 µM with the only exception of Ro 65-6570 and PWT2-N/OFQ that produced a significant decrease in photons emitted by RLuc. Thus 1 µM was chosen as the highest concentration tested in concentration-response curves to Ro 65-6570 and PWT2-N/OFQ (Table 4).

Table 4. Evaluation of CPS emitted in NOP/RLuc expressing membranes in presence of 1 or 10 μM of following compounds.

	1 μM	10 μM
PBS (and BSA 0.01%)	11330 ± 125	12022 ± 692
PBS/DMSO (0.1 - 0.01%)	11244 ± 756	11381 ± 137
N/OFQ	10482 ± 675	12315 ± 1833
N/OFQ(1-13)-NH$_2$	10662 ± 863	12767 ± 1737
[Arg^{14}Lys^{15}]N/OFQ	9864 ± 456	11949 ± 1911
UFP-112	13152 ± 436	13995 ± 843
PWT2-N/OFQ	11406 ± 912	*6018 ± 543
[F/G]N/OFQ(1-13)-NH$_2$	12950 ± 322	13886 ± 936
UFP-113	12496 ± 659	13455 ± 959
Ac-RYYRIK-NH$_2$	12746 ± 989	13555 ± 809
[Nphe^1]N/OFQ(1-13)-NH$_2$	12844 ± 434	13410 ± 566
UFP-101	12432 ± 851	11920 ± 512
Ro 65-6570	12190 ± 356	*7792 ± 563
SCH-221510	11616 ± 787	12012 ± 396
J-113397	10810 ± 663	11791 ± 981
SB-612111	10128 ± 846	11268 ± 1140
C-24	12298 ± 366	12709 ± 411
Naloxone	12146 ± 1065	12591 ± 445
GDP	11554 ± 1124	12601 ± 1012

Data are mean ± sem of 3 separate experiments. * $p < 0.05$ vs. PBS according to one way ANOVA followed by the Dunnett test for multiple comparisons.

Expression levels of RLuc/NOP receptor in Gβ$_1$/RGFP and β-arrestin 2/RGFP expressing cells - In order to compare the expression levels of NOP receptor in the two cell lines we measured photons emitted by RLuc in response to 5 μM coelenterazine as a function of membrane protein concentrations. As shown in Figure 1 in both cell lines there was a linear increase in CPS with the increase of the membrane protein concentration. The slopes of the regression lines, $3.66 \pm 0.065 \cdot 10^6$ and $4.09 \pm 0.068 \cdot 10^6$ CPS$\cdot 10^6 \cdot$μg^{-1} for Gβ1 and β-arrestin 2 cells, respectively, were not significantly different (Figure 17).
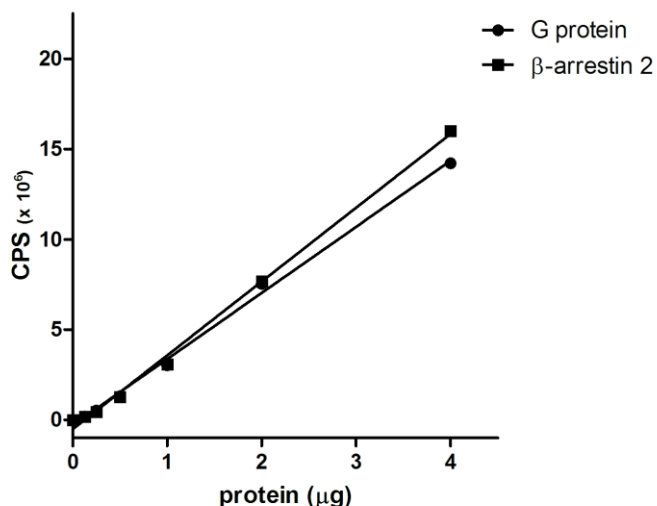
Figure 17. Light emitted (CPS) as function of the amount of protein (µg) in membranes prepared from NOP/RLuc cells expressing either $G\beta_1$/RGFP or β-arrestin 2/RGFP membranes.

Assessment of NOP/G-protein constitutive coupling - The GPCR/G-protein interaction assessed via BRET in cell membranes is abolished by the addition of guanine nucleotides. We thus examined the effect of GDP on NOP/ G-protein interaction to investigate the extent of constitutive activity in the NOP receptor under the present experimental conditions. GDP up to 10 µM did not significantly modify the basal BRET ratio, and only a very weak inhibitory effect (5% of basal BRET) was detected by prolonging incubation time to 15 min (Figure 18).
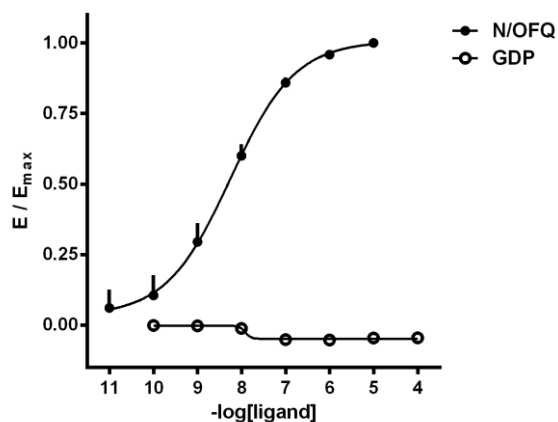

Figure 18. NOP receptor/G-protein interaction experiments - Concentration-response curves to N/OFQ and GDP following 15 minutes of incubation in membranes. Data are expressed as mean ± sem of 3 separate experiments performed in duplicate

Effect of Pertussis-toxin treatment - In order to elucidate the identity of the endogenous Gα subunits mediating the NOP/Gβ$_1$ interaction, and to evaluate their potential effects on NOP mediated β-arrestin 2 recruitment, HEK293 cells stably expressing the human NOP (NOP/RLuc) receptor and either the Gβ$_1$ subunit (Gβ$_1$/RGFP) or the β-arrestin 2 (β-arrestin 2/RGFP) were treated for 20 h with 10 ng PTX. As shown in Figure 2, right panel, PTX treatment abolished the ability of the agonist to stimulate NOP/G-protein interaction, but had negligible effects on the stimulation of NOP/β-arrestin 2 interactions (Figure 19).
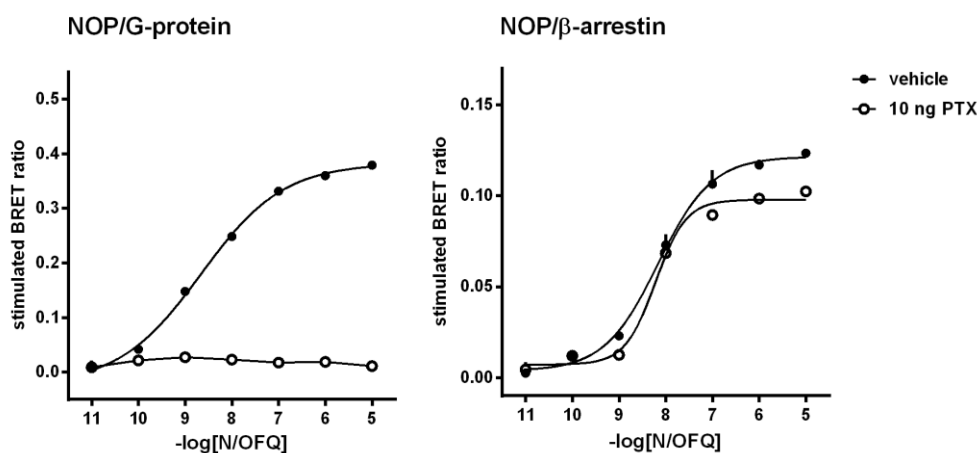

Figure 19. Concentration-response curves to N/OFQ - experiments performed in absence and in presence of PTX 10 ng 20 h treatment. NOP/G-protein (left panel) and NOP/β-arrestin 2 interaction experiments (right panel). Data are mean ± sem of 3 separate experiments performed in duplicate.

Effect of ligands on NOP/G-protein interaction - Membrane extracts taken from HEK293 cells stably expressing both the human NOP (NOP/RLuc) receptor and the Gβ$_1$ subunit (Gβ$_1$/RGFP) were used to perform concentration-response curves to NOP ligands. The endogenous NOP receptor agonist N/OFQ promoted NOP/G-protein interaction in a concentration-dependent manner. N/OFQ displayed high potency (pEC$_{50}$ 8.44) and a maximal effect which corresponded to a stimulation of 0.42 ± 0.01 BRET ratio units over the baseline (Figure 20, Panel A). Under the same experimental conditions synthetic peptides such as, [Arg^{14}Lys^{15}]N/OFQ, PWT2-N/OFQ, UFP-112, and N/OFQ(1-13)-NH$_2$ produced similar stimulatory effects, with E$_{max}$ values comparable to those induced by the natural peptide. N/OFQ(1-13)-NH$_2$ was equipotent with N/OFQ, while [Arg^{14}Lys^{15}]N/OFQ, PWT2-N/OFQ, and UFP-112 were 7, 5, and 8 fold more

potent than N/OFQ (Figure 20, Panel B). The non-peptide NOP ligands SCH-221510, Ro 65-6570, J-113397, SB-612111, C-24, and the opioid receptor antagonist naloxone were also investigated. SCH-221510 and Ro 65-6570 exhibited maximal effect not significantly different from those of N/OFQ, but were 2 and 5 fold less potent then the natural peptide (Figure 3, Panel C). In contrast, J-113397, SB-612111, C-24, and naloxone did not modify the basal BRET ratio. In a separate series of experiments the peptides UFP-101, UFP-113, [Nphe^{1}]N/OFQ(1-13)-NH$_2$, Ac-RYYRIK-NH$_2$, and [F/G]N/OFQ(1-13)-NH$_2$ were tested. All such peptides exhibited maximal effects that were significantly lower than that of N/OFQ, ranging from 0.14 (UFP-101) to 0.72 ([F/G]N/OFQ(1-13)-NH$_2$). As far as potency is concerned, all these ligands were less potent than the natural peptide, with the exception of UFP-113, which was 8 fold more potent than N/OFQ (Figure 20, Panel D). However, due to its very low E$_{max}$ value, the potency of UFP-101 could not be precisely estimated. All the data obtained in this series of experiments have been summarized in Table 5.

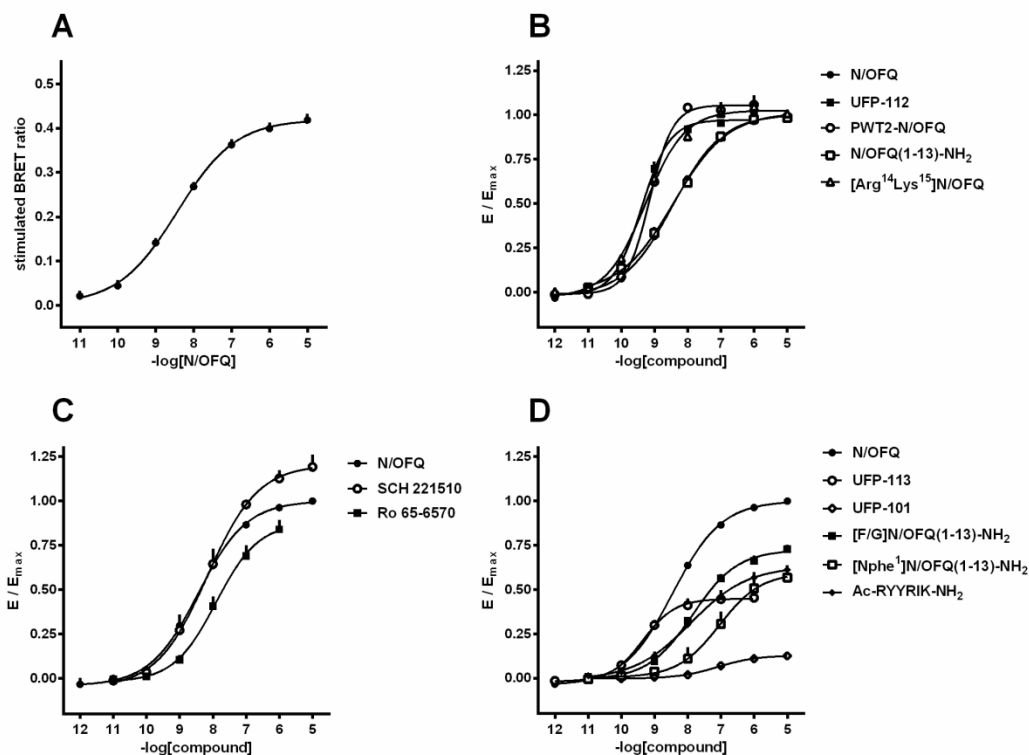Ligands with very weak or no agonist effects were assessed as antagonists.

Figure 20. NOP receptor/G-protein interaction experiments - Concentration-response curves to N/OFQ (Panel A); N/OFQ, UFP-112, PWT2-N/OFQ, N/OFQ(1-13)-NH$_2$, and [Arg^{14}Lys^{15}]N/OFQ (Panel B); N/OFQ, SCH-221510, and Ro 65-6570 (Panel C); N/OFQ, UFP-113, UFP-101, [F/G]N/OFQ(1-13)-NH$_2$, [Nphe^1]N/OFQ(1-13)-NH$_2$, and Ac-RYYRIK-NH$_2$ (Panel D). Data are expressed as mean ± sem of at least 5 separate experiments performed in duplicate.

In a series of pilot experiments, UFP-101, SB-612111 and C-24 were tested at fixed concentrations against the concentration-response curve of N/OFQ. All ligands produced the expected shift of agonist EC$_{50}$, however, unlike UFP-101, SB-612111 and C-24 also caused a depression of the maximal effect elicited by N/OFQ under such conditions. On repeating the experiments by increasing the time of incubation from 5 to 15 min, the decrease of N/OFQ E$_{max}$ value was no longer evident (Figure 21). Thus, a longer incubation time was used to assess antagonist potency for both G protein interaction and arrestin interaction (see below).
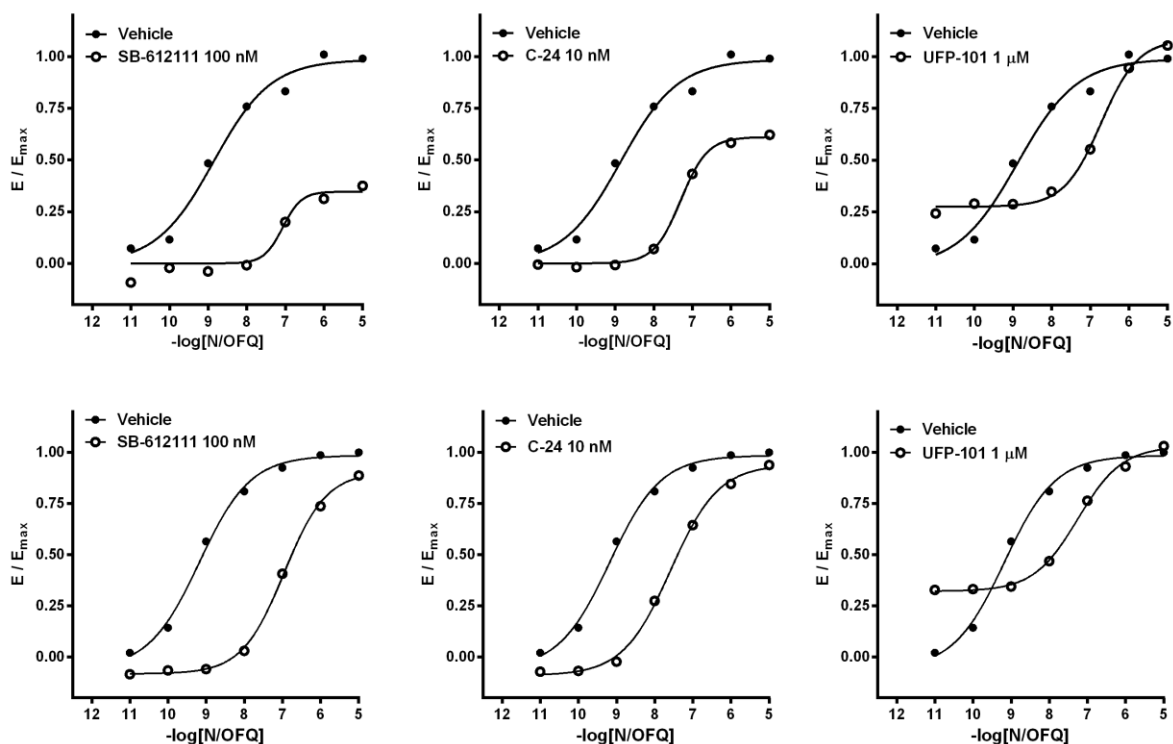
Figure 21. NOP receptor/G protein interaction experiments - concentration-response curves to N/OFQ in the absence and in presence of SB-612111 (left panels), C-24 (middle panels), and UFP-101 (right panels). Antagonists were injected 15 min before N/OFQ and BRET ratio was measured 5 min (top panels) or 15 min (bottom panels) after agonist injection. Data are from a single representative experiment performed in duplicate.

The ligands C-24 (10 nM), UFP-101 (1 µM), and J-113397 (30 nM) added to the concentration-response curve of N/OFQ produced a rightward shift of the curve without significantly changing the maximal effect. From these experiments the following pK_B values were derived: C-24, 9.11, UFP-101, 7.66, and J-113397, 7.95 (Figure 22). In similar experiments naloxone (1 µM) did not modify the concentration response curve to N/OFQ.
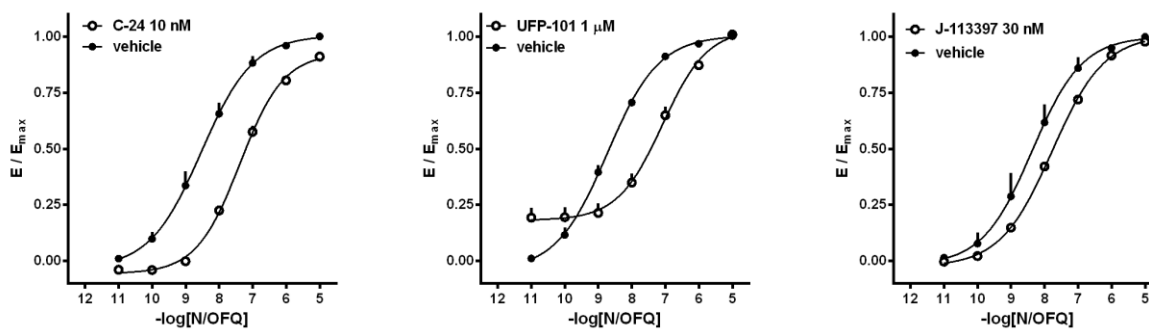
Figure 22. NOP receptor/G protein interaction experiments - concentration-response curves to N/OFQ in absence and in presence of C-24, UFP-101, and J-113397. Data are mean ± sem of 5 separate experiments performed in duplicate.

Schild analysis was used to obtain a more detailed analysis of the antagonist properties of SB-612111. Concentration-response curves of N/OFQ were generated in the absence and presence of increasing concentrations (1 - 100 nM) of the antagonist. SB-612111 produced a parallel rightward shift of the N/OFQ curves in a concentration dependent manner, without modifying the maximal effect elicited by the agonist (Figure 23, left panel). The resulting Schild plot was linear with a slope value of 1.16 ± 0.03; a pA_2 value of 8.96 was derived from these experiments (Figure 23, middle panel). Finally, the antagonist potency of SB-612111 was also estimated from inhibition response curves. Increasing concentrations of SB-612111 (10 pM - 10 µM) were tested against a fixed concentration of N/OFQ (30 nM); the pK_B derived from these experiments was 9.13 (Figure 23, right panel). All the data obtained in this series of experiments are summarized in Table 6.
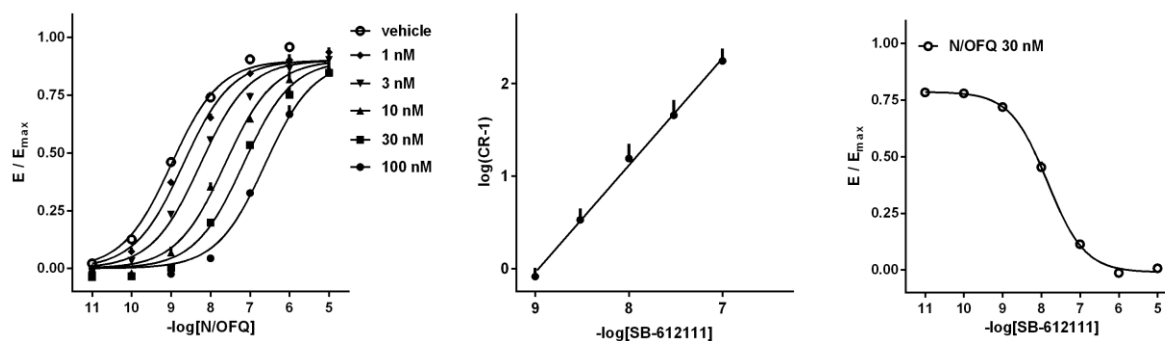
Figure 23. NOP receptor/G protein interaction experiments - concentration-response curves to N/OFQ in absence and in presence of increasing concentrations (1 - 100 nM) of SB-612111 (left panel). The corresponding Schild plot is shown in the middle panel. The inhibition response curve to SB-612111 vs. N/OFQ 30 nM is shown in the right panel. Data are mean ± sem of 4 separate experiments performed in duplicate.

Effect of ligands on NOP/β-arrestin 2 interactions - HEK293 cells stably expressing both the human NOP (NOP/RLuc) receptor and the β-arrestin 2 (β-arrestin 2/RGFP) protein were used for performing concentration-response curves to NOP ligands. N/OFQ promoted receptor/arrestin interaction in a concentration dependent manner displaying high potency (pEC$_{50}$ 8.02), and maximal effects that corresponded to a stimulation of 0.07 ± 0.004 BRET ratio units over the baseline (Figure 24, Panel A). The synthetic peptides [Arg^{14}Lys^{15}]N/OFQ, UFP-112, and N/OFQ(1-13)-NH$_2$ mimicked the stimulatory effect of N/OFQ and showed similar maximal effects. With regards to potency, UFP-112 was slightly more potent, whereas [Arg^{14}Lys^{15}]N/OFQ and PWT2-N/OFQ were 2 and 3 fold less potent than N/OFQ (Figure 24, Panel B). The non-peptide compounds SCH-221510, Ro 65-6570, J-113397, SB-612111, C-24, and naloxone were also investigated for their ability to promote NOP receptor/β-arrestin 2 interactions. SCH-221510 was 10 fold less potent than N/OFQ (Figure 24) and Ro 65-6570 exhibited a similar decrease of potency, although we should note that the incomplete concentration-response curves of this compound did not allow an experimentally verified assessment of the asymptotic plateau, thus the pEC$_{50}$ and E$_{max}$ values obtained for this compound (6.3 and 0.84) are extrapolated from the fitting routine (Table 5). J-113397, SB-612111, C-24, and naloxone did not modify the basal BRET ratio. The synthetic peptides that are partial agonist at G protein coupling (i.e., [F/G]N/OFQ(1-13)-NH$_2$, [Nphe^1]N/OFQ(1-13)-NH$_2$, UFP-101, UFP-113, [Nphe^1]N/OFQ(1-13)-

50

NH$_2$, and Ac-RYYRIK-NH$_2$) showed only a variable and weak stimulation of receptor / arrestin interaction (Figure 24, Panel D).
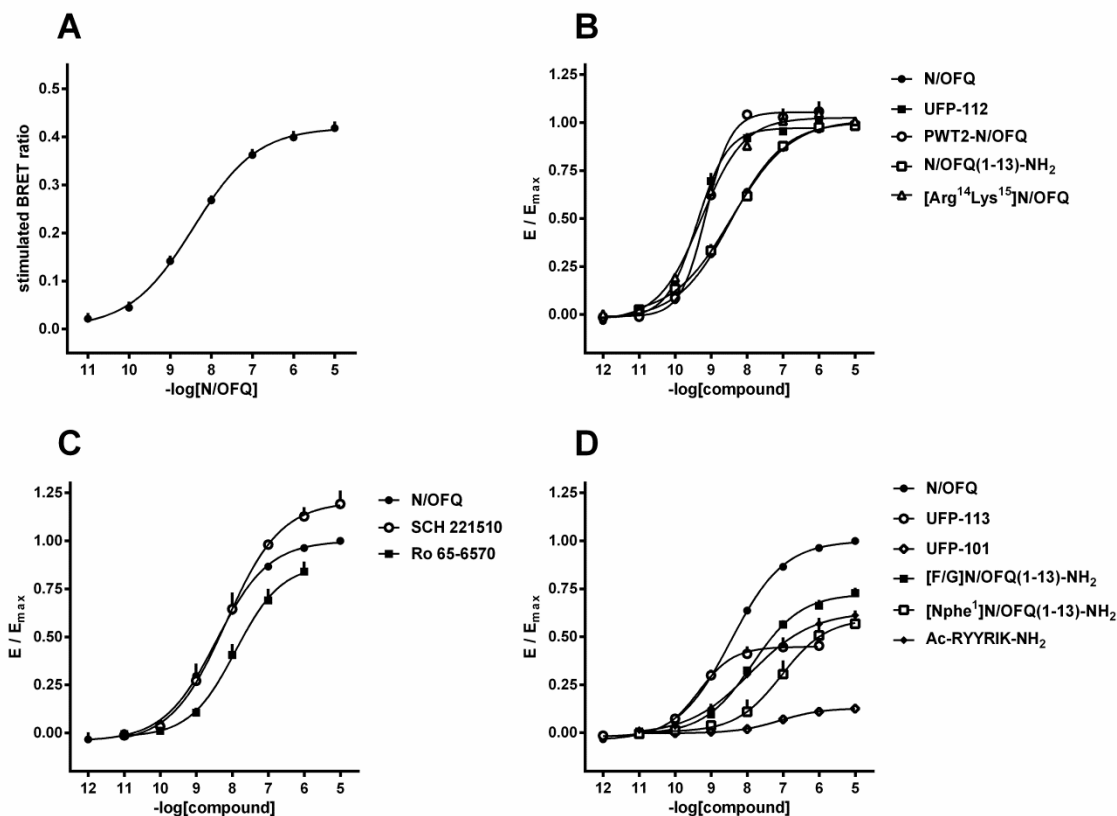

Figure 24. NOP receptor/β-arrestin 2 interaction experiments - Concentration-response curves to N/OFQ (Panel A); N/OFQ, UFP-112, PWT2-N/OFQ, N/OFQ(1-13)-NH$_2$, [Arg^{14}Lys^{15}]N/OFQ (Panel B); N/OFQ, SCH-221510, and Ro 65-6570 (Panel C); N/OFQ, UFP-113, UFP-101, [F/G]N/OFQ(1-13)-NH$_2$, [Nphe^1]N/OFQ(1-13)-NH$_2$, and Ac-RYYRIK-NH$_2$ (Panel D). Data are expressed as mean ± sem of at least 5 separate experiments performed in duplicate.

All such ligands were thus analyzed as antagonists. They behaved as competitive antagonists, by producing a rightward shift in the concentration-response curve of N/OFQ for arrestin coupling without affecting the E$_{max}$ value. The following pA$_2$ values were computed from such experiments: [F/G]N/OFQ(1-13)-NH$_2$, 7.52, Ac-RYYRIK-NH$_2$, 7.11, [Nphe1]N/OFQ(1-13)-NH$_2$, 7.00, UFP-101, 9.42 (Figure 25). All the data obtained in this series of experiments have been summarized in Table 6. Of note, the antagonist potencies estimated for these ligands in inhibiting arrestin coupling are very close to their agonistic potency in stimulating G protein

coupling. This indicates that the lack of agonistic effect on arrestin is not due an insufficient concentration of ligand that was used in the assay.

We also measured the inhibitory potency for arrestin coupling of the other antagonists, such as J-113397, SB-612111, C-24, J-113397, and, naloxone. With the exception of the latter, which was inactive, all antagonists produced the expected competitive inhibition with a rightward shift of the concentration-response curve of N/OFQ, from which pA_2 values were computed. All the data obtained in this series of experiments are summarized in Table 6.
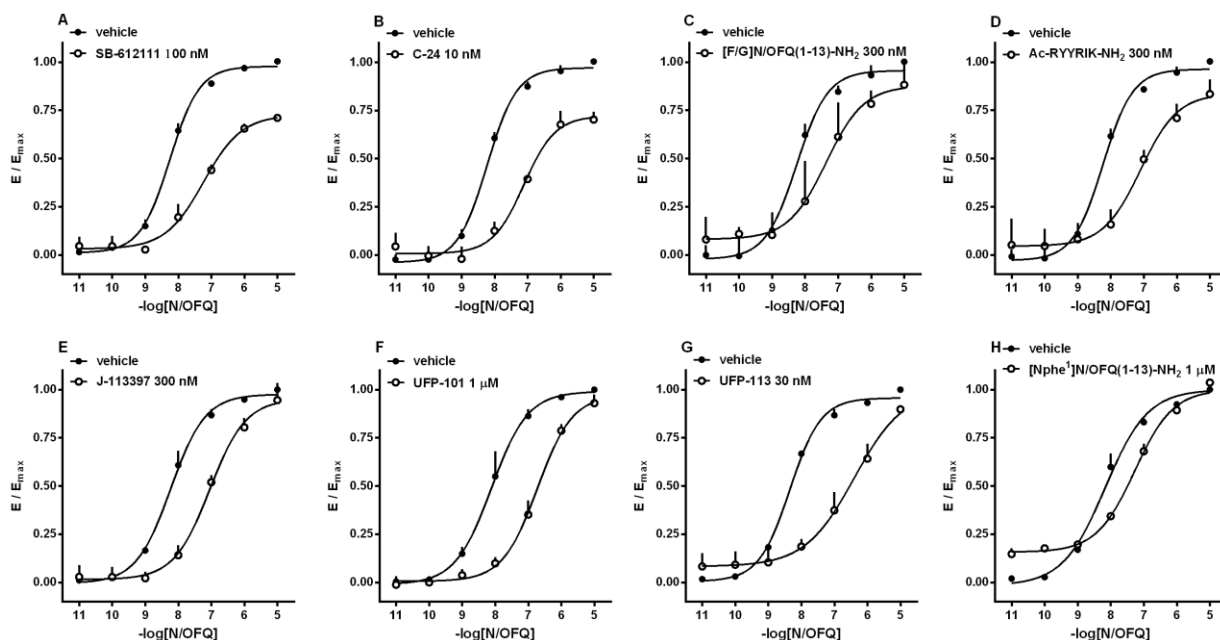
Figure 25. NOP receptor / β-arrestin 2 protein interaction experiments - concentration-response curves to N/OFQ in absence and in presence of SB-612111 (100 nM, panel A), C-24 (10 nM, panel B), [F/G]N/OFQ(1-13)-NH$_2$ (300 nM, panel C), Ac-RYYRIK-NH$_2$ (300 nM, panel D), J-113397 (300 nM, panel E), UFP-101 (1 μM, panel F), UFP-113 (30 nM, panel G), and [Nphe^1]N/OFQ(1-13)-NH$_2$ (1 μM, panel H). Data are mean ± sem of at least 3 separate experiments performed in duplicate.

Table 5. Potencies (pEC_{50}), concentration ratio (CR), and maximal effects (E_{max}) of the compounds tested on the interaction of NOP with G protein and β-arrestin 2.

	G protein			β-arrestin 2		
	pEC_{50} ($CL_{95\%}$)	CR	E_{max} ± sem	pEC_{50} ($CL_{95\%}$)	CR	E_{max} ± sem
N/OFQ	8.44 (8.33 - 8.56)	1	1	8.02 (7.81 - 8.23)	1	1
N/OFQ(1-13)-NH$_2$	8.46 (7.94 - 8.99)	0.95	1.00 ±0.03	8.02 (7.72 - 8.32)	1	1.00 ±0.08
[Arg^{14}Lys^{15}]N/OFQ	9.27 (9.21 - 9.33)	0.15	1.00 ±0.05	7.83 (7.63 - 8.03)	1.55	1.10 ±0.04
UFP-112	9.35 (9.10-9.60)	0.12	0.98 ±0.03	8.37 (8.18-8.57)	0.45	0.89 ±0.07
PWT2-N/OFQ	9.17 (8.97-9.48)	0.19	1.10 ±0.01	7.53 (7.30-7.77)	3.09	1.3 ±0.07
[F/G]N/OFQ(1-13)-NH$_2$	7.85 (7.75-7.96)	3.89	0.72* ±0.03	inactive		
UFP-113	9.35 (9.29 - 9.41)	0.12	0.45* ±0.04	inactive		
Ac-RYYRIK-NH$_2$	7.90 (7.45 - 8.34)	3.39	0.63* ±0.02	inactive		
[Nphe^1]N/OFQ(1-13)-NH$_2$	6.85 (6.70-6.99)	38.9	0.55* ±0.04	inactive		
UFP-101	7.01 (6.79 - 7.24)	26.9	0.14* ±0.04	inactive		
Ro 65-6570	7.77 (7.35 - 8.18)	4.68	0.96 ±0.05	6.37 (6.08-6.65)	44.67	0.84 ±0.06
SCH-221510	8.26 (7.06 - 9.46)	1.51	1.20±0.03	6.96 (6.43-7.48)	11.48	0.75 ±0.10
J-113397	inactive			inactive		
SB-612111	inactive			inactive		
C-24	inactive			inactive		
naloxone	inactive			inactive		

Inactive means the compound did not stimulate BRET ratios up to 10 μM. *p < 0.05 vs. N/OFQ, according to one way ANOVA followed by the Dunnett test for multiple comparison.

Table 6. Effects on NOP/G protein and NOP/β-arrestin 2 interactions of NOP ligands showing reduced efficacy.

	G protein			β-arrestin 2		
	pEC_{50}	E_{max}	pK_B	pEC_{50}	E_{max}	pK_B
N/OFQ	8.44	1.00	-	8.02	1.00	-
[F/G]N/OFQ(1-13)-NH$_2$	7.85	0.72*	-	inactive		7.52 (6.88-8.16)
UFP-113	9.35	0.45*	-	inactive		9.42 (8.44-10.40)
Ac-RYYRIK-NH$_2$	7.90	0.63*	-	inactive		7.11 (6.85-7.38)
[Nphe^1]N/OFQ(1-13)-NH$_2$	6.85	0.55*	-	inactive		7.00 (6.33-7.66)
UFP-101	7.01	0.14*	7.66 (7.23-8.10)	inactive		7.34 (6.73-7.94)
J-113397	inactive		7.95 (6.06-9.83)	inactive		7.27 (6.24-8.30)
SB-612111	inactive		8.96 (8.84-9.08)	inactive		7.91 (7.26-8.56)
C-24	inactive		9.11 (8.19-10.05)	inactive		9.09 (8.56-9.63)
Naloxone	inactive		Inactive	inactive		inactive

Inactive means that the compound was inactive up to 1 μM.

The pharmacological activity of ligands for promoting NOP receptor-G protein interaction was found to be in close agreement with the available data obtained in the [^{35}S]GTPγS binding assay. In fact the potency of N/OFQ in evoking stimulation of BRET ratio (pEC$_{50}$ 8.44) is very similar to that previously reported for the stimulation of [^{35}S]GTPγS binding (e.g. 8.95, (Fischetti *et al.*, 2009)). Moreover, compounds such as UFP-112, [Arg^{14}Lys^{15}]N/OFQ, PWT2-N/OFQ, and N/OFQ(1-13)-NH$_2$ behaved as full agonists in both assays and in both exhibited an identical rank order of potency: UFP-112 > [Arg^{14}Lys^{15}]N/OFQ > PWT2-N/OFQ > N/OFQ(1-13)-NH$_2$ = N/OFQ (Calo' & Guerrini, 2013; Rizzi *et al.*, 2014). Likewise, the results observed for number of synthetic peptides, known as NOP partial agonists, were also in best agreement with

pharmacological activities characterized in [^{35}S]GTPγS binding assays. The order of potency measured for these ligands (UFP-113 > Ac-RYYRIK-NH$_2$ > [F/G]N/OFQ(1-13)-NH$_2$ > [Nphe^1]N/OFQ(1-13)-NH$_2$) is in line with previously reported results (Calo' & Guerrini, 2013). The very high potency exhibited by UFP-113 in the BRET assay (pEC$_{50}$ 9.35) associated with a relative efficacy of 0.45, is also consistent with the similar profile reported in [^{35}S]GTPγS binding experiments (pEC$_{50}$ 9.73, E$_{max}$ 0.79, (Arduin *et al.*, 2007)). Non-peptide ligands such as Ro 65-6570 and SCH-221510 displayed similar maximal effects but a reduced potency (5 and 2 fold lower, respectively) compared to N/OFQ. The same results were observed previously using a [^{35}S]GTPγS binding assay (Varty *et al.*, 2008).

The correspondence between BRET and GTPγS activities is also evident on comparing the estimates of antagonist potencies (pK$_B$ values). For example, the BRET assay potency of SB-612111 estimated either using a classic Schild protocol (pA$_2$ 8.96) and from inhibition-response curves (pK$_B$ 9.13) was compatible with the previous estimate (9.70) obtained in [^{35}S]GTPγS binding studies (Spagnolo *et al.*, 2007).

In this study the pharmacological profile of the human NOP receptor was investigated using a BRET assay, which is based on the fusion of a RLuc donor to the receptor and a RGFP acceptor to the transduction protein. The same technology was employed to investigate the interaction of the NOP receptor with Gβ$_1$ subunits (which is mediated by endogenous Gα subunits of the membrane) and with β-arrestin 2 (which is recruited to the membrane upon receptor activation). Thus, receptor/G-protein interactions were studied in isolated membranes while receptor/arrestin interactions were determined in whole cells. The pharmacological profile for NOP receptor coupling to the two transduction proteins was evaluated using a large panel of peptide and non-peptide ligands, all of which are selective for the NOP receptor and enclose molecules that are known to display a broad range of receptor efficacy, from full agonism to inverse agonism. This allows an exhaustive and meaningful comparison of the molecular characterization of NOP receptor activity presented in this study with pharmacological results reported in a variety of previous investigations.

Control experiments indicate that the BRET signals reported here represent an accurate determination of the ligand-induced changes of NOP receptor coupling to the two fluorescently-

55

tagged transduction proteins, and that the comparison of such activities are not biased by large differences in receptor expression between the cell clones employed in this work. In fact, we found that within the range of concentrations used in this study ligands did not exert unspecific effects on the enzymatic activity of the Rluc used as BRET donor (Auld *et al.*, 2008). Moreover, the analysis of the intrinsic luminescence of the cell membranes, which quantifies the abundance of Rluc-tagged receptor, indicated that the NOP receptors were expressed at comparable levels in the two cell clones.

The NOP/Gβ_1 BRET signal measured in cell membrane preparations cannot be influenced by β-arrestin 2, since the amount of this transducer in the plasma membrane is negligible prior to ligand activation of the receptor. However, the NOP/Gβ_1 interaction may be mediated by a plurality of Gα subunits that can interact with the receptor. As shown here, PTX treatment abolished the BRET signal, indicating that the measured activity is primarily accounted for by the pertussis-sensitive family of Gα subunits (i.e., G$\alpha_{i/o}$). Thus the pharmacological parameters of NOP/G protein interaction reported here can be meaningfully compared with the results of pertussis toxin-dependent signalling studies of the NOP receptor (Cheng *et al.*, 1997; Margas *et al.*, 2008; McDonald *et al.*, 2003). In contrast, the NOP/β-arrestin 2 signal measured in whole cells was resistant to the toxin, indicating that the interaction with G protein does not interfere with the measurement or receptor-arrestin interactions. In conclusion, unlike the results of studies based on measurements of signalling activities occurring downstream of the transduction proteins, the receptor-transducer coupling activities reported in this study represent determinations that are largely unaffected by the mutual antagonism existing between arrestin and G protein for complex formation with the receptor. Thus, these results are independent estimates of the ability of NOP receptor to associate with each of the two proteins.

In the present study we found that GDP was not able to significantly inhibit the baseline of BRET ratio in membranes from cells expressing NOP-RLuc and Gβ_1-RGFP. This indicates that the level of spontaneous coupling between the NOP receptor and G proteins is negligible in isolated membranes, and stands in contrast with data reported earlier on delta/RLuc or mu/RLuc opioid receptors using the same type of BRET assay (Vezzi *et al.*, 2013). This result suggests that the NOP receptor has very low propensity to adopt a constitutively active conformation, particularly if compared to the delta receptor. Also in support of this suggestion is the observation that the ligand C-24, which was previously reported to behave as NOP inverse agonist (Mahmoud *et al.*,

2010), did not produce any significant inhibition of the basal BRET ratio. In agreement with such a conclusion, little evidence for NOP receptor constitutive activity has been described so far, at least under physiological conditions. Data suggesting NOP constitutive activity were only obtained by electrophysiological recording of neurons in which the over expression of the receptor was induced by microinjection of coding cDNA (Mahmoud *et al.*, 2010). In another study, in which the ability to constitutively activate G-protein-coupled pathways was investigated in a series of NOP receptor point mutations, only the N133W mutant displayed increased ligand-independent signalling (Kam *et al.*, 2002). Interestingly, this mutated residue (N3.35) was recently found to contribute to the network of interactions that establish a sodium binding pocket in the structure of several GPCRs (Katritch *et al.*, 2014), including the delta opioid receptor (Fenalti *et al.*, 2014). It was suggested that sodium binding may favor the inactive conformation of the receptor (Katritch *et al.*, 2014). Thus, additional comparative BRET experiments on the G protein interactions of delta and NOP receptors bearing cross-mutations in the residues that generate the sodium pocket will be necessary to evaluate if this structural domain is responsible for the large difference in constitutive activity observed between the two receptor subtypes.

In the first part of this study we appraised the pharmacological profile of the ligands in promoting NOP receptor interaction with the pertussis toxin-sensitive family of G-protein. As detailed in the Results section, the pharmacological parameters derived from this investigation are in best agreement with the results previously reported from the analysis of GTPγS binding data (Calo' & Guerrini, 2013; Fischetti *et al.*, 2009; Rizzi *et al.*, 2014). This finding is not surprising, as both assays are performed in isolated membranes and both measure the same early event of the signalling cascade, i.e., receptor-mediated G-protein activation. Yet, the good correlation that we found in this study is important, because it suggests that there is no dissociation between ligand-induced coupling to the G protein and ligand-promoted changes in the nucleotide-exchange properties of the G protein, within the studied ligands. In other words, we found no evidence for the existence of ligands that on promoting receptor-G protein coupling might produce a non proportional or even opposite effect on G protein activation. Moreover, this satisfactory agreement between NOP/G protein coupling and NOP stimulated GTPγS binding further demonstrate that the BRET assay used in the study provides a robust and precise assessment of the ligand ability to activate the NOP receptor.

On comparing the data with a wider range of pharmacological assays carried in vitro or in vivo, noticeable discrepancies are only apparent for a number of synthetic peptides that are known as NOP partial agonists. Such divergences are likely explained by the variations in stimulus/response coupling efficiency that characterize different pharmacological preparations. In fact, in accordance with classical receptor theory, the effect of a partial agonist can range from none to an almost full response, depending on the extent of amplification that the sensitivity of the signaling pathway exerts on the initial biological signal triggered by the receptor in complex with the transduction protein. For example, the peptide analog [F/G]N/OFQ(1-13)-NH$_2$ that shows a significant level of partial agonism (E$_{max}$ 0.72) in this study, was previously reported to behave as pure antagonist in a low-efficiency coupled preparation, such as the electrically stimulated mouse vas deferens (Guerrini *et al.*, 1998). The same ligand displayed varying level of efficacy in other studies in vitro or in vivo (Calo' & Guerrini, 2013); it was also specifically shown that the relative response of this agonist can be varied on manipulating the levels of NOP receptor expression, which is a typical feature of partial agonism (McDonald *et al.*, 2003). Analogous considerations apply to UFP-113, which shows weak and variable agonism in the mouse vas deferens (Arduin *et al.*, 2007), or to the hexapeptide Ac-RYYRIK-NH$_2$, for which conflicting and variable levels of efficacy were reported in the literature (Calo *et al.*, 2000a; Dooley *et al.*, 1997). Also consistent with this interpretation are the results obtained with the analog UFP-101. Although this peptide is known to behave as pure antagonist in a vast range of pharmacological tests (Calo' & Guerrini, 2013; Calo *et al.*, 2005), it displayed a faint but detectable level of residual efficacy (E$_{max}$ 0.14) in our assay. This is in line with the observation that a weak partial agonism in UFP-101 could only be revealed after receptor over-expression in neurons microinjected with plasmid coding for the NOP sequence (Mahmoud *et al.*, 2010).

In conclusion, we suggest that the rank order of relative effects that we measured for these partial agonists in the BRET assay (i.e. [F/G]N/OFQ(1-13)NH$_2$ > Ac-RYYRIK-NH$_2$ > [Nphe[1]]N/OFQ(1-13)-NH$_2$ > UFP-113 >> UFP-101, see table 2) provides a more accurate description of the level of efficacy endowed in these ligands.

Also the estimates of antagonist potency derived from BRET analysis were in substantial agreement with similar determinations made in a variety of different pharmacological studies. However, one interesting observation is that two of such antagonists, SB-612111 and C-24, displayed a pattern of agonist inhibition suggesting insurmountable behavior under some assay conditions (i.e. 5 min incubation with agonist); this is in contrast with a plurality of previous

studies, were the competitive nature of these compounds was demonstrated (Fischetti *et al.*, 2009; Spagnolo *et al.*, 2007; Zaratin *et al.*, 2004). We found, however, that a 3-fold increase in incubation time was sufficient to restore an essentially competitive pattern of antagonism in these compounds, while other antagonists with lower potency, such as UFP-101 or J-113397, did not show similar time-dependent changes. Thus, it is conceivable that the very slow dissociation rate of these ligands and the consequent effect on the agonist ability to reach a steady-state level of receptor occupancy are responsible for the phenomenon. Also in line with these findings is the intriguing observation that the antagonist action of UFP-101 in the isolated mouse vas deferens is immediately reversible on washing, while the effect of SB-612111 remains unchanged even after 3 hours of repeated washing (Spagnolo *et al.*, 2007).

In the second part of the study, we report the pharmacological profile of the same panel of ligands for the induction of NOP receptor interaction with β-arrestin 2. Although this is the first study in which a systematic assessment of the efficacy of NOP agonists for arrestin was made, previous results based on NOP receptor internalization show that agonists active in promoting internalization of the NOP receptor (Corbani *et al.*, 2004; Spampinato *et al.*, 2007) are among those that in this study display a robust effect on arrestin coupling. This supports the notion that NOP receptor internalization requires a clathrin-dependent rapid endocytosis mechanism that is mediated by arrestins (Zhang *et al.*, 1996).

The most prominent finding in our data is that the agonists showing relative E_{max} values ≤ 0.7 in G protein coupling produced negligible or no effects on arrestin recruiting. In fact, we also found that these inactive ligands behaved as virtually pure competitive antagonists in inhibiting the effect of the endogenous agonist N/OFQ on arrestin interaction. These results remind similar observations reported for delta and mu receptor interaction with arrestin, where the relationships between G protein and arrestin couplings for both receptors were strongly hyperbolic (Molinari *et al.*, 2010). Perhaps this hyperbolic relation may be stronger in the NOP receptor, judging from the greater threshold of partial G protein agonism that is necessary in order to observe a measurable effect on arrestin interaction. In addition, our results indicate that the potencies of agonists for NOP/arrestin interaction were systematically lower that those measured for NOP/G protein interaction, by factors ranging between 0.4 – 1.6 log units.

As far as pure antagonists are concerned, these compounds were similarly active at NOP/G protein and NOP/arrestin interaction and displayed an identical rank order of potency i.e. C-24 >

SB-612111 > J-113397 $\geq$ UFP-101, with potency values that were only slightly lower at NOP/β-arrestin 2 than NOP/G-protein.

Altogether the comparison of the pharmacological profile of NOP receptor interacting with G-protein or with β-arrestin 2 suggests minor differences for receptor antagonists, loss of efficacy for partial agonists and decrease of potency for synthetic full agonists. Collectively, these findings indicate that the activation induced by most NOP agonists is significantly biased towards promoting receptor-G protein interaction rather than receptor-arrestin interaction. Thus, the question is whether this preference is caused by system bias or reflects a true difference in agonist efficacy for driving the NOP receptor to interact with the two transduction proteins.

Two common sources of system bias are the difference in the efficiency of the signalling pathway that couples the activation of each transducer to the measured biological signals, or the difference in the sensitivity of the assay methods employed to evaluate divergent transduction pathways. Yet, neither kind of system bias is likely to affect the results presented in this study. In fact, the BRET signals reported here quantify the extent of protein-protein interaction between receptor and transducer; this is not influenced, unlike biological responses, by the differences in efficiency of the signalling pathways. Furthermore, the methodology adopted in this study is based on exactly the same pair of donor/acceptor reporters that were used to both assess G protein and arrestin interactions. Thus, it is unlikely that major differences in the efficiency of the resonance energy transfer system may alter the sensitivity of the two determinations.

However, there is a third source of system bias that may play a fundamental role in our results: i.e., the difference in binding affinity for the interaction of the two transduction proteins with the empty receptor. On comparing G protein vs. arrestin interactions, this difference is particularly difficult to evaluate, because under the generic term "affinity" one must factor additional biochemical events that regulate the ability of arrestin to associate to the receptor, such as GRK-mediated phosphorylation and the intracellular process of translocation that brings arrestin to the receptor in the plasma membrane. Thus, it is possible that a globally lower susceptibility of the NOP receptor to be docked by arrestin than by G protein might generate the systematic reduction in agonist effects observed here, despite a conserved efficacy of the ligands in promoting the two interactions.

A qualitative criterion that helps to distinguish between ligand and system bias is the rank of ligand effects at the two transduction systems; in fact, system bias, regardless of the source, cannot alter this ordering. An inversion in the rank order of potency was noted for some agonists.

For example, $[Arg^{14}Lys^{15}]$N/OFQ and PWT2-N/OFQ were more potent than the natural agonist in promoting G protein interaction, but less potent than N/OFQ in inducing arrestin interaction. In contrast, UFP-112 and the non peptide agonists (SCH-221510 and Ro-656570) maintained the same rank of potency at the two transduction proteins.

To obtain a quantitative estimate of biased efficacy, approximate values for the difference in intrinsic efficacies of the agonists for the two transduction proteins (i.e. $\varepsilon_{Gprotein}/\varepsilon_{arrestin}$) were computed as bias factors. Agonists such as Ro-656570 and PWT2-N/OFQ, displayed a 10-fold greater efficacy for G protein interaction. Smaller differences were observed in other agonists, such as UFP-112 and SCH-221510, whereas no biased efficacy was found in N/OFQ(1-13)-NH$_2$ (Table 7). Although the large propagated error in this calculation prevents an accurate assessment of the significance of the computed differences, the data suggest that several synthetic agonists, including perhaps those that behave as pure antagonists of receptor-arrestin interaction, may display significant losses of intrinsic efficacy at this transduction protein. This trend might result from the fact that these synthetic NOP analogs were designed and selected on the basis of SAR studies derived from G-protein-dependent signalling assays. Thus, it is possible that SAR studies focused on receptor/β-arrestin interaction will allow the discovery of arrestin biased agonist for the NOP receptor in the future.

Table 7. Bias factors obtained from at least 5 independent E_{max}/EC_{50} values from both NOP/G-protein and NOP/arrestin experiments.

	bias factor ± sem
N/OFQ	0.00
N/OFQ(1-13)-NH$_2$	0.00 ± 0.40
$[Arg^{14},Lys^{15}]$N/OFQ	0.25 ± 0.46
UFP-112	0.71 ± 0.37
SCH 221510	0.77 ± 0.75
Ro-65 6570	1.07 ± 0.38
PWT2-N/OFQ	1.09 ± 0.28

Ligand bias has important implications in drug development. In principle, using biased agonists that selectively activate a single transduction pathway it might be possible to maximize therapeutically useful responses and minimize side effects. Some examples of this innovative strategy were already described in literature. G-protein biased agonists acting at the mu opioid receptor are under development as analgesics with higher tolerability (DeWire *et al.*, 2013) while G-protein biased agonists at GPR109 may reduce serum fatty acids without inducing cutaneous flushing (Walters *et al.*, 2009). Similarly, β-arrestin biased agonists acting at the AT1 receptor may be effective drugs for the treatment of heart failure (Violin *et al.*, 2010), while biased β-arrestin PTH receptor ligands are potential innovative drugs for promoting bone formation (Ferrari *et al.*, 2005).

N/OFQ via selective NOP receptor activation can control several biological functions, however the relative role of G-protein and arrestin in mediating these actions is presently unknown. Further studies are needed to identify new lead molecules that will help to understand the structural requirements underlying the difference in efficacy of NOP agonists for G-proteins and arrestins, and the potential therapeutic indications of G-protein or arrestin biased NOP agonists. N/OFQ can produce robust antinociceptive effects following spinal administration both in rodents and non human primates (Schroder *et al.*, 2014). Thus, it is important to clarify whether the extent of G-protein bias, which is present in some NOP agonists as shown in this study, may be a crucial determinant for the antinociceptive response; this may lead to the discovery of innovative spinal analgesics. Interestingly, compounds such as UFP-112 and PWT2-N/OFQ demonstrated robust and extremely long acting antinociceptive properties after spinal administration in rodents and monkeys (Hu *et al.*, 2010; Rizzi *et al.*, 2014; Rizzi *et al.*, 2007). It has been suggested that the long lasting action of these compounds may reflect reduced susceptibility to peptidase action (Rizzi *et al.*, 2014; Rizzi *et al.*, 2007). However, according to the present data, we may speculate that the G protein bias nature of these compounds could contribute to their persistent antinociceptive effect. Further studies and the use of mice knockout for the β-arrestin 2 gene are needed to validate this hypothesis.

3.2. Ligands for classical opioid receptors

3.2.1. Pharmacological characterization of N-substituted derivatives of morphine and oxymorphone.

Morphine and structurally related derivatives are highly effective analgesics, and the mainstay in the medical management of moderate to severe pain. Pharmacological actions of opioid analgesics are primarily mediated through agonism at the MOP receptor. Position 17 in morphine has been one of the most manipulated sites on the scaffold and intensive research has focused on replacements of the 17-methyl group with other substituents. Structural variations at the N-17 of the morphinan skeleton led to a diversity of molecules appraised as valuable and potential therapeutics and important research probes. Discovery of therapeutically useful morphine-like drugs has also targeted the C-6 hydroxyl group, with oxymorphone as one of the clinically relevant opioid analgesics, where a carbonyl substitutes an hydroxyl group at position 6 (Figure 26).
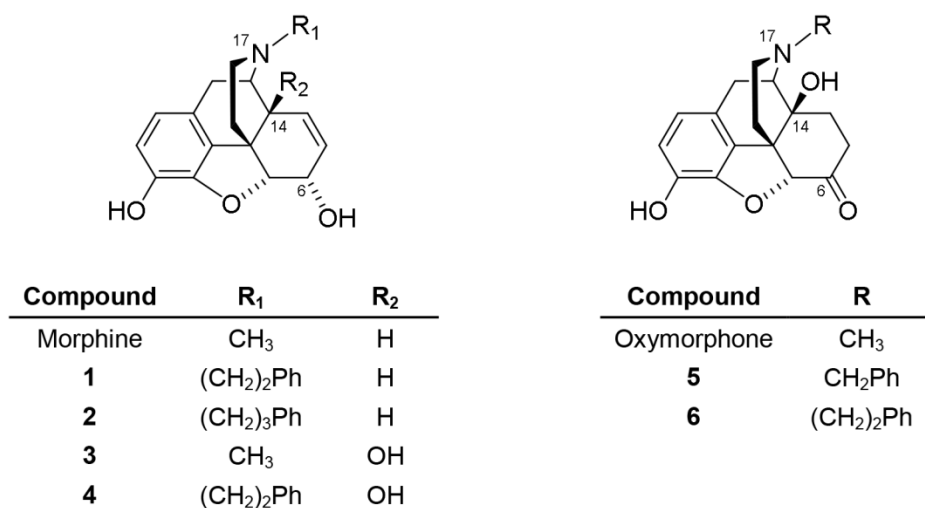

Compound	R₁	R₂
Morphine	CH_3	H
1	$(CH_2)_2Ph$	H
2	$(CH_2)_3Ph$	H
3	CH_3	OH
4	$(CH_2)_2Ph$	OH

Compound	R
Oxymorphone	CH_3
5	CH_2Ph
6	$(CH_2)_2Ph$

Figure 26. Structures of morphine, oxymorphone and N-substituted morphinans (compounds 1-6).

In the present study, we tested derivatives 1, 4 and 6 in the calcium mobilization assay. In CHO cells expressing the human MOP receptor and the $G_{\alpha qi5}$ chimeric protein, all compounds produced a concentration-dependent stimulation of calcium mobilization (Figure 27). DAMGO

was able to concentration dependently stimulate the calcium mobilization with high potency (EC$_{50}$ 42.7 nM) and maximal effects (217±21% over the basal value), all other effects are then expressed as intrinsic activities α, fraction of the DAMGO maximal effects. Morphine and oxymorphone were also tested for their ability to stimulate calcium mobilization displaying EC$_{50}$ values of 140 and 44.3 nM, respectively, with maximal effects being significantly lower than DAMGO (α 0.55 and 0.52, respectively). N-phenethylnoroxymorphone (6) was about 2-fold more potent than DAMGO. Among the two morphine derivatives, N-phenethylnormorphine (1) was about 3-fold more potent than morphine and equipotent to DAMGO, and about 3-fold more active than its 14-hydroxy analogue 4 in terms of potency at the MOP receptor. Among the two morphine derivatives, N-phenethylnormorphine (1) was about 3-fold more potent than morphine and equipotent to DAMGO, and about 3-fold more active than its 14-hydroxy analogue 4 in this assay (Table 8). As far as maximal effect is concerned, compounds 1, 4, and 6 displayed lower maximal effects to that of DAMGO (α 0.70, 0.70, and 0.78, respectively). The same compounds were tested in CHO cells expressing the human DOP receptor and the Gα$_{qG66Di5}$ chimeric protein, and in cells expressing the human KOP receptor and the Gα$_{qi5}$ chimeric protein, compound 4 was inactive at both DOP and KOP receptors, compounds 1 and 6 both displayed a weak stimulation of calcium mobilization in CHO$_{DOP}$ cells only in the high micromolar range of concentrations, while being completely inactive at the KOP receptor (Figure 27).
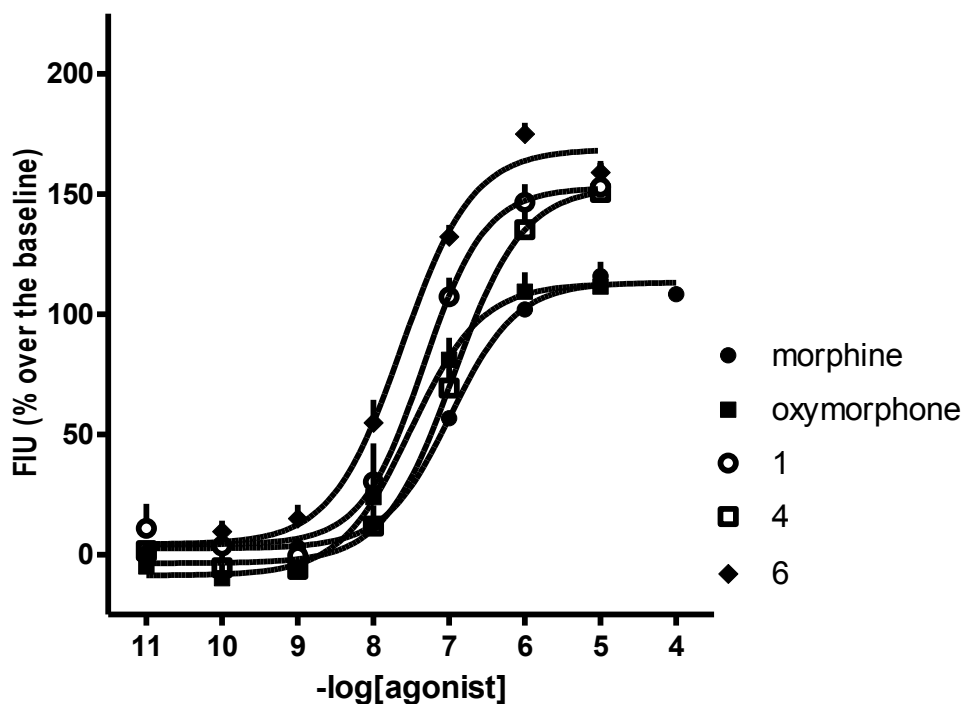
Figure 27. Concentration response experiments to morphine, oxymorphone, derivatives 1, 4, and 6, in calcium mobilization experiments performed in CHO$_{MOP}$ stably expressing the chimeric Gα_{qi5} chimeric protein. Agonists effects were expressed as FIU % over the basal value. Data are the mean ± sem of at least 3 separate experiments performed in duplicate.

Table 8. Potency and efficacy values at MOP, DOP, and KOP receptors in calcium mobilization assay.

	MOP		DOP		KOP	
	EC$_{50}$ (nM)	α	EC$_{50}$ (nM)	α	EC$_{50}$ (nM)	α
Morphine	140±31	0.55±0.03	inactive		2185±451	0.51±0.02
Oxymorphone	44.3±9.7	0.52±0.05	inactive		inactive	
1	48.8±14.0	0.70±0.04	crc incomplete		inactive	
4	124±20	0.70±0.07	inactive		inactive	
6	23.4±4.7	0.78±0.02	crc incomplete		Inactive	

Data are mean ± sem of at least 3 separate experiments performed in duplicate. Inactive: the compound was inactive up to 10 µM. Crc incomplete: concentration response curve does not reach the maximal effect up to 10 µM. α is expressed as a fraction of the maximal stimulation produced by DAMGO (MOP), DPDPE (DOP) or U69,593 (KOP).

The rank order of potency (6 > 1 > 4) and the high selectivity for the MOP receptor found, are in line with data obtained in the stimulation of [^{35}S]GTPγS binding assay (Table 9). Potency and efficacy values obtained in calcium mobilization assay and in the stimulation of [^{35}S]GTPγS binding, and receptor binding affinities at the MOP receptor (Table 10), together with previous in vivo data from the literature for compounds 1 (Winter *et al.*, 1957) and 6 (Loew & Berkowitz, 1978) were used for establishing an appropriate dose range for in vivo investigations.

Table 9. Potency and efficacy values at MOP, DOP, and KOP receptors in the stimulation of stimulation of [^{35}S]GTPγS binding assay, performed in membranes from CHO cells stably expressing the human MOP, DOP, or KOP receptors.

	MOP		DOP		KOP	
	EC_{50} (nM)	α	EC_{50} (nM)	α	EC_{50} (nM)	α
Morphine	34.4±5.1	0.89±0.17	668±65	1.09±0.14	710±23	0.76±0.02
Oxymorphone	4.38±0.76	0.98±0.11	259±33	0.87±0.40	463±116	0.48±0.11
1	10.3±0.9	1.13±0.08	712±86	1.38±0.17	1049±29	0.19±0.02
4	46.3±7.1	1.19±0.03	1247±356	1.25±0.15	nd	
6	2.63±1.06	0.97±0.03	131±60	1.01±0.09	225±74	0.08±0.01

Data are mean ± sem of at least 3 separate experiments performed in duplicate. ND, not determined due to very low binding affinity at the KOP receptor. α is expressed as a fraction of the maximal stimulation produced by DAMGO (MOP), DPDPE (DOP) or U69,593 (KOP).

Table 10. Receptor binding assays were performed with membranes from rat brain (MOP and DOP receptors) and guinea pig brain (KOP receptors).

	MOP	DOP	KOP
	K_i (nM)	K_i (nM)	K_i (nM)
Morphine	6.55±0.74	217±19	113±9
Oxymorphone	0.97±0.05	80.5±5.5	61.6±1.2
1	0.93±0.14	37.0±5.5	107±18
2	79.5±1.1	869±171	565±24
3	16.4±1.1	1081±271	789±77
4	4.60±0.01	163±17	513±66
5	359±31	1078±35	75.0±8.0
6	0.54±0.03	12.8±0.2	84.2±7.2

Data are mean ± sem of at least 6 separate experiments.

Antinociceptive properties of morphine derivatives 1 and 4, and oxymorphone analogue 6 were assessed in mice after subcutaneous (s.c.) administration using two nociceptive tests, hot-plate and tail-flick tests (Spetea *et al.*, 2010). All three MOP agonists produced time- and dose-dependent effects in both nociceptive assays with compounds 1 and 6 being the most effective against acute thermal nociception. The antinociceptive peak occurred generally 30 min after drug s.c. administration. Antinociceptive potencies expressed as ED_{50} values with 95% confidence limits are summarized in Table 9, and were compared with those of the reference opioids drugs, morphine and oxymorphone. In agreement with pivotal works in this field (Winter *et al.*, 1957), the morphine derivative 1 elicits a stronger antinociceptive effect than morphine. In the hot-plate and tail-flick tests, it was 22- and 28-fold, respectively, more effective than morphine. First data on the antinociceptive effect of N-phenethyl-14-hydroxynormorphine (4) revealed that this MOP agonist is a potent antinociceptive agent with a 2- to 3-fold increased potency than morphine. Compound 6, the N-phenethyl analogue of oxymorphone, was found to be highly active with about 2-fold higher potency than oxymorphone, and comparable potency to 1. It was 8-fold more potent than its 6-hydroxy counterpart 4 in inducing an antinociceptive response, indicating that a 6-keto substitution leads to improved analgesic properties. Besides analgesia, MOP agonists are well-known to induce other behavioral changes. In general, no major alterations in locomotor activity and no sedative effects were observed at any of the tested doses of compounds 1, 4 and 6, representing about 3- to 4-fold the analgesic ED_{50} dose, further investigations will be needed to establish the therapeutic index of these compounds (Ben Haddou *et al.*, 2014a).

In conclusion, position 17 in morphine has been one of the most manipulated sites on the scaffold and intensive research has focused on replacements of the 17-methyl group with other substituents. Structural variations at the N-17 of the morphinan skeleton have resulted in a diversity of compounds appraised as valuable and therapeutic agents and important research tools (Furst & Hosztafi, 2008; Pasternak & Pan, 2013; Spetea *et al.*, 2013; Spetea & Schmidhammer, 2012). Furthermore, discovery of therapeutically useful morphine-like drugs has also targeted the C-6 hydroxyl group, with oxymorphone as one example of the clinically relevant opioid analgesics, where a carbonyl instead of a hydroxyl group is present at position 6 (Furst & Hosztafi, 2008; Schmidhammer *et al.*, 2013). Taken together, in the present study we highlight on the significant outcomes of N-substituent variation in morphine and oxymorphone on in vitro and in vivo biological properties and the emerging SAR. The presented data clearly reflect that a

Nphenethyl moiety in position 17 is highly favorable regarding enhanced affinity and selectivity at the MOP receptor, potent agonism and antinociceptive action. The increased lipophilicity of the N-phenethyl derivatives compared to the parent compounds may also contribute to the increased potency. Besides, it was also demonstrated that a carbonyl group at position 6 is preferable to a hydroxyl function in the N-phenethyl substituted molecules, augmenting MOP receptor affinity and agonist potency in vitro and in vivo. Though morphine derivatives, N-phenethylnormorphine (1) and N-phenethyl-14-hydroxynormorphine (4), and the oxymorphone analogue N-phenethylnoroxymorphone (6) have been developed many years ago, this is the first report on their opioid receptor binding and signaling, and antinociceptive efficacy. This report clarifies the activity of these molecules at the opioid receptors for the first time, serving as a systematic study of understanding their mode of action and the link between agonist-induced G protein signaling events leading to the high analgesic efficacy. Moreover, these results reveal that targeting position 17 is a viable approach toward improving the pharmacological properties, and may be instrumental to the development of new opioids for therapeutic use in the clinic. Considering the interesting functional profile of these MOP agonists and their high efficacy as antinociceptive agents, it is of interest to investigate other intracellular signaling pathways (i.e. interactions with regulatory proteins such as β-arrestins) and their side-effect profile in future studies.

3.2.2. Exploring pharmacological activities of morphinans substituted in position 6 as potent MOP agonists

A series of structurally related derivatives of morphine, substituted in position 6 with acrylonitrile and amid functions (Figure 28) were characterized for their pharmacological activities.
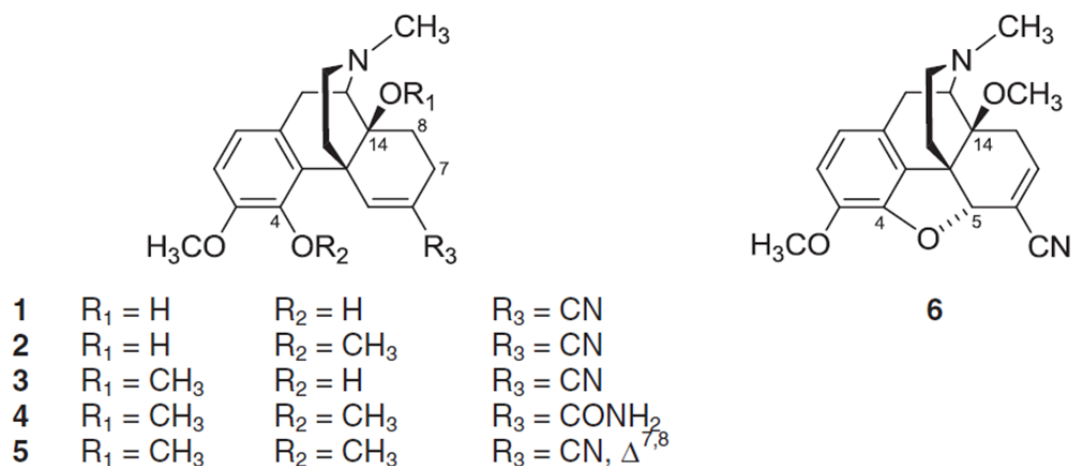

1	$R_1 = H$	$R_2 = H$	$R_3 = CN$
2	$R_1 = H$	$R_2 = CH_3$	$R_3 = CN$
3	$R_1 = CH_3$	$R_2 = H$	$R_3 = CN$
4	$R_1 = CH_3$	$R_2 = CH_3$	$R_3 = CONH_2$
5	$R_1 = CH_3$	$R_2 = CH_3$	$R_3 = CN, \Delta^{7,8}$

Figure 28. Structures of N-methylmorphinans (compounds 1-6).

Compounds 1-6 were tested in CHO cells stably expressing the human MOP receptor and the $G\alpha_{qi5}$ chimeric protein. All compounds evoked a concentration-dependent stimulation of calcium mobilization (Figure 29). Compound 5 was the most potent with an EC_{50} value of 21.7 nM, being 2-fold more potent than DAMGO, with lower maximal effects than the standard MOP agonist (intrinsic activity α 0.70, fraction of DAMGO maximal stimulation). Analogue 4 also showed high potency and maximal effect lower than that of DAMGO (EC_{50} 56.1 nM, α 0.59). The other 6-cyano substituted derivatives 1, 2, 3 and 6 exhibited up to 10 times higher potency than oxycodone and 14-OMC. In terms of efficacy, compounds 1–6 and 14-OMC showed intermediate maximal effects between oxycodone (α 0.38) and DAMGO (Table 11). Compounds 1–6, oxycodone and 14-OMC were also functionally evaluated in the stimulation of $[^{35}S]GTP\gamma S$ binding assay, their effects are reported as percentage of DAMGO maximal effects (Table 11). Compounds 1-6 concentration dependently stimulated the binding of $[^{35}S]GTP\gamma S$, showing that the 6-cyano substituted 2, 3, 5 and 6, and their amido analogue 4 were approximately 10-fold more potent than oxycodone and 14- OMC, while the 4,14-dihydroxy-6-cyanomorphinan 1 displayed similar potency. Similarly to calcium mobilization, derivative 5 was the most potent

agonist with an EC_{50} value of 1.64 nM. This 6-cyanomorphinan derivative was also 12-fold more potent than DAMGO (EC_{50} 20.2 nM), while the analogues 1‑4 showed similar or lower potencies. The 6-amido substituted 4 was 16 fold more potent than its 6-cyano analogue 5, but similar potency to the other two 6-cyanomorphinans 2, 3 and 6. The 4-methoxy analogue 2 had an about 6 times greater potency than its 4-hydroxy counterpart 1. A further increase in potency resulted upon methylation of the hydroxyl group in position 14, leading to compound 3 with about 10 fold lower EC_{50} value than its analogue 1.
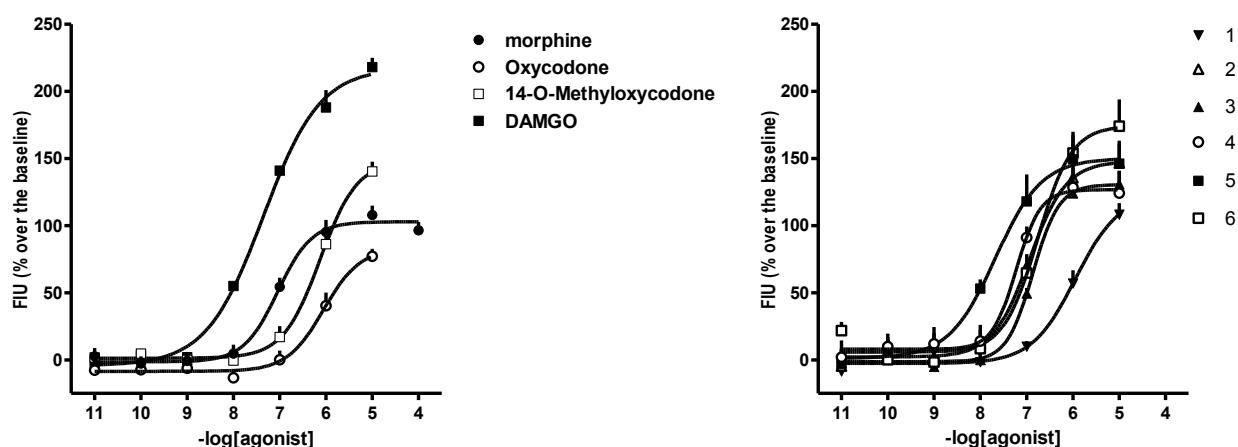
Figure 29. Concentration response experiments to morphine, DAMGO, oxycodone, and 14-OMC (left panel), and derivatives 1-6 (right panel), in calcium mobilization experiments performed in CHO_{MOP} stably expressing the chimeric $G\alpha_{qi5}$ chimeric protein. Agonists effects were expressed as FIU% over the basal value. Data are the mean ± sem of at least 3 separate experiments performed in duplicate.

Table 11. Potency and efficacy values in the stimulation of $[^{35}S]GTP\gamma S$ binding assay, in membranes from CHO cells expressing the human MOP receptor, and in calcium mobilization assay in CHO cells expressing both the human MOP receptor and the chimeric G protein.

	$[^{35}S]GTP\gamma S$ binding		Calcium mobilization	
	EC_{50} (nM)	α	EC_{50} (nM)	α
Oxycodone	500±128	0.92±0.09	1176±347	0.38±0.03
14-OMC	325±94	1.37±0.55	973±204	0.72±0.07
1	273±24	0.98±0.04	957±233	0.57±0.04
2	42.5±14.9	0.97±0.15	116±9	0.69±0.07
3	26.2±1.7	0.85±0.03	140±21	0.61±0.06
4	25.6±9.5	1.07±0.26	56.1±11.3	0.59±0.08
5	1.64±0.19	1.33±0.07	21.7±5.5	0.70±0.08
6	25.1±3.6	1.21±0.27	173±21	0.84±0.10
DAMGO	20.2±5.6	1.00	42.7±7.6	1.00

Data are mean ± sem of at least 3 separate experiments performed in duplicate.

Binding affinities at MOP, DOP and KOP receptors of the new 6-acrylonitrile incorporated N-methylmorphinans (5 and 6) and the corresponding amido derivative 4 were determined by radioligand binding assays in rat brain membranes. Data were reported as inhibition constant (K_i) values and summarized in Table 11. All three new derivatives 4-6 displayed a marked increase in MOP receptor affinity than the parental oxycodone. Compounds 4-6 showed high affinity for the MOP receptor, with derivative 5 showing a very high affinity (K_i 0.54 nM) and selectivity for the MOP receptor in rat brain membranes. Compound 4-6 showed 10/100 fold lower affinities at DOP and KOP receptors. The 6-amido substituted derivative 4 also showed high MOP receptor affinity in the low nanomolar range (K_i value of 1.61 nM), but reduced MOP selectivity. The presence of a 6-cyano group in 5 appears to be favorable for both affinity and selectivity for the MOP receptor, while a 6-amido substitution (4) leads to 3 to 9 fold lower MOP receptor affinity, and up to 5 and 7 fold reduced MOP receptor selectivity vs DOP and KOP receptors, respectively. In addition, the high affinity at the MOP receptor displayed by the 6-cyanomorphinan 5 in the rat brain was also demonstrated at the recombinant rat MOP receptor expressed in C6 glioma cells (C6rMOP, K_i = 0.70 nM). In line with findings in the rat brain, low binding affinities were determined for this compound in C6 cells transfected with rat DOP

receptors (K_i = 56 nM) and Chinese hamster ovary (CHO) expressing human KOP receptors (K_i = 229 nM), thus extending the outcomes on the high MOP selectivity of 5 (80 fold vs DOP and 327 times vs KOP). Comparison of the new 6-acrylonitrile 4,5-oxygen bridged 6 to the earlier developed non-bridged analogue 3 depicted no major changes in the MOP affinity and selectivity. It was also noted that methylation of the 4-hydroxy group in compounds 2, 4 and 5 gives rise to an improved interaction with the MOP receptor. The comparison between 14-methoxy and 6-cyano substituted 6 to its 6-keto counterpart 14-O-methyloxycodone (14-OMC), it was observed that the presence of a 6-acrylonitrile moiety increases binding to the MOP receptor by about 5 times (Table 12). Also, a similar increase was observed in the case of the other two new 14-methoxy substituted derivatives 4 and 5. The presence of a hydroxyl group in both 4 and 14 positions (compound 1) appears to largely affect binding at the MOP receptor. Compared to 6- cyano-N-methylmorphinans 1–3 described earlier (Spetea *et al.*, 2005), the new analogues 4 and 5 had one order of magnitude lower Ki values at the DOP receptor, with the 6-cyano derivative 6 showing comparable and reduced affinity. Also, like the 6-cyanomorphinans 1–3, compounds 4– 6 retained the decreased binding at the KOP receptor (Table 12).

Table 12. Receptor binding assays performed in membranes from rat brain.

	MOP K_i (nM)	DOP K_i (nM)	KOP K_i (nM)
Oxycodone	43.6±1.5	1087±246	2658±367
14-OMC	35.3±2.1	116±15	454±6
1	31.7±2.1	498±79	1648±201
2	2.44±0.13	107±5	364±7
3	5.38±0.42	197±29	378±155
4	1.61±0.05	28.8±2.3	105±45
5	0.54±0.04	30.3±2.9	200±40
6	7.39±0.34	239±40	194±68

Data are mean ± sem of at least 3 separate experiments performed in duplicate.

The new derivatives 4–6 were evaluated in vivo for their antinociceptive effects in mice after subcutaneous (s.c.) administration using three well-established and commonly used tests, hot-plate, tail-flick and PPQ abdominal stretching (Schutz *et al.*, 2003). Both hot-plate and tail-flick assays are valuable models for acute thermal nociception. Activity in the hot-plate test suggests that a drug acts at the supraspinal level, whereas the tail-flick may reflect spinal activity (Le Bars *et al.*, 2001). The PPQ assay evaluates chemical sensitivity, and is established as a model for visceral pain (Le Bars *et al.*, 2001). Antinociceptive potencies expressed as ED_{50} values are listed in Table 13 from (Ben Haddou *et al.*, 2014b), and were compared with those of the previously reported N-methyl-6-cyanomorphinans 1–3 (Spetea *et al.*, 2005), oxycodone and 14-OMC. As shown in Table 13, compounds 4–6 produced potent antinociceptive effects in all three in vivo assays. The 6-cyano substituted 5 and 6 exhibited markedly higher antinociceptive potencies than the 6-amido analogue 4, and were up to 165 times more active than oxycodone. The 6-acrylonitrile 4,5-oxygen bridged 6 showed comparable potency to its analogue 5 in the hot-plate and PPQ tests, and it was 3 times less potent in the tail-flick test. Compared to the earlier described derivatives 1–3 (Spetea *et al.*, 2005), the new 6-cyanomorphinans 5 and 6 were overall more potent as antinociceptive agents in mice after s.c. administration being highly effective against thermal and chemical nociception. The 6-amido derivative 4 was as potent as compound 1 in the tailflick and PPQ assays, while it was about 3 times less active in the hot-plate test (Table 3). Antinociceptive potencies of compound 4 were also found to be comparable to those of 14-OMC and oxycodone. The 14- methoxy-6-cyanomorphinan 6 was 11, 7, and 72 times more potent than its 6-keto counterpart 14-OMC in inducing an antinociceptive response in the hot-plate, tailflick, and PPQ assays, respectively. In addition to antinociception, MOP agonists are well-recognized to elicit other behavioral changes in rodents. In the current study, there were no sedative effects observed at any of the tested doses. Some increase in locomotor activity was noticed in mice, however, this only occurred at doses in the upper end of the dose–response curve, i.e. 90% of analgesia. Further investigations will be needed to establish the side effect profile of these opioids.

Table 13. Antinociceptive activities in the hot-plate (HP), tail-flick (TF), and PPQ abdominal stretching test.

	ED$_{50}$ (mg/kg, s.c.) (CL$_{95\%}$)		
	HP	TF	PPQ
Oxycodone[a]	1.37 (0.48-3.92)	0.94 (0.40-2.30)	0.38 (0.19-0.75)
14-OMC	1.02 (0.52-2.01)	0.80 (0.32-2.04)	0.22 (0.12-0.41)
1[a]	0.50 (0.12-2.02)	1.88 (1.25-2.83)	0.18 (0.076-0.42)
2[a]	0.15 (0.054-0.41)	0.12 (0.061-0.23)	0.026 (0.012-0.055)
3[a]	0.25 (0.11-0.59)	0.21 (0.11-0.40)	0.11 (0.072-0.16)
4	1.30 (0.56-3.03)	1.34 (0.53-3.03)	0.18 (0.08-0.43)
5	0.080 (0.011-0.61)	0.040 (0.020-0.090)	0.0023 (0.0009-0.0060)
6	0.089 (0.037-0.21)	0.12 (0.070-0.20)	0.003 (0.0007-0.012)

Antinociceptive potencies in mice after s.c. administration shown as ED50 values with 95% confidence limits (95% CL) (n = 6–10 mice per group). [a]Data from (Ben Haddou *et al.*, 2014b)

Though natural opioid alkaloids such as morphine and codeine (Figure 1) contain a 6-hydroxyl group, synthetic approaches have uncovered that functionalizing position 6 gives rise to a wide range of diverse activities (Schmidhammer *et al.*, 2013). Thus, position 6 of the morphinan skeleton has been a major target for successful drug developments over the years, leading to various opioid agonists and antagonists that are of importance both for clinical use and research. Oxycodone and oxymorphone, clinically used as opioid analgesics, are two representative examples of structural variation at C-6, where a carbonyl instead of a hydroxyl group is present in position 6. By targeting the chemically highly versatile 6-keto function of morphinan- 6-ones as in oxycodone, we have previously reported on a chemically innovative modification giving rise to a novel class of morphinans with acrylonitrile incorporated substructures (Greiner *et al.*, 2001; Spetea *et al.*, 2005). The resulted acrylonitrile incorporated 4,5-oxygen bridge-opened N-methylmorphinans (1–3, Figure 1) emerged as high affinity and potent MOP antinociceptive agents, with a pharmacological profile comparable to that of their 6-keto counterparts (Spetea *et al.*, 2005). The interesting approach to incorporate acrylonitrile substructures into morphinans was further explored by our group and resulted in new derivatives (Schutz *et al.*, 2005).

In the present study, combining in vitro ligand binding and functional assays and in vivo behavioral approaches, we show that the presence of a cyano group in position 6 in N-methylmorphinans has a strong influence on opioid receptor binding and post-receptor molecular

events. In line with our previous findings, having a 6-cyano group in N-methylmorphinans (5 and 6) results in increased MOP receptor activity compared to the lead molecule oxycodone both in vitro and in vivo. In the series of 6-cyanomorphinans, the new derivative 5 was consistently identified to exhibit the highest affinity and selectivity at the MOP receptor and to be the most potent MOP agonist. The design of compound 5 having a 4,14-dimethoxy substitution was attained based on our earlier observations, when a 4-methoxy group and/or a 14-methoxy group, like in compounds 2 and 3, is more favorable for binding and selectivity for the MOP receptor and antinociceptive activity than the corresponding hydroxy counterpart 1 (Spetea *et al.*, 2005). Herein, we also establish that the presence of a methoxy group in both positions, 4 and 14, has a major impact not only on binding affinities to all three opioid receptor types, and MOP receptor selectivity, but also on agonist potencies and efficacies at this receptor. We have also examined how the combination of a C-6 cyano functionality together with a closed 4,5-oxygen bridge (compound 6) will affect in vitro and in vivo opioid activities. The two 6-cyanomorphinans 3 and 6 show high and similar affinities at the MOP receptor, and low binding to DOP and KOP receptors. In both functional studies, [^{35}S]GTPγS binding and intracellular calcium mobilization, compounds 3 and 6 acted as potent MOP agonists with comparable EC50 values, and a somewhat reduced efficacy showed by derivative 3. In vivo, the 6- cyanomorphinan 6 with a closed 4,5-oxygen bridge was more potent than its 4,5-oxygen bridge-opened analogue 3 in inducing an antinociceptive effect in mice after s.c. administration (ca. 3 times in the hot-plate, 2 times in the tail-flick and 37 times in the PPQ tests). Closing of the 4,5-oxygen bridge in the 6-acrylonitrile substituted 3 produces no major changes in interaction with the MOP receptor in vitro, but augmented antinociceptive potency. On the other hand, the 14-methoxy-6-cyanomorphinan 6 showed greater MOP receptor affinity and agonist potency than 14-OMC and the 14-hydroxy substituted oxycodone, together with much better antinociceptive properties. It was of interest to assess the result of the conversion of the 6-acrylonitrile to a 6-amido group on the interaction with opioid receptors, signaling, and the link between antinociceptive efficacy and the mode of action. Since the presence of 4- and 14-methoxy groups was favorable in the case of the 6-cyano substituted N-methylmorphinan 5, the same substitution pattern was applied to the 6-amido analogue 4. It was remarkable to note that the presence of an amido group in position 6 resulted in high affinity at the MOP receptor and also good MOP selectivity. In the [^{35}S]GTPγS functional assay, the 6- amido substituted 4,5-oxygen bridge-opened 4 acted as a highly efficacious agonist at the MOP receptor with several times increased potency than oxycodone, 14-OMC and 4,14-

dihydroxy substituted 6-cyanomorphinan 1. The same profile was depicted for compound 4 when stimulating G protein signaling and intracellular calcium release through MOP receptors. When compared to the 6-cyano analogue 5, the 6-amido group in 4 appears to largely affect agonist potency, leading to reduced activity, especially in antinociceptive potency. It is possible that differential metabolism of derivatives 4 and 5 may determine the differences in the in vivo activity. Primary aliphatic amides are known to be rapidly metabolically hydrolyzed (Testa & Mayer, 2006) whilst the nitrile group is more stable (Fleming *et al.*, 2010). In this study, we described the in vitro functional activities of the previously reported 6-cyanomorphinans 1–3 and oxycodone based on the assessment of MOP receptor-mediated G protein activation and intracellular calcium mobilization. Replacement of the 4-hydroxy group in 6-cyanomorphinan 1 with a 4-methoxy group in analogue 2, or substitution of 14-hydroxyl in compound 1 with a 14-methoxy group in 3 results in 6 to 10 times enhanced agonist potencies and comparable efficacies, upon the test being used. Compared to the 6- ketomorphinans oxycodone and 14-OMC, the 6-cyano substituted N-methylmorphinans 1–3 generally displayed higher agonist activity in vitro, which correlates well with the in vivo results on antinociceptive properties. Among all investigated N-methylmorphinans, derivative 5 is the most potent agonist in terms of G protein coupling and changes in intracellular calcium concentration. This MOP agonist potency enhancement of the new 6-cyanomorphinan 5 compared to the other derivatives established in the two functional assays is in agreement with the outcomes from in vitro binding assays and nociceptive tests, and supports the importance of the presence of both methoxy groups in positions 4 and 14 in this class of opioid morphinans (Spetea *et al.*, 2005). The clinically relevant analgesic oxycodone was found as the MOP ligand with the lowest agonist potency in the series of the investigated morphinans. In CHO_{hMOP} cell membranes, oxycodone stimulated [^{35}S]GTPγS binding with a EC_{50} value of 500 nM, which is lower than the EC_{50} value of 1.40 μM reported by Thompson et al. in the same cell line (Thompson *et al.*, 2004). In the same work, a lower relative efficacy as percentage stimulation compared to DAMGO at the human MOP receptor in CHO cells was found for oxycodone (67%), while in this study a higher efficacy, i.e. 92% stimulation relative to DAMGO, was determined. Comparable potency (EC_{50} 373 nM) and lower relative efficacy (66%) for oxycodone to our data was reported in C6rMOP cells (Peckham & Traynor, 2006). Similarly, in CHO_{hMOP} cells stably expressing the $Gα_{qi5}$ chimeric protein, oxycodone exhibited low activity, by producing stimulation of calcium release with an EC_{50} value of 1,176 nM and an efficacy of 38%. A recent study (Zhang *et al.*, 2012) reported on changes in

intracellular calcium levels produced by oxycodone in human embryonic kidney-293 (HEK293) cells co-expressing the human MOP receptor and $G\alpha_{qi3}$ chimeric protein, with low potency (1.74 µM) and high efficacy (100%). Although 14-OMC also displays low agonist potencies at the human MOP receptor in both functional systems, it shows a similar efficacy compared to oxycodone in $[^{35}S]$GTPγS binding and in calcium mobilization, that is also seen in antinociceptive potency. Mostly, compounds 1–6, oxycodone and 14-OMC were found to be more potent MOP agonists in the terms of G protein activation based on the lower EC_{50} values by one order of magnitude than the EC_{50} values for the calcium signaling, and with lesser efficacies measured in the latter. Presumably these differences may be due to variances in receptor reserve in the two cell lines, and/or possibly membranes vs. intact cells. Differences in signaling may also be regulated by the MOP receptor localization within the plasma membrane (Ge *et al.*, 2009; Zheng *et al.*, 2008). Receptor localization within the lipid rafts after agonist binding can promote G protein coupling or recruitment of other intracellular regulatory proteins (Levitt *et al.*, 2009; Raehal *et al.*, 2011). Over the past years, increased attention has been drawn to the understanding of intracellular signaling pathways that mediate the therapeutic and/or adverse effects of opioid agonists acting at the MOP receptor (Kelly, 2013; Pradhan *et al.*, 2012; Raehal & Bohn, 2014). In vitro and in vivo studies demonstrate that different opioids can initiate distinct cellular and physiological responses downstream of receptor activation (Pradhan *et al.*, 2012; Raehal *et al.*, 2011). The nature of MOP receptor signaling and regulation are functions not only of the type and structure of the agonist acting at the receptor but also of the cellular environment in which the receptor is expressed (Raehal *et al.*, 2011). Moreover, the present understanding of MOP receptor function is persistently increasing, as the crystal structure is now available (Manglik *et al.*, 2012). For a detailed discussion of these data see (Ben Haddou *et al.*, 2014b).

3.2.3. Pharmacological characterization of endomorphin-2-based cyclicpentapeptides with methylated phenylalanine residues

The cyclization of linear peptide sequences has been shown to result as a possible way to modify the pharmacological properties of opioid peptides (Piekielna *et al.*, 2013). The aim of the present study was to pharmacologically characterize a panel of endomorphin-2 (EM-2, Tyr-Pro-Phe-Phe-NH_2) cyclic derivatives, modified from the previously described structure (compound 1) Dmt-c[D-Lys-Phe-Phe-Asp]NH_2 (Fichna *et al.*, 2011). The derived compounds are: 2 (Dmt-c[D-Lys-2'-MePhe-Phe-Asp]NH_2), 3 (Dmt-c[D-Lys-3'-MePhe-Phe-Asp]NH_2), 4 (Dmt-c[D-Lys-4'-MePhe-Phe-Asp]NH_2), 5 (Dmt-c[D-Lys-Phe-2'-MePhe-Asp]NH_2), 6 (Dmt-c[D-Lys-Phe-3'-MePhe-Asp]NH_2), and 7 (Dmt-c[D-Lys-Phe-4'-MePhe-Asp]NH_2).

The in vitro biological activities of this series of compounds were evaluated at MOP, DOP, and KOP receptors, in the calcium mobilization assay. CHO cells stably expressing either the human MOP, DOP, or KOP, and chimeric G proteins were used to monitor calcium changes. Concentration response curves to EM-2 and compounds 1-6 are shown in Figure 30, the calculated agonist potencies (pEC$_{50}$) and efficacies (α) are summarized in Table 14. Dermorphin, DPDPE, and dynorphin A were used as the reference agonists at the MOP, DOP, and KOP receptors, respectively. In general, all the analogs behaved as agonists displaying high potency at all three opioid receptors.

In the CHO$_{MOP}$ cells both dermorphin and EM-2 evoked a concentration dependent stimulatory effect, displaying high potency (pEC$_{50}$ 8.11 and 7.81) and maximal effect of 221 ± 13% and 202 ± 7% over the basal value, respectively (Figure 30, panel A). The EM-2 analogs 1, 2, 5–7 mimicked the stimulatory effect of dermorphin, showing similar potencies and maximal effects. Compounds 3 and 4 displayed high potencies associated with a significant reduction in efficacies. In the CHO$_{DOP}$ cells, the DOP receptor selective ligand, DPDPE, showed high potency (pEC$_{50}$ 8.20), while EM-2 did not stimulate calcium release up to 1 μM. All tested compounds were able to stimulate calcium mobilization, displaying moderate/high potency (pEC$_{50}$ 6.53-7.90) and low maximal effects (Figure 30, panel B). In the CHO$_{KOP}$ cells dynorphin A evoked a concentration dependent stimulation of calcium release displaying high potency (pEC$_{50}$ 8.88) and maximal effect (186 ± 10% over the basal values), while EM-2 did not stimulate calcium mobilization up to 1 μM (Figure 30, panel C). Analogs 3, 5, 6 and 7 exhibited high potencies; their maximal

effects were slightly but significantly lower than those evoked by dynorphin A. Compound 4 showed lower maximal effect and potency as compared with dynorphin A. Compounds 1 and 6 elicited maximal effects similar to those of dynorphin A but lower potencies.

Collectively, analogs 5–7 with MePhe substitutions in position 4 displayed the highest potency at the MOP receptor (Figure 30, panel A). All cyclic analogs acquired agonist activity at the DOP receptor, where 2'-MePhe[4] substitution produced the strongest effect (Figure 30, panel B). Additionally, analogs 1–7 showed very high potency for the KOP receptor (Figure 30, panel C). The highest potency at all three receptors was found for analog 5 with 2'-MePhe[4], while analogs with 4'-MePhe[3] were the least potent.
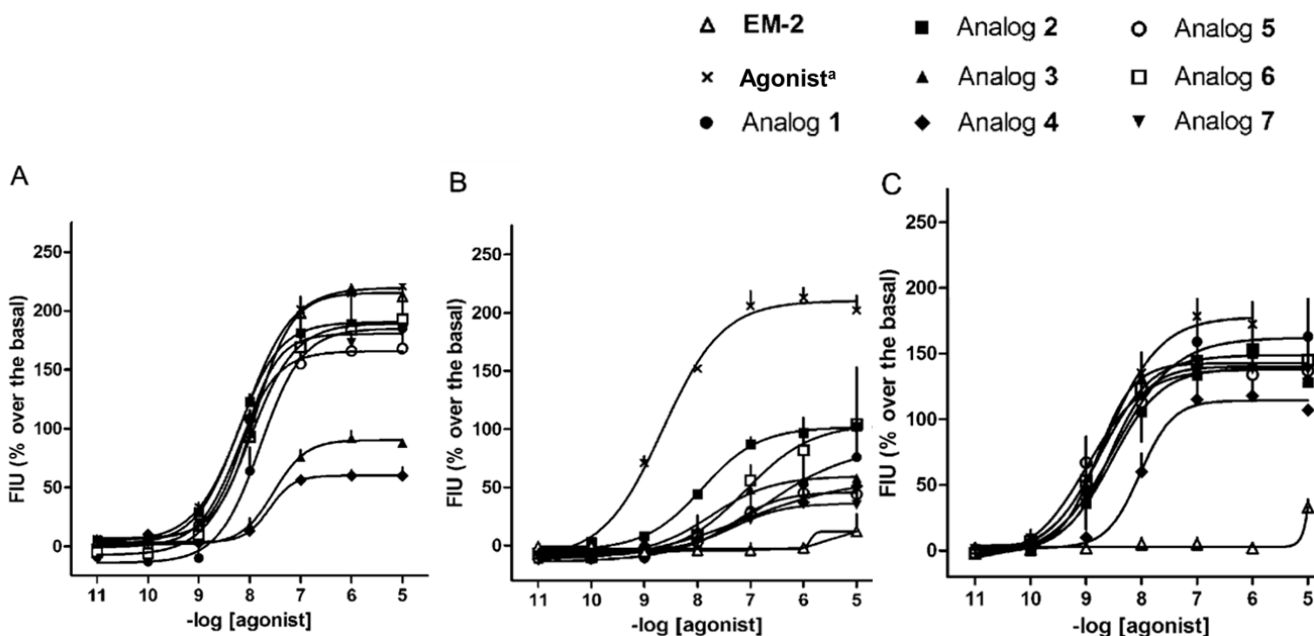
Figure 30. Concentration response curves to EM-2, cyclic analogs and dermorphin[a] (A), DPDPE[a] (B) and dynorphin A[a] (C) in calcium mobilization experiments performed in CHO_{MOP}, CHO_{DOP} and CHO_{KOP} cells, respectively. Data are mean ± sem of at least 4 separate experiments performed in duplicate.

Table 14. Effects of the cyclic pentapeptides at human recombinant opioid receptors coupled with calcium signaling via chimeric G proteins.

	MOP		DOP		KOP	
	pEC_{50} (CL$_{95\%}$)	$\alpha \pm sem$	pEC_{50} (CL$_{95\%}$)	$\alpha \pm sem$	pEC_{50} (CL$_{95\%}$)	$\alpha \pm sem$
EM-2	7.81 (7.69-7.93)	1.00	Inactive		Inactive	
dermorphin	8.11 (7.95-8.27)	0.99 ± 0.01	6.43 (6.04-6.82)	1.03±0.07[a]	Inactive	
DPDPE	Inactive		8.20 (7.78-8.61)	1.00	Inactive	
dynorphin A	6.67 (6.17-7.17)	0.83 ± 0.10[a]	7.73 (7.46-8.00)	0.99 ± 0.04[a]	8.88 (8.58-9.17)	1.00
1	7.76 (7.38-8.14)	0.84 ± 0.04	≈ 6.7	0.34 ± 0.15*	8.50 (7.72-9.28)	1.03 ± 0.19
2	8.25 (8.11-8.39)	0.94 ± 0.01	7.94 (7.81-8.07)	0.46 ± 0.10*	8.51 (7.84-9.18)	0.74 ± 0.04*
3	7.53 (7.16-7.90)	0.45 ± 0.02*	7.57 (6.81-8.33)	0.26 ± 0.01*	8.72 (7.75-9.69)	0.78 ± 0.02*
4	7.55 (7.15-7.95)	0.30 ± 0.01*	7.34 (6.62-8.06)	0.39 ± 0.09*	7.97 (7.35-8.59)	0.63 ± 0.05*
5	8.25 (7.98-8.52)	0.82 ± 0.03	7.95 (7.74-8.16)	0.44 ± 0.02*	8.92 (8.16-9.68)	0.74 ± 0.03*
6	7.96 (7.50-8.42)	0.87 ± 0.01	≈ 7.1	0.55 ± 0.18*	8.74 (8.01-9.48)	0.96 ± 0.10
7	8.11 (8.04-8.18)	0.90 ± 0.02	7.34 (6.78-7.90)	0.21 ± 0.01*	8.56 (8.27-8.85)	0.75 ± 0.04*

Inactive means that the compound was inactive as agonist up to 1 μM.
EM-2, DPDPE, and dynorphin A were used as reference agonists for calculating intrinsic activity at MOP, DOP, and KOP receptor, respectively. [a] these data are from Camarda and Calo', 2013. * p < 0.05 according to one way ANOVA followed by the Dunnett test for multiple comparisons.

In receptor binding studies, parent compound 1 showed sub-nanomolar MOP receptor affinity and three rows of magnitude lower affinity for the DOP receptor (Fichna *et al.*, 2011). Analogs 2–4 with 2'-, 3'-or 4'-MePhe, respectively, in position 3 displayed also high but3–4-fold lower MOP binding affinity, increased DOP affinity and therefore decreased MOP versus DOP selectivity. The same modification (2'-, 3'-or 4'-MePhe) introduced into position 4 (analogs 5–7) resulted in the increased affinities for both, MOP and DOP receptors, as compared with the parent compound. The obtained results showed that introduction of methylated Phe residues generally enhanced binding to the DOP receptor. The effect of methyl groups on MOP binding depended on the position of MePhe. Introduction of the MePhe residue into position 3 resulted in a slight decrease, and into position 4, in a significant increase of MOP affinity. The position of the methyl group in the phenyl ring of Phe[4] was also important: the rank order of affinity was 4'-MePhe ≥ 2'-MePhe ≥ 3'-MePhe (data reported in (Perlikowska *et al.*, 2014)). The resistance of cyclic analogs against protolithic degradation was evaluated in vitro, using rat brain homogenates. Cyclic pentapeptides and EM-2, were incubated with the homogenate for 90 min and then the mixtures were analyzed by RP-HPLC. All cyclic peptides displayed low degradation, not higher than 15%, while EM-2 was almost completely digested after 90 min of incubation (data reported in (Perlikowska *et al.*, 2014)).

The antinociceptive effects of the analogs were assessed in the hot-plate test in mice after i.c.v. administration. All cyclic analogs produced dose-dependent antinociceptive responses (Figure 31). The incorporation of the MePhe residues into position 4 produced extremely potent analogs 5–7, with ED_{50} values 4.9, 14.3 and 0.6 ng/animal, respectively (Table 15) (data are from (Perlikowska *et al.*, 2014)).
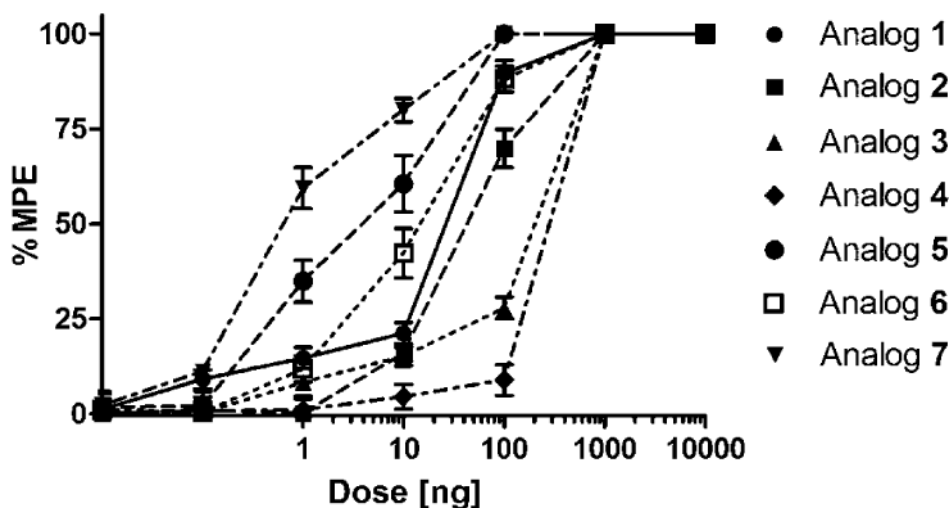
Figure 31. Dose–response curves determined in the hot-plate test in mice for the inhibition of jumping induced by i.c.v. injection of cyclic analogs 1–7. Data are mean ± sem of 10 mice per group.

Table 15. ED_{50} values for cyclic pentapeptides in the hot-plate test in mice.

	ED_{50} (jumping)
	ng/animal
1	20.0 ± 3.1
2	31.9 ± 1.2
3	220.5 ± 13.7
4	389.0 ± 23.0
5	4.9 ± 0.2
6	14.3 ± 0.9
7	0.6 ± 0.05

Data are mean ± SEM of 10 animals per group. Table is from (Perlikowska *et al.*, 2014)

It is generally accepted that the aromatic amino acids in the structure of EM-2 and other opioid peptides are essential structural elements for receptor binding and activation (Janecka *et al.*, 2007; Keresztes *et al.*, 2010; Liu & Wang, 2012). The aromatic portions of the ligands can be positioned in close proximity to the hydrophobic pockets belonging to the receptor domains and exhibit significant non-covalent interactions in such areas. The introduction of substituents, especially methyl groups, into the aromatic rings of Tyr and Phe can influence the conformation of the opioid ligands because of the increased bulkiness of the side-chains. The development of

Dmt paved the way for achieving increased bioactivities in opioid peptides (Hansen *et al.*, 1992; Li *et al.*, 2005). The substitution of 2',6'-dimethylphenylalanine (Dmp) into position 3 of EM-2 produced analog with about 5-fold lower MOP receptor affinity (Sasaki *et al.*, 2003).The combined introduction of Dmt1and alkylated analogs of Phe3(2'-ethyl-, 3'-,5'- and 2'-, 6'-dimethyl-, 2'-ethyl- 6'-methyl-) into EM-2 structure did not produce potent MOP receptor agonists but was associated with DOP receptor antagonism (Li *et al.*, 2007). Methylation of the Phe[4] residue in EM-2 analogs was not explored so far. I was recently reported the synthesis and pharmacological activity of Dmt[1]-substituted cyclic analogs of EM-2 (Fichna *et al.*, 2011). One of them, Dmt-c[D-Lys-Phe-Phe-Asp]NH$_2$ (analog 1), showed high MOP receptor affinity and a strong, long-lasting MOP receptor-mediated antinociceptive effect after i.c.v. administration.

In the present study, further modifications of analog 1, in particular the incorporation of bulkier, 2'-, 3'- or 4'-methylated Phe residues in either the third or fourth position of the cyclic structures were studied. These modifications introduce an additional steric hindrance which may result in conformational changes. The more interesting is the series with MePhe substitutions in position 4 (analogs 5–7). These analogs displayed extremely high affinities at the MOP receptor and simultaneously drastically enhanced affinities at the DOP receptor. The binding of the analogs to the KOP receptor was not tested, but the calcium mobilization functional assay was performed which, as opposed to the GPI/MVD assays, allows for the determination of the activity of peptides at all three types of opioid receptors. At the molecular level, opioids modulate calcium channel conductance through MOP, DOP and KOP receptors (Standifer & Pasternak, 1997). In the present study the pharmacological activities of the novel compounds have been evaluated by measuring calcium mobilization in cells expressing a recombinant human receptor and chimeric G proteins. This approach has been previously used and validated by investigating the pharmacological profile of non-peptide ligands of classical opioid receptors (Camarda & Calo, 2013; Zhang *et al.*, 2012) and of NOP receptor ligands (Camarda *et al.*, 2009; Fischetti *et al.*, 2009; Marti *et al.*, 2013; Trapella *et al.*, 2009). Here, this functional assay was used for the first time to characterize and compare the potencies and efficacies of the novel cyclic analogs of a peptide structure. These analogs preferentially inter-acted with KOP and MOP receptors with the following order of potency: 5 > 6 > 3 > 7 (for the KOP receptor) and 2 ≥ 5 > 7 > 6 (for the MOP receptor), while potencies at the DOP receptor were following 5 > 2 > 3 > 4. In the past it was demonstrated that analogs that are KOP/MOP-receptor agonists may be effective for the

treatment of cocaine or other psychostimulant abuse (Greedy *et al.*, 2013) which opens further possibilities for pharmacological testing of these analogs. In the in vivo hot-plate test, position 3 substituted analogs 2–4 produced weaker – and position 4-substituted analogs 5–7 – much stronger antinociceptive effects than the parent compound 1 after i.c.v. injection. These results may suggest that the combined high agonist potency at both, the MOP and KOP receptors results in the great enhancement of the antinociceptive effect. The obtained data indicate that EM-2 analogs cyclized through a side-chain to side-chain amide bond show in opioid bioassays preference for MOP and KOP receptors while EM-2 and many of its linear analogs are MOP receptor selective (Janecka *et al.*, 2007). According to the accumulated data reviewed recently by Schiller (Schiller, 2010), it is now widely accepted that biological activity at a single receptor is often insufficient and ligands that bind to more than one receptor type may have much improved potency due to synergistic effects. Extremely high antinociceptive activity of the new cyclic analogs that activate MOP and KOP receptors with similar potency and show even some affinity to the DOP receptor open new possibilities in designing compounds with mixed opioid profile (Perlikowska *et al.*, 2014).

3.3. Ligands for NOP receptor

3.3.1. The nociceptin/orphanin FQ receptor antagonist NiK-21273

The purpose of the present study was to characterize the in vitro pharmacological profile of the novel NOP receptor ligand NiK-21273 (2-[3-[4-(2-Chloro-6-fluoro-phenyl)-piperidin-1-ylmethyl]-2-(morpholine-4-carbonyl)-indol-1-yl]-acetamide, Figure 32). The effects of this molecule were assessed in calcium mobilization studies performed with cells expressing the human recombinant NOP or the classical opioid receptors as well as in bioassay studies performed with isolated tissues expressing animal native NOP receptors.
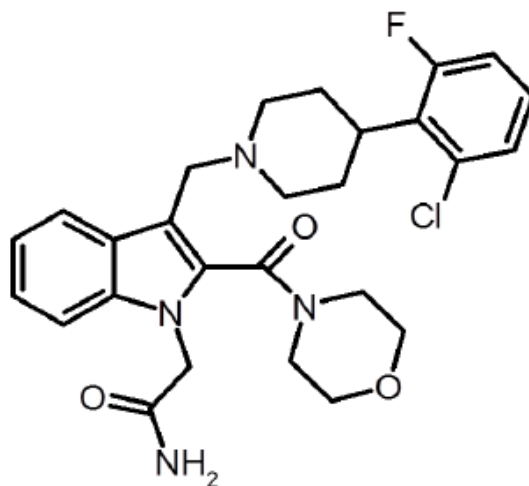
Figure 32. Chemical structure of NiK-21273

N/OFQ concentration dependent stimulated the calcium signal in CHO_{NOP} cells stably expressing the $G\alpha_{qi5}$ protein, displaying high potency (pEC_{50} 9.19 (8.85–9.53)) and maximal effects of 200±12% fluorescence over baseline. NiK-21273 inhibited the stimulatory effect of N/OFQ (10 nM) in a concentration dependent manner with a pK_B of 7.38, whereas naloxone was ineffective (Table 16). SB-612111 also inhibited N/OFQ effects in a concentration-dependent manner, with a pK_B of 8.18 (not shown). NiK-21273 selectivity was then evaluated in CHO cells stably expressing classical opioid receptors (CHO_{MOP}, CHO_{KOP} and CHO_{DOP} cells) and the chimeric G proteins ($G\alpha_{qi5}$ for MOP and KOP, $G\alpha_{qG66Di5}$ for DOP). In these cell lines, dermorphin, dynorphin

A and DPDPE evoked concentration-dependent stimulations of calcium mobilization showing different potencies (pEC$_{50}$ 8.26, 9.19 and 8.36, for MOP, KOP, and DOP, respectively) and efficacies (~189, ~226 and ~102% over baseline, respectively). Naloxone antagonized the stimulation evoked by 30 nM dermorphin (pK$_B$ 8.73), 30 nM dynorphin A (pK$_B$ 7.00) and 30 nM DPDPE (pK$_B$ 6.80) in a concentration-dependent manner, whereas NiK-21273 was ineffective (Table 16) (Figure 33).
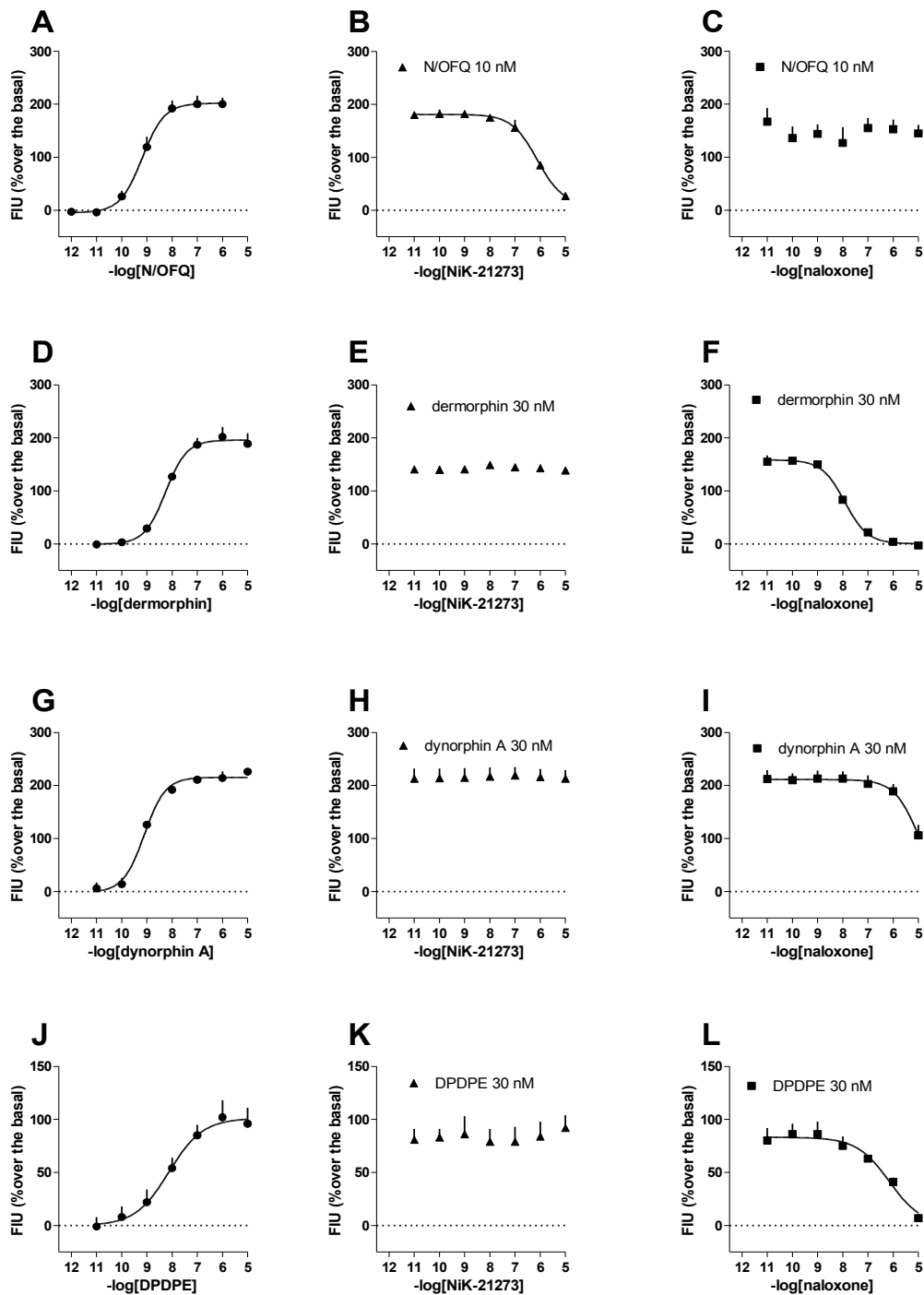
Figure 33. Calcium mobilization experiments. Concentration response curves to agonists (left panels) and inhibition response curves to NiK-21273 (middle panels) and naloxone (right panels) in cells expressing the NOP (panels A, B, C), the MOP (panels D, E, F), the KOP (panels G, H, I), and the DOP (panels J, K, L) receptors. Data are mean ± sem of at least 3 separate experiments performed in duplicate.

Table 16. Antagonist potencies of NiK-21273 and naloxone obtained in inhibition response experiments performed in CHO cells expressing NOP or classical opioid receptors and Gα chimeric proteins.

	NOP	MOP	KOP	DOP
NiK-21273	7.38 (7.06-7.70)	< 6	< 6	< 6
naloxone	< 6	8.73 (8.38-9.08)	7.00 (6.68-7.32)	6.80 (6.09-7.51)

Data are mean ($CL_{95\%}$) of at least 3 separate experiments performed in duplicate.

In order to assess the nature of NiK-21273 antagonism at the NOP receptor, a classical Schild analysis was performed. NiK-21273 produced a concentration-dependent rightward shift of the N/OFQ curve without modifying its maximal effect (Figure 34, panel A). The corresponding Schild plot (Figure 34, panel B) was linear, yielding a pA_2 of 7.77. SB-612111 (10 nM–1 µM) replicated this behavior (Figure 34, panel C), the corresponding Schild plot (Figure 34, panel D) yielding a pA_2 of 7.74.
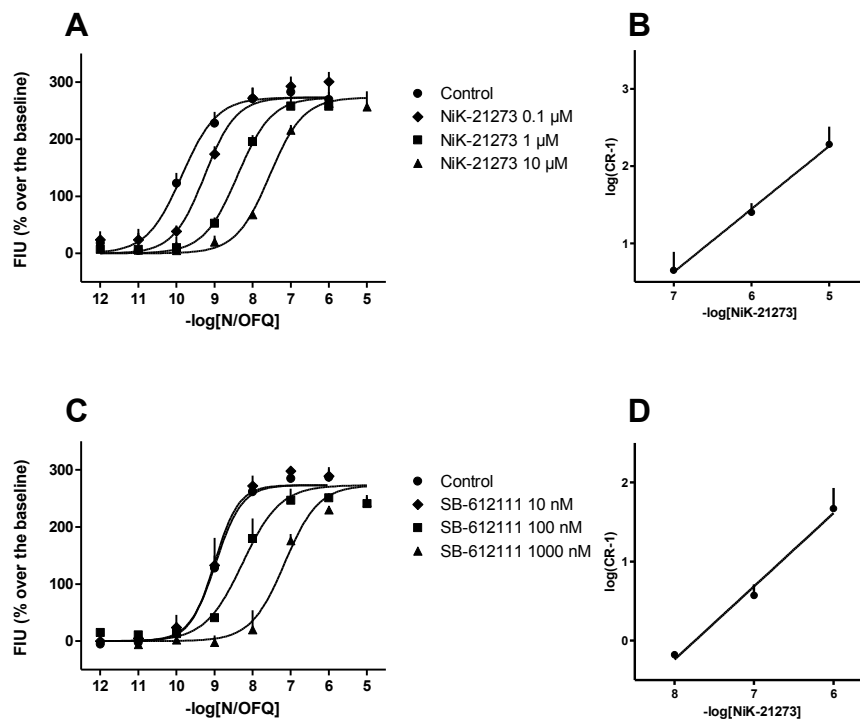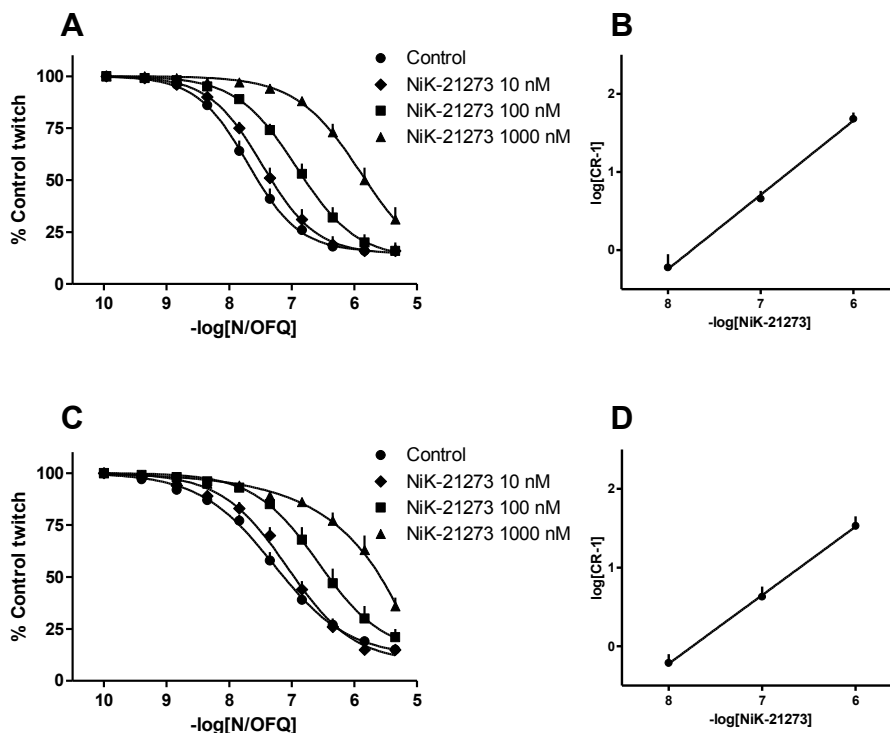
Figure 34. Concentration-response curve to N/OFQ obtained in the absence (control) and in presence of increasing concentrations of NiK-21273 (panel A) and SB-612111 (panel C). The corresponding Schild plots are shown in panels B and D. Data are the mean of at least 4 separate experiments performed in duplicate.

NiK-21273 was also assessed in the electrically stimulated mouse and rat vas deferens. N/OFQ inhibited the twitch response in a concentration-dependent manner, both in the mouse (pEC_{50} 7.70; Emax -84 ± 3%; Figure 35, Panel A) and rat (pEC_{50} 7.48; Emax -86±2%; Figure 35, Panel C) vas deferens. NiK-21273 alone was ineffective up to 1 µM in both preparations, but produced a concentration-dependent rightward shift of the N/OFQ curve without affecting its maximal effect (Figure 35, Panel A and C). Schild analysis (Figure 35, Panel B and D) yielded a pA_2 value of 7.74 and 7.75 in the mouse and rat tissues respectively. SB-612111 (100 nM) replicated this behavior with pK_B values of 8.77 (mouse) and 8.05 (rat) (data not shown).

In functional washout experiments performed in the electrically stimulated mouse vas deferens, the reversibility of NiK-21273 and SB-612111 action at equieffective concentrations (1 and 0.1 µM, respectively) was evaluated. The concentration–response curves to N/OFQ performed 1, 2 and 3 h after washing were superimposable to the control curve. The antagonist effect of 1 µM NiK-21273 (CR 30, where CR is the ratio between the EC_{50} of the agonist in the presence and in the absence of the antagonist) was easily, although not completely, reversed by washing the

tissues for 1 h (CR 3). On the contrary, the antagonist effect exerted by 0.1 μM SB-612111 (CR 30) could not be reversed even after 3 h of washing (CR 10).

Figure 35. Concentration-response curve to N/OFQ obtained in the absence (control) and in presence of increasing concentrations of NiK-21273 in the electrically stimulated mouse (panel A) and rat (panel C) vas deferens. The corresponding Schild plots are shown in panels B and D. Data are the mean of at least 4 separate experiments.

The present results demonstrated that NiK-21273 behaves in vitro as a pure, fairly potent and highly selective NOP receptor antagonist. This molecule represents a novel and useful tool for investigating the role played by the N/OFQ – NOP receptor system in physiology and pathology. For results and discussion of the in vivo activity of NiK-21273 in animal models of Parkinson's disease see (Marti *et al.*, 2013).

3.3.2. Spiroxatrine derivatives, pharmacological activity for the NOP receptor

Spiroxatrine (Figure 36) is an alpha2-adrenoceptor and 5-HT1A receptor antagonist able to bind the NOP receptor with moderate affinity ($pK_i \sim 7$, (Zaveri *et al.*, 2001)).
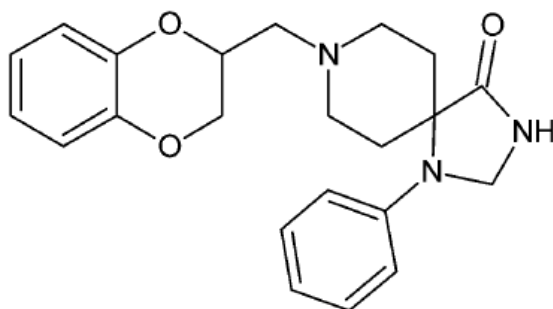
Figure 36. Spiroxatrine (1).

It was known that the 1-phenyl-1,3,8-triazaspiro[4.5]decan-4-one portion of 1, due to its chemical features, is responsible for the NOP affinity of this class of compounds. The resulting spiropiperidine analogues exhibited high affinity for the NOP receptor. In particular, the spiropiperidine series developed by Roche and Pfizer demonstrated high affinity associated with moderate selectivity for the NOP receptor (Largent-Milnes & Vanderah, 2010).

Herein this study reports the results of three different SAR studies aimed at identifying a series of triazaspirodecanone derivatives as NOP receptor ligands.

The first SAR development plan was to investigate possible substitutions of the chromane core of 8-(chroman-4-yl)-1-phenyl-1,3,8-triazaspiro[4.5]decan-4-one.
Compounds 1-18, S-4 and R-4 were tested in the calcium mobilization assay in CHO cells stably expressing the human NOP receptor and the $G\alpha_{qi5}$ chimeric protein. The compounds were tested as agonists together with N/OFQ as standard (Figure 37). Under the present experimental conditions, N/OFQ produced a concentration-dependent stimulatory effect showing high potency (pEC_{50} 9.68) and maximal effect (254±16% over the basal value), in line with previously published data (Fischetti *et al.*, 2009; Trapella *et al.*, 2009). Spiroxatrine (1) behaved as a low potency NOP full agonist (pEC_{50} 6.49 and α 0.81). Compounds 4 and 18 produced a

91

concentration-dependent calcium mobilization with pEC_{50} values of 6.80 and 6.37, respectively. Compounds 5–10, 13–15 and 17 produced a weak stimulation of the NOP receptor, generating incomplete concentration response curves. Thus these molecules behaved as very low potency NOP agonists. Differently, compounds 11, 12 and 16 did not stimulate calcium mobilization up to 10 µM.

These compounds were further evaluated in antagonist-type experiments. In these studies SB-612111 was used as a positive control. Inhibition response curves were performed against a fixed concentration of N/OFQ, approximately corresponding to its EC_{80}. As shown in Figure 37, right panel, under the present experimental conditions SB-612111 elicited a complete and concentration-dependent inhibition of the N/OFQ stimulatory effect, with a pK_B value of 8.10. This value is in line with previously reported findings (Camarda *et al.*, 2009; Fischetti *et al.*, 2009). Compounds 11, 12, and 16 up to 10 µM did not modify the stimulatory effect of N/OFQ. In addition, compounds 7 and 13, which displayed a weak stimulatory effect only at 10 µM, were also evaluated as NOP antagonists up to 1 µM. These compounds produced a weak inhibitory effect only at the highest concentration tested.

All the data were summarized in Table 17.
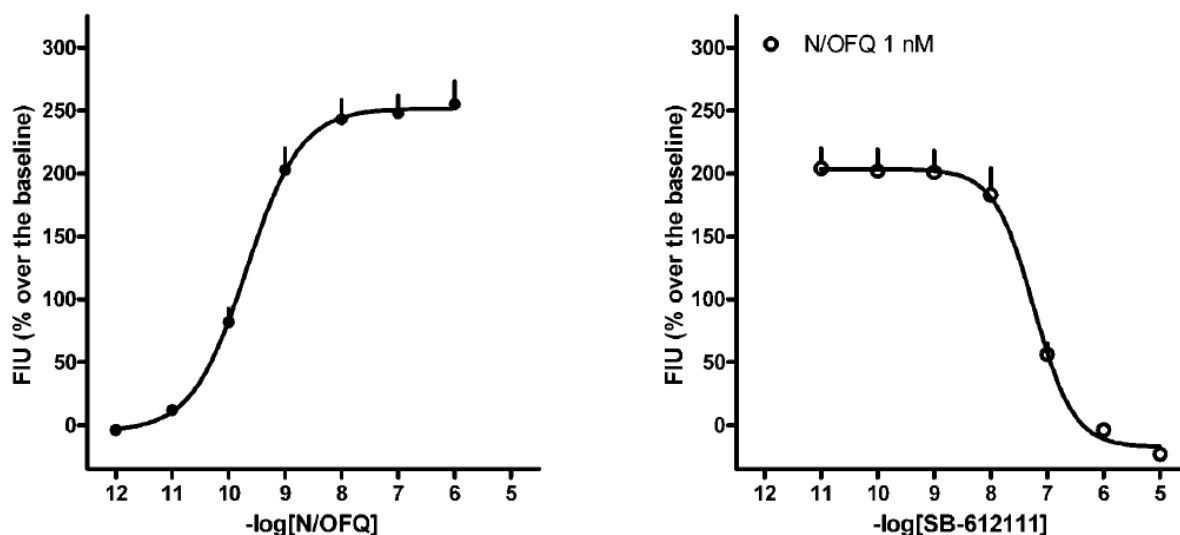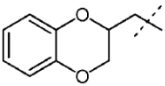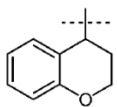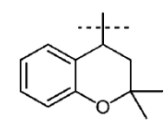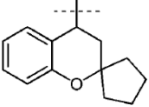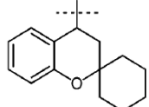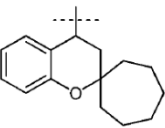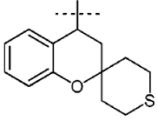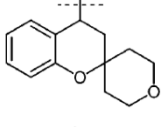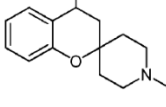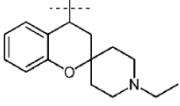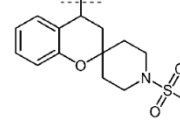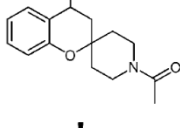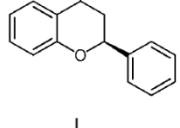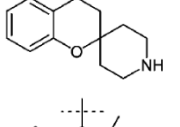
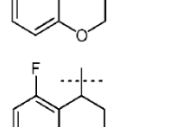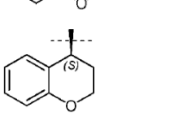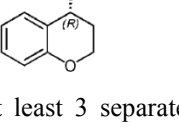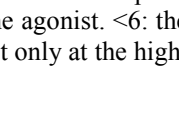**Figure 37.** Calcium mobilization experiments performed in CHO_{NOP} cells stably expressing the $G\alpha_{qi5}$ protein. Concentration response curve to N/OFQ (left panel) and inhibition response curve to SB-612111 vs 1 nM N/OFQ (right panel). Data are the mean ± sem of at least 4 separate experiments performed in duplicate.

Table 17. Effects of standard and novel ligands in calcium mobilization experiments performed in CHO cells coexpressing the human NOP receptor and the $G\alpha_{qi5}$ chimeric protein.

		agonist		antagonist
		pEC_{50} ($CL_{95\%}$)	$\alpha\pm sem$	pK_B ($cl_{95\%}$)
N/OFQ		9.68 (9.59–9.78)	1.00	nd
SB-612111		inactive		8.10 (7.95–8.24)
1		6.49 (5.95-7.03)	0.81±0.03	nd
4		6.80 (5.79–7.63)	1.02±0.04	nd
5		crc incomplete		nd
6		crc incomplete		nd
7		crc incomplete		<6
8		crc incomplete		nd
9		crc incomplete		nd
10		crc incomplete		nd
11		inactive		inactive

12		inactive		inactive
13		crc incomplete		<6
14		crc incomplete		nd
15		crc incomplete		nd
16		inactive		inactive
17		crc incomplete		nd
18		6.37 (6.31–6.43)	1.00±0.09	nd
S-4		6.68 (6.57–6.80)	0.95±0.04	nd
R-4		7.34 (7.29–7.39)	0.98±0.04	nd

Data are mean of at least 3 separate experiments performed in duplicate. n.d.: not determined. Inactive: inactive up to 10 μM. Crc incomplete: the concentration response curve could not be completed because of the low potency of the agonist. <6: the pKB could not be precisely determined because the ligand produced a weak inhibitory effect only at the highest concentration tested, i.e. 1 μM.

The introduction of the chromane core on the piperidine nitrogen of 1-phenyl- 1,3,8-triazaspiro [4.5]decan-4-one, as in compound 4, moderately increases the agonist activity with respect to 1. Introduction of a halogen atom at position 5 of compound 4, to give 18, leads to a slight decrease in potency. The presence of a steric hindrance at position 3 of the chromane moiety as in compound 17 decreases the ligand potency. A similar trend was observed for the introduction of alkyl and aromatic substituents on position 2 of the chromane as in compounds 5 and 15. By increasing the steric hindrance at position 2 of the chromane core, compounds 6 and 15 did not

show promising activity, suggesting very low steric tolerance on the chromane ring. The homologation of the spiro structure of 6, to give 7, seems to convert the compound into a weak antagonist. However, the very low potency of this compound does not allow a detailed characterization of its pharmacological activity. Further homologation of the spiro alkyl substituents (8) led to a decrease in activity both as agonist and antagonist. The same behavior was observed for the isosters of 7, compounds 9, 10 and 16. Indeed the latter was completely inactive as its methyl and ethyl derivatives (11 and 12, respectively), probably because at physiological pH the nitrogen atom is protonated and the positive charge may negatively interfere with the binding process. Compound 13, with a non-protonable sulfonamidic nitrogen which also carries the hindered substituent such as the methanesulfonyl group, showed a weak antagonist activity similar to compound 7. However, this is not observed with compound 14 which has a similar nitrogen atom (acetamidic), indicating the relevant and discriminating role of steric interactions in the antagonist activity.

Single enantiomers (S-4 and Z-4) of the most potent spiroxatrine derivative i.e. compound 4, were also tested in calcium mobilization assay. (+)-(R)-4 and (-)-(S)-4 produced a concentration-dependent stimulation of NOP receptor with pEC_{50} values of 7.34 and 6.68, respectively (Table 17 and Figure 39). Thus the results identified the (R)-enantiomer as the most active component being 5-fold more potent than the (S)-enantiomer. Moreover, in order to demonstrate the direct involvement of the NOP receptor in the biological action of (+)-(R)-4 and (-)-(S)-4 inhibition response experiments were performed by testing increasing concentrations of SB-612111 against fixed concentrations of (+)-(R)-4 and (-)-(S)-4 (1 μM), approximately corresponding to their EC_{80}. The pK_B values obtained for SB-612111 vs. (+)-(R)-4 and (-)-(S)-4 were 8.67 and 8.58, respectively (Figure 38), indicating that the latter compounds behaved as full agonists interacting with the NOP receptor at the orthosteric binding site.
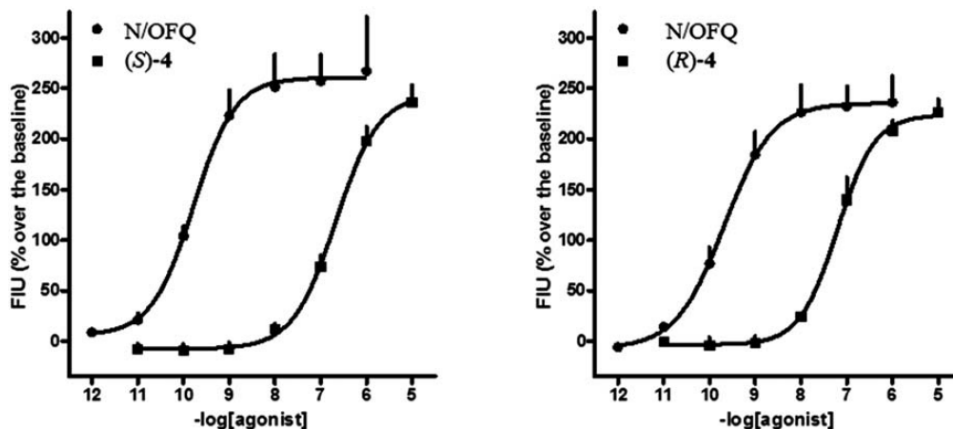
Figure 38. Calcium mobilization experiments performed in CHO_{NOP} cells stably expressing the $G\alpha_{qi5}$ protein. Concentration response curve to N/OFQ and S-4 (left panel), and R-4 (right panel). Data are the mean ± sem of at least 4 t experiments performed in duplicate.
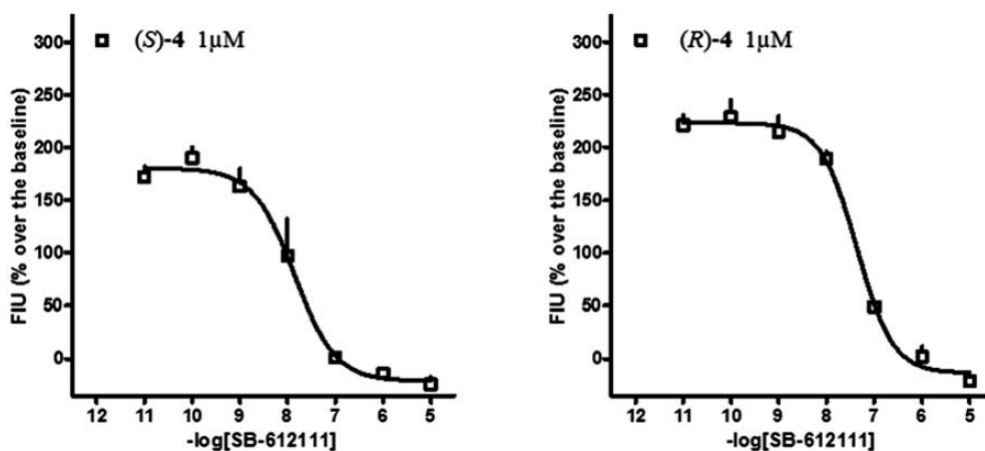

Figure 39. Inhibition response experiments performed in CHO_{NOP} cells stably expressing the $G\alpha_{qi5}$ protein. Inhibition response curve to SB-612111 vs 1 µM S-4 (left panel), or 1 µM R-4 (right panel). Data are the mean ± sem of at least 4 t experiments performed in duplicate.

This first series of spiroxatrine derivatives, led to characterize several small molecule ligands for their ability to bind and stimulate the NOP receptor, among them compound 4 demonstrated a good activity as a NOP receptor agonist. Then an enantioseparative method led to obtain single enantiomers of 4. Further biological studies have shown (R)-4 as the eutomer, indicating a clear stereospecific interaction. Docking studies were performed on the NOP receptor crystal structure in order to understand the binding mode of the two stereoisomers of 4. These results would help guide further developments of N-substituted spiropiperidine-based NOP agonists (Battisti *et al.*, 2014).

For the second SAR, a new series of spiroxatrine derivatives was characterized in the calcium mobilization assay, in CHO cells coexpressing the human NOP receptor and the $G\alpha_{qi5}$ chimeric protein. N/OFQ produced a concentration dependent stimulation of calcium mobilization with a pEC_{50} of 9.27 and maximal effects of 157 ± 19 % over the basal value. Compound 1 mimicked the stimulatory effect of N/OFQ showing similar maximal effects but lower potency (pEC_{50} 6.49). Similar results were obtained with compounds 21 and 23 that were slightly less potent than compound 1. Compound 22 also behaved as a full agonist showing, however, a further decrease in potency (pEC_{50} 5.91). Compounds 21, 22 and 23 were also tested in CHO cells expressing the $G\alpha_{qi5}$ protein but not the human NOP receptor. In these cells, ATP produced concentration dependent stimulatory effect with a pEC_{50} value of 6.94 and E_{max} of 278 ± 44 %, while 21, 22 and 23 were inactive up to 10 µM. These findings demonstrate that the stimulatory effects of 21, 22, and 23 are due to NOP receptor activation. Compounds 23, 24 and 25, isosters of 21, produced weak stimulatory effects only at micromolar concentrations thus generating incomplete concentration response curves (Table 18). Compound 29 did not stimulate calcium mobilization up to 10 µM suggesting a complete loss of agonist activity. The same results were obtained with all azaspiro derivatives 26, 28, 30–32. In order to investigate putative NOP antagonist properties of these compounds, inhibition response curves were performed against a fixed concentration of N/OFQ (10 nM). The NOP antagonist J-113397 was used as positive control (Kawamoto *et al.*, 1999). As shown in Figure 40 right panel, under the above presented experimental conditions, J-113397 elicited a complete and concentration-dependent inhibition of the N/OFQ stimulatory effect. A pK_B value of 7.73 was derived from these experiments; this value is in line with previously reported findings (Camarda *et al.*, 2009). In parallel experiments compounds 26, 28–32 did not modify up to 10 µM the stimulatory effects induced by 10 nM N/OFQ (Table 18). Thus, these compounds were found inactive also as NOP antagonists.
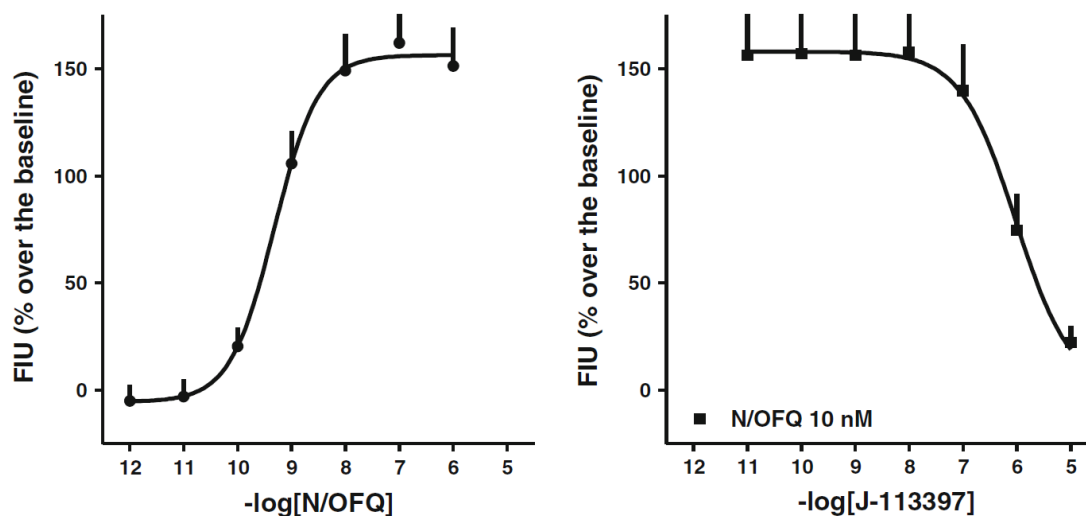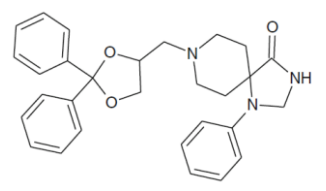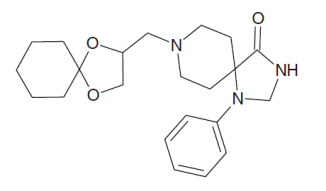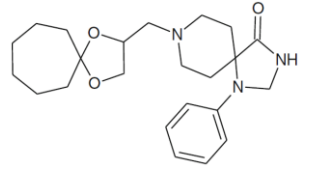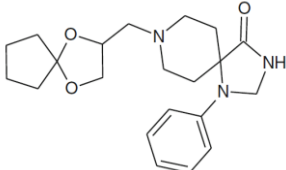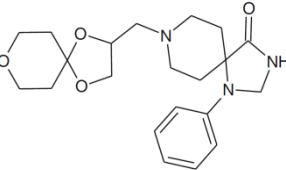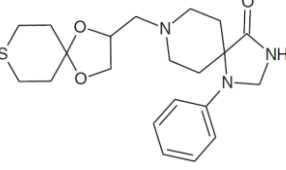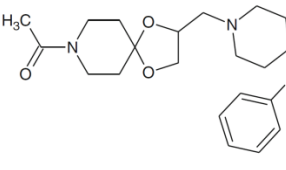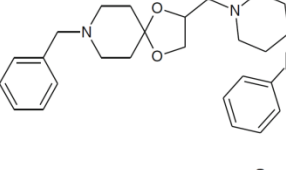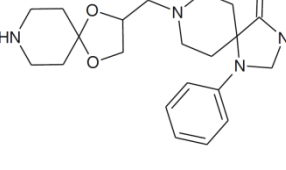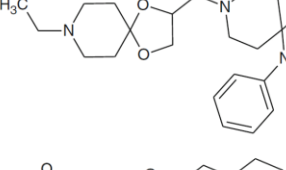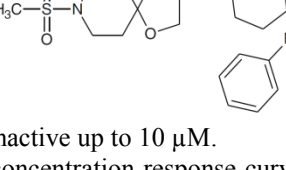
Figure 40. Calcium mobilization experiments performed in CHO_{NOP} cells stably expressing the $G\alpha_{qi5}$ protein. Concentration response curve to N/OFQ (left panel) and inhibition response curve to J-113397 vs 10 nM N/OFQ (right panel). Data are the mean ± sem of at least 4 separate experiments performed in duplicate.

Table 18. Effects of standard and spiroxatrine derivatives in calcium mobilization experiments performed on CHO cells co-expressing the human NOP receptor and the $G\alpha_{qi5}$ chimeric protein.

		agonist		antagonist
		pEC_{50} (CL$_{95\%}$)	α±sem	pK_B (CL$_{95\%}$)
N/OFQ		9.27 (8.98–9.55)	1.00	nd
J-113397		inactive		7.73 (7.45–8.01)
Spiroxatrine (1)		6.49 (5.95-7.03)	0.81±0.03	nd
20		crc incomplete		nd
21		6.29 (6.02–6.56)	0.87±0.04	nd
22		5.91 (5.83–6.00)	1.17±0.11	nd

98

23		6.23 (5.93–6.53)	1.01±0.09	<6
24		crc incomplete		nd
25		crc incomplete		nd
26		inactive		nd
28		inactive		inactive
30		inactive		inactive
31		inactive		inactive
32		inactive		inactive

Inactive: compound inactive up to 10 μM.
Crc incomplete: the concentration response curve could not be completed because of the low potency of the agonist tested.

The analysis of these biological results suggests different molecular effects of these ligands on calcium release in CHO$_{NOP}$ cells stably expressing the Gα_{qi5} chimeric protein. Replacement of 1,4-benzodioxane fragment with 2,2-diphenyl-1,3-dioxolane moiety as in compound 20 caused a slight decrease of agonist activity. When the geminal phenyl rings were replaced by a spiro group, as in 21, the agonist activity is maintained both in terms of potency and efficacy. Compound 21 was taken as a new starting point in order to further explore a possible structure-activity relationship. Homologation of the spiro structure, as in compound 22 and 23, produced a decrease in ligand potency; this was more pronounced for 22 with respect to compound 23. Moreover, it was observed that the polarity of the atom at position 8 of the 1,4-dioxaspiro[4.5]decane derivatives has a critical influence. Indeed increasing the polarity of that atom led to a decrease (24 and 25, incomplete concentration response curves) or even to a complete loss of activity (29). For compound 29, another parameter may be responsible of the observed loss of activity: at physiological pH, the nitrogen atom is protonated, and the positive charge may interfere with the binding process. The same explanation may be put forward in order to interpret the inactivity of compound 28 and 30 which in addition carry hydrophobic sterically hindered substituents such as benzyl and ethyl groups respectively. Steric hindrance may also be a negative factor in the case of compounds 26, 31, and 32 (in these cases the nitrogen atom is not protonated at physiological pH), obtained by the introduction of hydrogen bond acceptor or electron donor/ acceptor moieties on the nitrogen atom of compound 29. Compounds inactive as agonists were further evaluated as NOP antagonists. The azaspiro derivatives 26–32 did not affect the stimulatory effects of N/OFQ up to 10 μM. This evidence suggests that these compounds are not able to bind NOP receptor. As a conclusion of these studies, 1,4-dioxolane-triazospirodecanone derivatives showed unique and significant SAR as NOP receptor agonists. In particular, the present study demonstrated that 1-phenyl-1,3,8-triazaspiro[4.5]decan-4-one portion, together with an appropriate 1,4-dioxolane substituent might represent a new promising class of NOP receptor ligands.

The third series of SAR studies on spiroxatrine molecule has been pharmacologically evaluated at the NOP receptor in the calcium mobilization assay using again, the endogenous peptide N/OFQ as standard agonist (Figure 41, left panel). Under the present experimental conditions N/OFQ produced a concentration dependent stimulation of calcium mobilization with a pEC_{50} of 9.55 and maximal effects of 198 ± 29% over the basal values. Results obtained with the novel compounds are summarized in Table 19. Spiroxatrine (compound 1), taken as lead compound for the present study, mimicked the stimulatory effect of N/OFQ, showing similar maximal effect with 1000-fold lower potency (pEC_{50} 6.49). Compounds cis-4, cis-18 and cis-22 produced a concentration-dependent calcium mobilization with pEC_{50} values of 6.67, 6.57 and 6.38 respectively. The maximal effects elicited by these compounds were not significantly different from that of N/OFQ (Table 19). Compound 6 also behaved as a full agonist showing however lower potency (pEC_{50} 5.97). Compound trans-4 stimulated calcium mobilization in a concentration dependent manner with a potency value of 6.45. However the maximal effect induced by this compound was significantly lower than those produced by the standard agonist N/OFQ (Table 19 and Figure 42, Panel A). Thus, trans-4 behaved as a partial NOP agonist (Figure 42, Panel A). These compounds were inactive up to 10 μM when assayed in CHO cells expressing the Gαqi5 protein but not the NOP receptor. Thus the stimulatory effects of compounds 6, trans-4, cis-4, cis-18 and cis-22 are due to the ability of these molecules to bind and activate the NOP receptor. trans-22 produced an incomplete concentration response curve at 10 μM, stimulating calcium mobilization to 39 ± 14% over the basal value. Similar results were obtained testing compounds 5, 10, 17 and 23. Thus these molecules behaved as low potency NOP agonists. On the contrary, compounds 3, 14 and 21 did not modify calcium levels up to 10 μM. Therefore these compounds were further evaluated in antagonist-type experiments. In these studies SB-612111 was used as positive control (30). Inhibition response curves were performed against a fixed concentration of N/OFQ, approximately corresponding to its EC80. As shown in Figure 41, right panel, under the present experimental conditions, SB-612111 elicited a complete and concentration-dependent inhibition of the N/OFQ stimulatory effect. A pK_B value of 8.50 was derived from these experiments. This value is in line with previously reported findings (Camarda *et al.*, 2009; Fischetti *et al.*, 2009). In parallel experiments, compound 3 did not modify the N/OFQ stimulatory effect up to 10 μM. Compound 14 and 21 displayed weak antagonist activity only at the higher concentration tested, i.e. 10 μM.
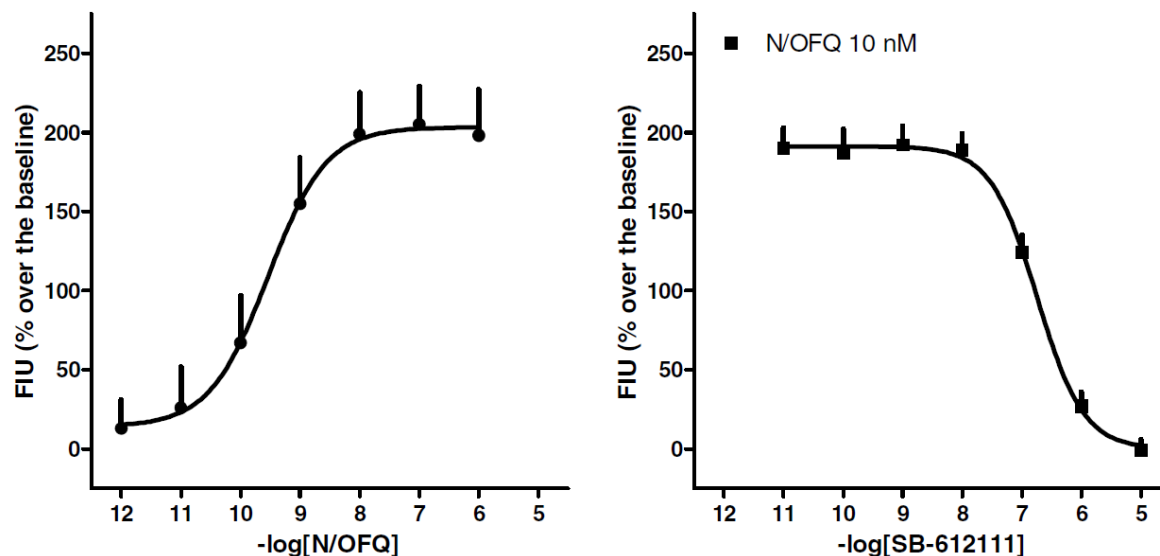
Figure 41. Calcium mobilization experiments performed in CHO$_{NOP}$ cells stably expressing the Gα_{qi5} protein. Concentration response curve to N/OFQ (left panel) and inhibition response curve to SB-612111 vs 10 nM N/OFQ (right panel). Data are the mean ± sem of at least 4 separate experiments performed in duplicate.

Finally the selectivity of compounds trans-4, cis-4 was evaluated measuring calcium mobilization in CHO cells stably expressing the Gα chimeric protein and either the MOP, DOP or KOP receptors. The results obtained are summarized in Table 19 and Figure 42. Compounds trans-4, and cis-4 did not modify calcium levels up to 10 μM in agonist-type experiment for KOP and DOP receptors highlighting a fine NOP/DOP and NOP/KOP selectivity (Figure 42 panel C and D respectively). Differently trans-4 and cis-4 produced a concentration-dependent calcium mobilization for the MOP receptor with pEC$_{50}$ values of 6.21 and 6.17 respectively, with a low NOP/MOP selectivity ratio (<0.6 and 3.2 respectively, Table 20). Notably, a reversed behaviour in selectivity was observed in comparison to NOP agonist activity and trans-4 proved to be the most active isomer suggesting complete different stereointeractions with the two NOP/MOP receptors.
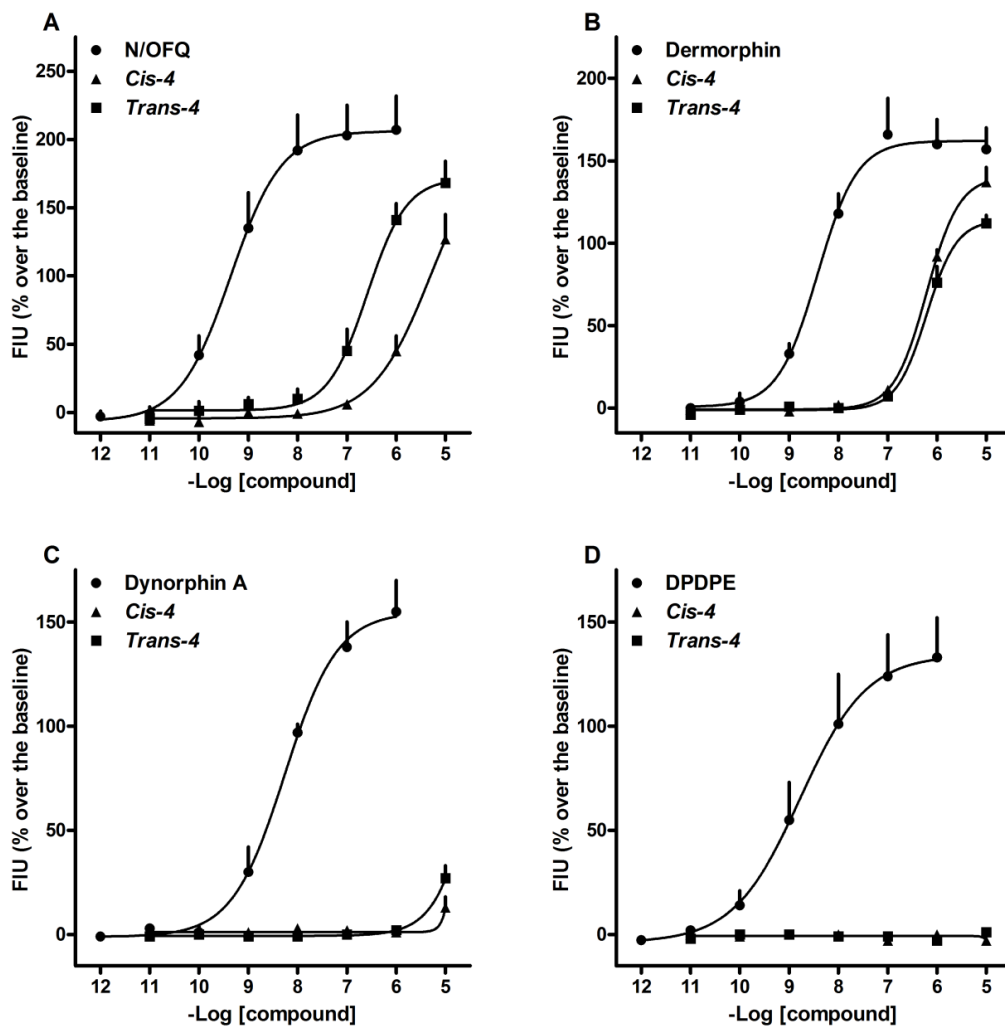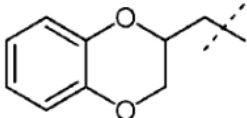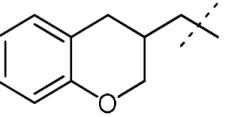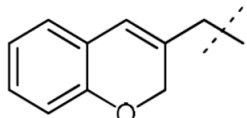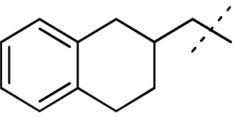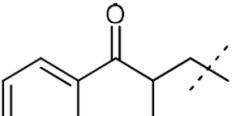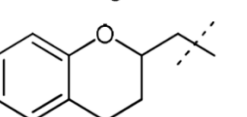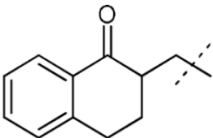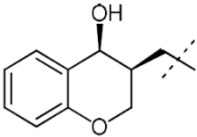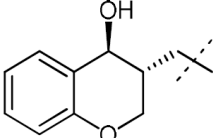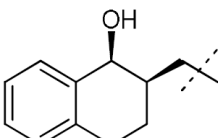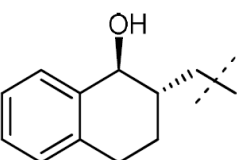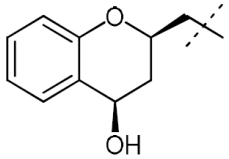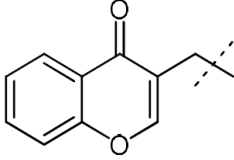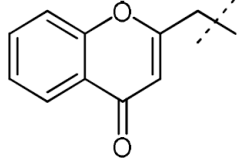
Figure 42. Calcium mobilization experiments performed in CHO cells coexpressing the chimeric G proteins and the human NOP, MOP, KOP, and DOP receptors (panels A, B, C, and D, respectively). Concentration response curves to standard agonists, cis-4 and trans-4. Data are the mean ± sem of at least 3 separate experiments performed in duplicate.

Table 19. Effects of standard and novel NOP ligands in calcium mobilization assays, performed in CHO cells coexpressing the human NOP receptor and the $G\alpha_{qi5}$ protein.
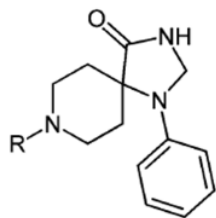
		agonist		antagonist
		pEC_{50} ($CL_{95\%}$)	$\alpha\pm$sem	pK_B ($CL_{95\%}$)
N/OFQ		9.55 (9.07–10.04)	1.00	nd
SB-612111		inactive		8.50 (8.03–8.97)
1		6.49 (5.95-7.03)	0.81±0.03	nd
6		5.97 (5.78–6.17)	1.09±0.05	nd
5		crc incomplete		nd
23		crc incomplete		nd
3		inactive		inactive
17		crc incomplete		nd

21		inactive		<6
cis-4		6.67 (6.43-6.91)	0.83±0.04	nd
trans-4		6.45 (5.77-7.13)	0.70±0.02*	nd
cis-22		6.38 (5.51-7.25)	1.01±0.41	nd
trans-22		crc incomplete		nd
cis-18		6.57 (6.06-7.08)	1.08±0.32	nd
10		crc incomplete		nd
14		inactive		<6

Agonist efficacy is expressed as intrinsic activity (α) using the maximal effect elicited by N/OFQ as internal standard (α = 1.00).
* $p < 0.05$ according to Anova followed by the Dunnett test for multiple comparisons.
inactive: inactive up to 10 μM.
crc incomplete: the concentration response curve could not be completed because of the low potency of the agonist.
< 6: the pKB could not be precisely determined because the ligand produced a weak inhibitory effect only at the highest concentration tested, i.e. 10 μM.

Table 20. Effects of trans-4, cis-4 and standard NOP, MOP, KOP, and DOP ligands in calcium mobilization.

	NOP		MOP		KOP		DOP	
	pEC_{50} (CL$_{95\%}$)	α ±sem	pEC_{50} (CL$_{95\%}$)	α ±sem	pEC_{50} (CL$_{95\%}$)	α ±sem	pEC_{50} (CL$_{95\%}$)	α ±sem
N/OFQ	9.35 (8.86–9.83)	1.00	< 5		< 6		< 5	
dermorphin	< 5		8.43 (7.98-8.87)	1.00	< 5		< 6	
dynorphin A	< 6		6.67 (6.17-7.17)	0.99 ±0.05[a]	8.29 (7.45-9.12)	1.00	7.16 (7.07-7.25)	1.10 ±0.20
DPDPE	inactive		Inactive		inactive		8.73 (8.39–9.07)	1.00
trans-4	< 6		6.21 (6.00-6.42)	0.87 ±0.06	inactive		inactive	
cis-4	6.68 (5. 96-7.41)	0.85 ±0.08	6.17 (5.88-6.45)	0.73 ±0.05	inactive		inactive	

Agonist efficacy is expressed as intrinsic activity (α) using the maximal effect elicited by N/OFQ as internal standard (α = 1.00)
Inactive: inactive up to 10 μM.
< 5 and < 6: the concentration response curve could not be completed because of the low potency of the agonist; the estimated pEC50 obtained by constraining the maximal effects were less than 5 or 6.

The isosteric substitution O-1/CH2 in the 1,4-benzodioxane nucleus of spiroxatrine (1) as represented by compound 6, results in a 3 fold decrease of agonist potency. A further decrease in potency was observed with the unsaturated benzopyran-derivative 5 and with the tetralin derivative 23 with respect to 6. These results indicate that both oxygen atoms are necessary for spiroxatrine activity at NOP receptors and the one at position 1 is probably more sensitive to isosteric replacement. By alternatively dislocation out of the ring the oxygen at position 1 and 4 of the 1,4-benzodioxane core of 1 produced the chroman-4-one derivatives 3 and 17 and it was

possible to determine that the introduction of a carbonyl group led to a severe loss of activity. These findings suggest that the introduction of an H-bond acceptor is not well tolerated. In addition, the replacement of oxygen at position 1 of the chroman-4-one derivative 3 provided the inactive α-tetralone derivative 21, confirming the role of this oxygen. Compounds 3, 17 and 21 proved to be inactive also in antagonist-type experiments; these data suggest that these compounds do not bind NOP receptor.

One moiety of 3, which gave chroman-4-ols cis- and trans-4, allowed the recovery of agonist activity, especially in the case of cis isomer that showed a pEC_{50} value of 6.67, higher than that of spiroxatrine (6.49). The favorable effect of carbonyl reduction was also observed for compound 22 obtained from the other chromanone derivative 21. Also in this case the cis isomer was more potent than the trans isomer, with a pEC_{50} value of 6.38. Further confirmation of the positive role of the hydroxyl group in this position came from the comparison of the activities of chromanone 17, regional isomer of chromanone 3, and its carbonyl-reduced derivative cis-18 which showed a pEC50 value of 6.57. Unfortunately, in the case of this 4-hydroxyl-derivative, only the cis isomer was obtained. We did not made any further effort to obtain the trans isomer since the same isomer of the alcohols 4 and 22 was less active than the cis one. For this reason, most likely also in the case of trans-18 it would have been obtained the same result.

Finally we wanted to investigate the effect of the introduction of a double bond in the chromanone structure of regional isomers 3 and 17 with the synthesized chromones 10 and 14. Proceeding from 3 to 10, a small and barely detectable agonist efficacy was seen, while the contrary seems to be true going from 17 to 14, since in this case the already weak activity disappears. Certainly such consideration is based on a very small variation of activity and might be speculative. However it is suggested that the more constrained structure of these chromones, that makes therefore planar this part of the molecule, does not favor agonist activity. This indirectly seems to confirm the importance first of a certain distortion of the lateral chain and secondly of the oxygenated function in position 4, indicating that the interaction at NOP receptor site is highly stereoselective.

In conclusion, this third panel of spiroxatrine derivatives also shown that these ligands might represent novel tools for better understanding the structural requirements necessary for NOP receptor binding and activation. Moreover with this last part of SAR studies we demonstrated that

by introducing specific group on the chromane core of this type of molecules it is possible to modulate the agonist activity notwithstanding the lipophilic portion is attached to the piperidine nitrogen by a 1-carbon linker. Since the majority of the agonists reported in literature are connected directly to the piperidine nitrogen these evidences could be useful for the development of new NOP ligands.

3.3.3. Structure activity studies of nociceptin/orphanin FQ(1-13)-NH$_2$ derivatives modified in position 5

N/OFQ and Dynorphin (Dyn) share some similarities, in particular the same length, the N-terminal part with two aromatic residues linked by a Gly-Gly spacer and a C-terminal part rich in basic residues. Despite these structural homologies, N/OFQ is highly selective for the NOP and Dyn for the KOP receptor. The systematic replacement in the C-terminus of the Dyn sequence with residues of the C-terminus of N/OFQ slightly increased affinity but did not affect potency at the NOP receptor. In contrast, further replacement of position 6 (Arg/Gly) and 5 (Lue/Thr) substantially increased affinity and produced a dramatic enhancement of NOP potency (Lapalu *et al.*, 1997). An important role of N/OFQ Thr^5 for NOP occupation/activation is also suggested by classical Ala scan studies that demonstrated a substantial loss of affinity and an even greater loss of potency of [Ala^5]N/OFQ (Dooley & Houghten, 1996; Reinscheid *et al.*, 1996).

This study was aimed to investigating the structure activity relationship of the Thr residue in position 5 of the N/OFQ sequence. To this aim N/OFQ(1-13)-NH$_2$ was used as chemical template and 28 [X^5]N/OFQ(1-13)-NH$_2$ derivatives, in which Thr was substituted with natural and unnatural residues (Figure 43), were synthesized, purified and characterized for their pharmacological action at the NOP receptor.
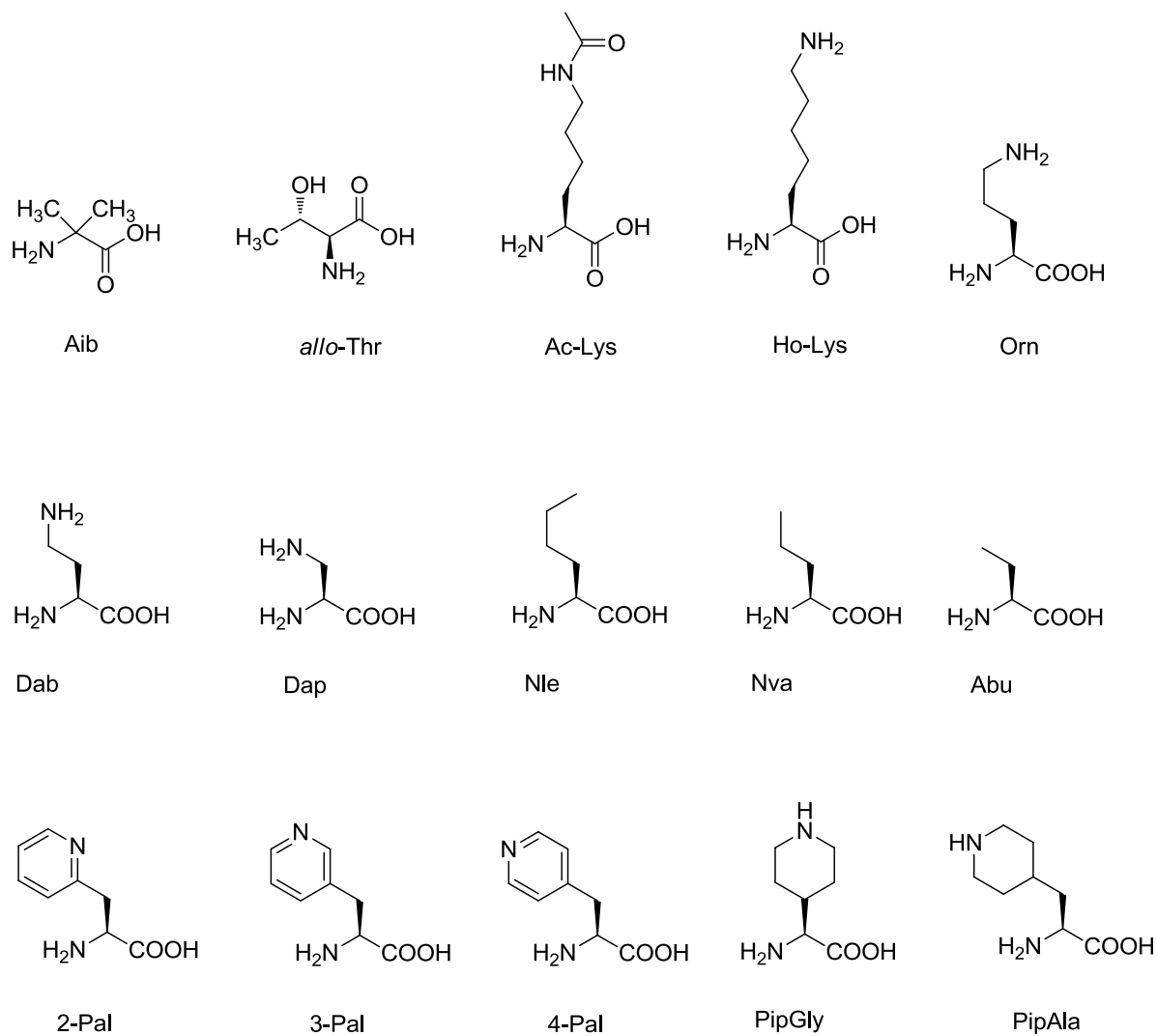
Figure 43. Chemical structure of the unnatural amino acids employed in the present study.

[^{35}S]GTPγS binding studies - N/OFQ was able to concentration dependently stimulate the [^{35}S]GTPγS binding to membranes from CHO cells stably expressing the human NOP receptor, in a concentration dependent manner showing a maximal effect of 210 ± 17 % over the basal value and a pEC$_{50}$ of 8.45. This stimulatory effect of N/OFQ was mimicked by N/OFQ(1-13)-NH$_2$ that produced a superimposable concentration response curve (E$_{max}$ 199 ± 16 %, pEC$_{50}$ 8.57). Under the same experimental conditions, [X^5]N/OFQ(1–13)-NH$_2$ analogues in which Thr was substituted with natural amino acids (compounds **1-13**) stimulated [^{35}S]GTPγS binding in a concentration dependent manner showing maximal effects similar to those evoked by the reference compound N/OFQ(1–13)-NH$_2$ (Table 1). As far as potency is concerned, compounds **5** and **10** displayed potency values similar to that of N/OFQ(1–13)-NH$_2$, while all the other analogues showed lower potency. In particular compounds **4**, **8**, **9** and **12** had EC$_{50}$ values from 3 to 10 fold lower than the reference peptide, compounds **1**, **2**, **6**, **7**, **11** and **13** had EC$_{50}$ values from 10 to 100 fold lower than N/OFQ(1–13)-NH$_2$, while compound **3** was 117 fold less potent than the standard.

In a second series of experiments the effects of [X^5]N/OFQ(1–13)-NH$_2$ analogues in which Thr was substituted with unnatural amino acids (compounds **14-28**) were investigated. All compounds stimulated [^{35}S]GTPγS binding in a concentration dependent manner with maximal effects similar to those evoked by N/OFQ(1–13)-NH$_2$ (Table 1). As far as potency is concerned, compounds **16** and **23** displayed similar potency to that of N/OFQ(1–13)-NH$_2$, while all the other analogues displayed lower potency. In particular compounds **15**, **19-22**, and **26** showed EC$_{50}$ values from 3 to 10 fold lower than the reference peptide, compounds **18**, **24**, **25**, **27**, and **28** had EC$_{50}$ values from 10 to 100 fold lower than N/OFQ(1–13)-NH$_2$, while compounds **14** and **17** were more than 100 fold less potent than the standard.

Calcium mobilization studies - N/OFQ stimulated calcium mobilization in a concentration dependent manner with a maximal effect of 238 ± 17 % over the basal values and a pEC$_{50}$ of 8.74. The stimulatory effect of N/OFQ was mimicked by N/OFQ(1-13)-NH$_2$ that produced a superimposable concentration response curve (E$_{max}$ of 232 ± 13, pEC$_{50}$ 9.07). Under the same experimental conditions, the effects of [X^5]N/OFQ(1–13)-NH$_2$ analogues in which Thr was substituted with natural amino acids were evaluated. All compounds stimulated calcium

mobilization with maximal effects similar to those evoked by the reference compound N/OFQ(1–13)-NH$_2$ (Table 2). As far as potency is concerned, compound **5** and **10** displayed potency similar to that of N/OFQ(1–13)-NH$_2$, while all the other analogues showed lower potency. In particular compounds **9** and **12** had EC$_{50}$ values from 3 to 10 fold lower than the reference peptide, compounds **1**, **4**, **6-8**, and **11** had EC$_{50}$ values from 10 to 100 fold lower than N/OFQ(1–13)-NH$_2$, while compound **2** and **13** were 159 and 760 fold less potent than the standard, respectively. Finally the potency of compound **3** could not be estimated because the compound produced an incomplete concentration response curve.

In the last series of experiments the effects of [X^5]N/OFQ(1–13)-NH$_2$ analogues in which Thr was substituted with unnatural amino acids (compounds **14-28**) were investigated. All compounds stimulated calcium mobilization in a concentration dependent manner showing maximal effects similar to those evoked by N/OFQ(1–13)-NH$_2$ (Table 2). As far as potency is concerned, compounds **21-23** displayed potency similar to that of N/OFQ(1–13)-NH$_2$, while all the other analogues showed lower potency. In particular, compound **16** was 4 fold less potent than the reference peptide, compounds **15**, **19**, **20**, and **26-28** had EC$_{50}$ values from 10 to 100 fold lower than N/OFQ(1–13)-NH$_2$, while compounds **14**, **17**, **18**, **24** and **25** were more than 100 fold less potent than the standard.

The results obtained in the [^{35}S]GTPγS binding and in the calcium mobilization assay have been compared in Figure 44: a determination coefficient (r^2) of 0.82 and a value of p<0.01 were derived from these data.

Table 21. Effects of N/OFQ, N/OFQ(1-13)-NH$_2$ and its [X^5] derivatives in [^{35}S]GTPγS binding experiments in membranes of CHO$_{hNOP}$ cells.

	Compound	pEC$_{50}$ (CL$_{95\%}$)	CR	α ± sem
	N/OFQ	8.45 (8.18-8.73)	1	1.04 ± 0.15
	N/OFQ(1-13)-NH$_2$	8.57 (8.28-8.86)	1	1.00
1	[Asp^5]N/OFQ(1-13)-NH$_2$	7.15 (6.69-7.62)	26	0.72±0.12
2	[Arg^5]N/OFQ(1-13)-NH$_2$	6.92 (5.95-7.90)	44	0.96 ±0.25
3	[Lys^5]N/OFQ(1-13)-NH$_2$	6.50 (5.23-7.77)	117	0.81 ±0.09
4	[Ser^5]N/OFQ(1-13)-NH$_2$	7.70 (6.28-9.12)	7	1.01 ±0.25
5	[Asn^5]N/OFQ(1-13)-NH$_2$	8.41 (7.87-8.96)	1	0.78 ±0.11
6	[His^5]N/OFQ(1-13)-NH$_2$	7.36 (6.59-8.12)	16	0.94 ±0.14
7	[Phe^5]N/OFQ(1-13)-NH$_2$	7.38 (6.69-8.08)	15	0.84 ±0.19
8	[Tyr^5]N/OFQ(1-13)-NH$_2$	7.75 (6.91-8.59)	7	0.85 ±0.14
9	[Leu^5]N/OFQ(1-13)-NH$_2$	7.88 (7.11-8.66)	5	0.88 ±0.11
10	[Val^5]N/OFQ(1-13)-NH$_2$	8.15 (7.31-8.99)	3	0.79 ±0.11
11	[Ala^5]N/OFQ(1-13)-NH$_2$	7.24 (6.30-8.18)	22	0.84 ±0.13
12	[Gly^5]N/OFQ(1-13)-NH$_2$	7.57 (7.19-7.94)	10	0.90 ±0.15
13	[Pro^5]N/OFQ(1-13)-NH$_2$	6.88 (6.51-7.25)	49	0.84 ±0.14
14	[Aib^5]N/OFQ(1-13)-NH$_2$	6.47 (5.66-7.28)	126	0.91 ±0.21
15	[AlloThr^5]N/OFQ(1-13)-NH$_2$	7.81 (6.97-8.65)	6	0.88 ±0.15
16	[Ac-Lys^5]N/OFQ(1-13)-NH$_2$	8.21 (7.80-8.61)	2	0.87 ±0.15
17	[HoLys^5]N/OFQ(1-13)-NH$_2$	6.36 (5.34-7.38)	163	0.94 ±0.11
18	[Orn^5]N/OFQ(1-13)-NH$_2$	6.61 (6.04-7.18)	92	0.82 ±0.11
19	[Dab^5]N/OFQ(1-13)-NH$_2$	7.87 (7.46-8.28)	5	1.01 ±0.16
20	[Dap^5]N/OFQ(1-13)-NH$_2$	7.66 (7.38-7.95)	8	1.08 ±0.14
21	[Nle^5]N/OFQ(1-13)-NH$_2$	7.90 (7.05-8.75)	5	0.77 ±0.15
22	[Nva^5]N/OFQ(1-13)-NH$_2$	8.01 (7.58-8.45)	4	0.94 ±0.09
23	[Abu^5]N/OFQ(1-13)-NH$_2$	8.44 (8.06-8.82)	1	0.98 ±0.14
24	[S-PipGly^5]N/OFQ(1-13)-NH$_2$	7.18 (6.87-7.50)	25	0.89 ±0.14
25	[PipAla^5]N/OFQ(1-13)-NH$_2$	6.65 (6.24-7.06)	84	1.07 ±0.14
26	[2-Pal^5]N/OFQ(1-13)-NH$_2$	7.79 (7.38-8.20)	6	0.91 ±0.17
27	[3-Pal^5]N/OFQ(1-13)-NH$_2$	7.45 (6.89-8.01)	13	0.75 ±0.18
28	[4-Pal^5]N/OFQ(1-13)-NH$_2$	7.31 (7.03-7.60)	18	0.90 ±0.17

CR: concentration ratio, N/OFQ(1-13)-NH$_2$ used as standard.
α: maximal effect expressed as fraction of that of N/OFQ(1-13)-NH$_2$

Table 22. Effects of N/OFQ, N/OFQ(1-13)-NH$_2$ and its [X^5] derivatives in calcium mobilization assay performed in CHO$_{hNOP}$ cells coexpressing the Gα_{qi5} protein.

	Compound	pEC$_{50}$ (CL$_{95\%}$)	CR	α ±sem
	N/OFQ	8.74 (8.57-8.92)	2	0.95 ±0.05
	N/OFQ(1-13)-NH$_2$	9.07(8.74-9.40)	1	1.00
1	[Asp^5]N/OFQ(1-13)-NH$_2$	7.37 (7.18-7.55)	35	0.99 ±0.05
2	[Arg^5]N/OFQ(1-13)-NH$_2$	7.02 (6.71-7.33)	159	0.75 ±0.03
3	[Lys^5]N/OFQ(1-13)-NH$_2$	crc incomplete		
4	[Ser^5]N/OFQ(1-13)-NH$_2$	8.44 (7.79-9.09)	30	0.87 ±0.11
5	[Asn^5]N/OFQ(1-13)-NH$_2$	8.72 (8.53-8.91)	2	1.03 ±0.06
6	[His^5]N/OFQ(1-13)-NH$_2$	7.87 (7.45-8.29)	22	0.79 ±0.05
7	[Phe^5]N/OFQ(1-13)-NH$_2$	7.24 (6.94-7.54)	48	0.99 ±0.00
8	[Tyr^5]N/OFQ(1-13)-NH$_2$	7.60 (7.37-7.82)	21	0.94 ±0.06
9	[Leu^5]N/OFQ(1-13)-NH$_2$	8.03 (7.17-8.88)	8	0.96 ±0.02
10	[Val^5]N/OFQ(1-13)-NH$_2$	8.65 (7.81-9.50)	2	0.79 ±0.13
11	[Ala^5]N/OFQ(1-13)-NH$_2$	7.71 (7.30-8.13)	16	0.90 ±0.08
12	[Gly^5]N/OFQ(1-13)-NH$_2$	8.01 (7.83-8.19)	8	0.97 ±0.06
13	[Pro^5]N/OFQ(1-13)-NH$_2$	6.04 (5.53-6.55)	760	0.85 ±0.05
14	[Aib^5]N/OFQ(1-13)-NH$_2$	6.44 (6.09-6.79)	300	0.90 ±0.04
15	[AlloThr^5]N/OFQ(1-13)-NH$_2$	7.13 (6.75-7.51)	62	0.96 ±0.01
16	[Ac-Lys^5]-N/OFQ(1-13)-NH$_2$	8.61 (7.44-9.78)	4	0.74 ±0.14
17	[HoLys^5]N/OFQ(1-13)-NH$_2$	6.61 (6.28-6.94)	406	0.71 ±0.03
18	[Orn^5]N/OFQ(1-13)-NH$_2$	6.44 (6.18-6.70)	597	0.66 ±0.10
19	[Dab^5]N/OFQ(1-13)-NH$_2$	7.82 (7.43-8.21)	25	0.64 ±0.05
20	[Dap^5]N/OFQ(1-13)-NH$_2$	7.86 (7.33-8.39)	23	0.67 ±0.06
21	[Nle^5]N/OFQ(1-13)-NH$_2$	8.91 (8.74-9.07)	2	0.86 ±0.01
22	[Nva^5]N/OFQ(1-13)-NH$_2$	8.78 (8.35-9.21)	3	0.88 ±0.04
23	[Abu^5]N/OFQ(1-13)-NH$_2$	8.80 (8.55-9.05)	3	0.90 ±0.13
24	[S-PipGly^5]N/OFQ(1-13)-NH$_2$	6.95 (6.26-7.63)	187	0.95 ±0.08
25	[PipAla^5]N/OFQ(1-13)-NH$_2$	6.33 (6.11-6.56)	773	0.74 ±0.05
26	[2-Pal^5]N/OFQ(1-13)-NH$_2$	7.65 (7.35-7.95)	37	0.81 ±0.05
27	[3-Pal^5]N/OFQ(1-13)-NH$_2$	7.57 (6.85-8.29)	45	0.80 (±0.06)
28	[4-Pal^5]-N/OFQ(1-13)-NH$_2$	8.05 (7.64-8.46)	15	0.69 (±0.05)

CR: concentration ratio, N/OFQ(1-13)-NH$_2$ used as standard.
α: maximal effect expressed as fraction of that of N/OFQ(1-13)-NH$_2$
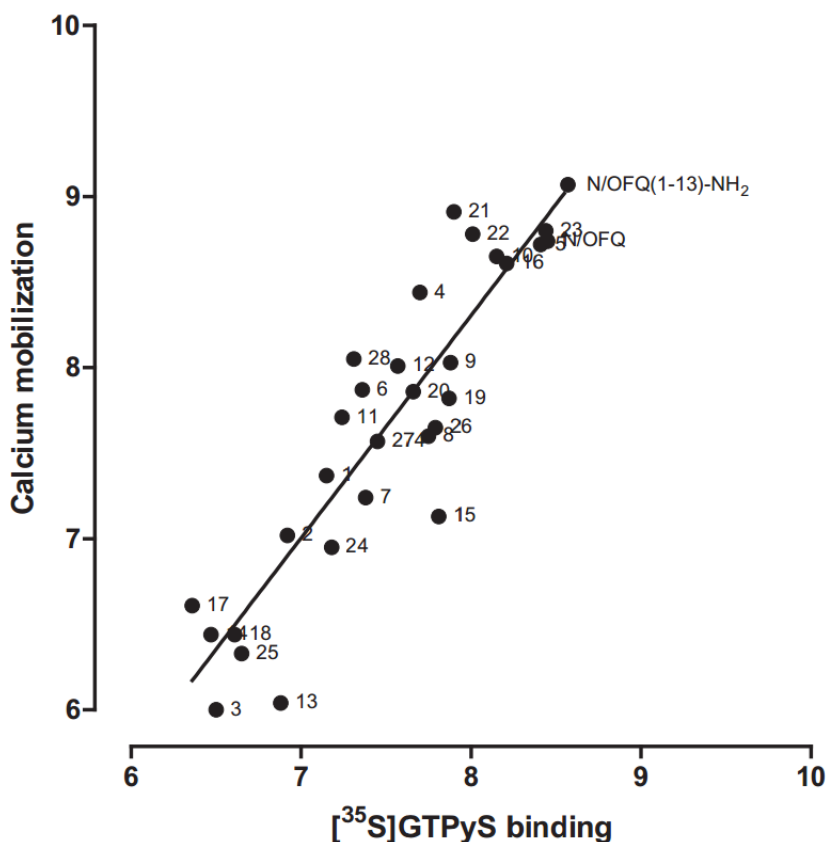
Figure 44. Correlation between agonist potency (pEC$_{50}$) of N/OFQ, N/OFQ(1-13)-NH$_2$ and its [X^5] derivatives at the human NOP receptor obtained in the [^{35}S]GTPγS binding and the calcium mobilization assays.

This study investigated the structure activity relationships of N/OFQ Thr^5. The shortest sequence maintaining the same potency and efficacy of the natural peptide namely N/OFQ(1-13)-NH$_2$ (Calo *et al.*, 1996; Guerrini *et al.*, 1997) has been used as chemical template. 13 [X^5]N/OFQ(1-13)-NH$_2$ derivatives were synthesized by substituting Thr^5 with natural amino acid residues. A further 17 [X^5]N/OFQ(1-13)-NH$_2$ derivatives were obtained using unnatural amino acids. All these compounds were assessed pharmacologically for their activity at human NOP receptors using two different functional assays: [^{35}S]GTPγS binding in cell membranes and calcium mobilization in whole cells co-expressing a chimeric G protein.

All the 28 [X^5]N/OFQ(1-13)-NH$_2$ derivatives produced maximal effects similar to those of the standard peptide in both the [^{35}S]GTPγS binding and the calcium mobilization assay, thus

consistently behaving as NOP receptor full agonists. This finding suggests that Thr^5 is important for receptor binding but not for receptor activation. Moreover the rank order of agonist potency obtained in [^{35}S]GTPγS binding and the calcium mobilization assay was virtually superimposable (determination coefficient of the correlation is r^2 = 0.82). This demonstrated that the pharmacological profile of the NOP receptor interacting with native G_i proteins and that of the same receptor artificially coupled with calcium signaling via the chimeric G protein is superimposable. In other words this result corroborates literature findings (Camarda *et al.*, 2009) demonstrating that the artificial coupling does not affect the ligand recognition features of the NOP receptor.

[X^5]N/OFQ(1-13)-NH$_2$ derivatives in which Thr^5 was substituted with natural residues displayed very different potencies. In particular, the most detrimental results were obtained using charged amino acids either with acid (compound **1**) or basic (compounds **2** and **3**) side chains. In contrast the best results were obtained using hydrophilic non charged residues such as Asn (compound **5**) or aliphatic branched side chain such as Val (compound **10**). In addition, the replacement of the secondary alcoholic function of Thr with the primary alcoholic function of Ser (compound **4**) caused a significant loss of potency. These findings suggest that the oxydryl group of Thr side chain is not crucial for receptor binding. However the spatial disposition of the alcoholic moiety of Thr may affect receptor binding. This is suggested by the loss of potency of compound **4** in which the primary alcoholic function is not chiral and of compound **15** in which the chirality of the side chain has been inverted. The replacement of Thr with aromatic residues as in compounds **6-8** caused a loss of potency. Similar results were obtained using the smallest chiral residue Ala (compound **11**). This confirms previous data obtained in classical Ala-scan studies (Dooley & Houghten, 1996; Reinscheid *et al.*, 1996). The increase in peptide flexibility obtained using the non chiral residue Gly produced a moderate loss of potency. In contrast replacement of position 5 with conformational inducer residues (the beta bend inducer Pro and the alpha helix inducer Aib) caused an important loss of potency. A similar conformational perturbation can be induced by using D residues and in line with the present findings it has been reported that [D-Thr^5]N/OFQ shows an important loss of affinity and a dramatic loss of potency compared to the natural peptide sequence (Reinscheid *et al.*, 1996). The huge effect of conformation inducing residues may probably be due to their interference with the formation of the beta bend centered on Gly^6-Ala^7 sequence which has been reported to play an important role for N/OFQ biological activity (Amodeo *et al.*, 2002).

Collectively these results suggest that the size of X^5 side chain as well as its lipo / hydrophilic balance and hydrogen bond capability are not crucial for receptor binding. In contrast the presence of an ionizable side chain, particulary in the case of Lys, produced a dramatic loss of potency.

In order to investigate in detail the reasons underlying the loss of potency induced by Thr/Lys replacement a series of $[X^5]N/OFQ(1-13)-NH_2$ derivatives generated using Lys analogues has been synthesized and assayed. The elimination of basic character of Lys by acetylation as in compound **16** restored ligand potency. This finding demonstrates that primary amino function of Lys side chain plays a crucial role in hindering receptor binding. Then we investigate the importance of the distance between the primary amino function and the peptide backbone. Increasing this distance as in compound **17** does not substantially affect ligand potency. However, reducing this distance by 1 to 3 carbon atoms (compounds **18-20**) caused a progressive recovery of potency. In addition the elimination of the primary amino function from the side chain of Lys, Orn and Dab as in compounds **21-23** produced NOP ligands almost as potent as the standard peptide. Interestingly, the presence of a secondary amino function obtained by cyclization of the side chain of Orn and Lys, and as in compounds **24** and **25**, respectively, generated ligands showing the same rank order of potency **24** > **25** displayed by their linear analogs **18** > **3**. Collectively these findings demonstrated that both the presence of the basic amino function and its distance from the peptide backbone play a very important role in disrupting peptide receptor binding.

Finally modulation of the distance from the peptide backbone of the nitrogen atom obtained with aromatic derivatives as in compounds **26-28** does not substantially affect ligand potency. This result is similar to that obtained with the natural aromatic residues Phe, Tyr and His. Thus, these findings corroborate the proposal that NOP receptor binding is sensitive to the spatial disposition of the positive charge of the basic nitrogen atom of the X^5 residue.

In conclusion this study investigated the structure activity relationship of the position 5 of N/OFQ sequence. The major findings of this investigation can be summarized as follows: i) position 5 does not play a pivotal role in receptor activation; ii) the secondary alcoholic function of Thr is not important for receptor binding; iii) side chain size, lipo / hydrophilic balance as well as hydrogen bond capability are also not crucial for receptor binding; iv) an aliphatic amino function

positively charged with at least 3 carbon atom distance from the peptide backbone has a huge disrupting effect on receptor binding.

This study in addition to extending our knowledge on the structure activity relationship of N/OFQ allowed the identification of N/OFQ(1-13)-NH$_2$ derivatives (i.e. compound 23) as potent as the natural sequence. The presence of unnatural residues e.g. Abu in the peptide sequence may at least partially prevent enzymatic degradation thus generating longer lasting effects in vivo. Further studies are needed to validate this proposal.

3.3.4. Pharmacological characterization of nociceptin/orphanin FQ tetrabranched derivatives

The present study was aimed to deeply investigate the pharmacological profile of three recently developed tetrabranched derivatives of N/OFQ (Guerrini *et al.*, 2014). These synthetic peptides were generated with an innovative chemical approach, named peptide welding technology (PWT), that allows the synthesis of multibranched peptides with extraordinary high yield, purity and reproducibility. The three N/OFQ derivatives have been named PWT1-N/OFQ, PWT2-N/OFQ, and PWT3-N/OFQ. These compounds differ exclusively in the core used: $(Lys)_2$-Lys-NH_2 for PWT1-N/OFQ, Cyclam for PWT2-N/OFQ, and $(Lys)_2$-ethylendiamine for PWT3-N/OFQ (Figure 45). The PWT N/OFQ derivatives activities were compared with those of the naturally occurring peptide in receptor binding, stimulation of $[^{35}S]GTP\gamma S$ binding, calcium mobilization, and electrically stimulated mVD assays. Results of the in vivo pharmacological activities of PWT derivatives of N/OFQ have been previously reported (Rizzi *et al.*, 2014)
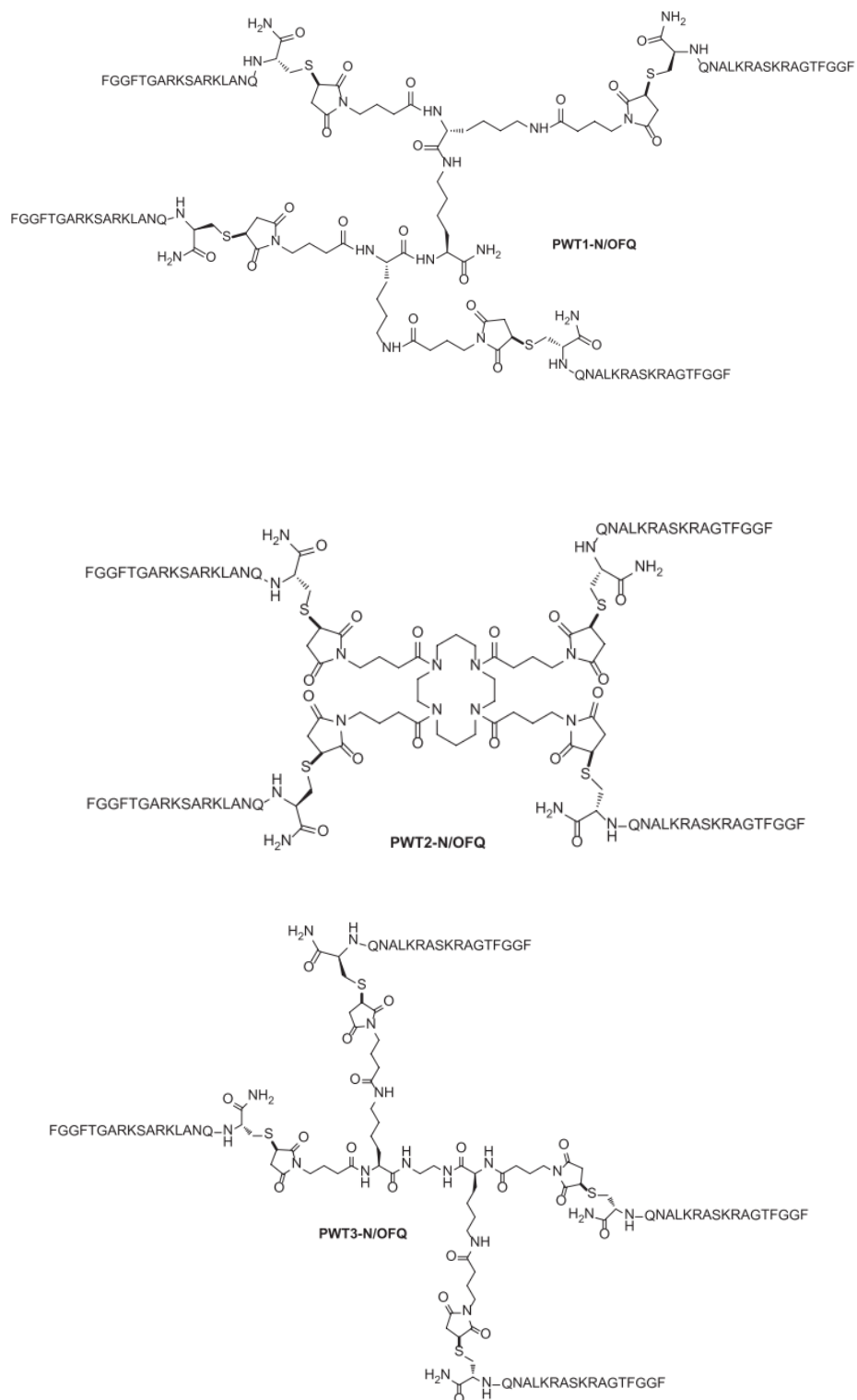
Figure 45. Chemical structures of PWT derivatives of N/OFQ.

Receptor binding - In CHO_{NOP} cell membranes N/OFQ displaced [^{3}H]UFP-101 binding in a concentration depend manner showing high affinity (pK$_i$ 9.42). Similar results were obtained with PWT derivatives of N/OFQ that displayed however increased affinity by 5 (PWT3-N/OFQ) up to 15 (PWT1-N/OFQ) fold (Table 23). To investigate selectivity over classical opioid receptors similar experiments were performed using membranes obtained from CHO cells expressing the MOP, KOP and DOP human receptors and [^{3}H]DPN as radioligand. N/OFQ up to 1 µM did not bind KOP and DOP sites while displayed micromolar affinity at MOP (pK$_i$ 6.06). All PWT derivatives showed higher affinity than N/OFQ at classical opioid receptors, however their NOP selectivity (range 2570 – 14125 fold) was never inferior to that displayed by the natural peptide (2291 fold). In parallel experiments standard ligands for classical opioid receptors displayed the expected high affinity (morphine pK$_i$ 8.57 for MOP, Dmt-Tic pK$_i$ 8.87 for DOP, and norbinaltorphimine pK$_i$ 10.69 for KOP).

Table 23 - Affinities of N/OFQ and its PWT derivatives in membranes of CHO cells expressing the human NOP or classical opioid receptors.

	NOP	MOP	KOP	DOP
	pK$_i$ (CL$_{95\%}$)	pK$_i$ (CL$_{95\%}$)	pK$_i$ (CL$_{95\%}$)	pK$_i$ (CL$_{95\%}$)
N/OFQ	9.42 (9.23 - 9.57)	6.06 (5.80 - 6.32)	< 6	< 6
PWT1-N/OFQ	10.60 (10.10 - 11.10)	6.45 (6.21 - 6.69)	6.40 (6.01 - 6.79)	6.38 (6.07 - 6.69)
PWT2-N/OFQ	10.30 (9.99 - 10.61)	6.60 (6.31 - 6.89)	6.36 (5.80 - 6.92)	< 6
PWT3-N/OFQ	10.10 (9.74 - 10.46)	6.69 (6.19 - 7.19)	6.33 (5.98 - 6.68)	< 6

Data are the mean of 3 separate experiments performed in duplicate.

Stimulated [^{35}S]GTPγS binding - In CHO_{NOP} cell membranes N/OFQ stimulated [^{35}S]GTPγS binding in a concentration dependent manner with maximal effects equal to 3.5 ± 0.2 and pEC$_{50}$ of 8.84 (Figure 45, top panel). PWT derivatives of N/OFQ mimicked the stimulatory effect of the natural peptide showing similar maximal effects but higher potency (7-19 fold more potent than N/OFQ). In fact the pEC$_{50}$ of PWT compounds were in the range 9.71 - 10.12 (Figure 45, top panel).

Calcium mobilization assay - In CHO$_{NOP}$ cells stably expressing the Gα_{qi5} chimeric protein and human NOP recombinant receptor, N/OFQ and its PWT derivatives evoked a concentration dependent stimulation of calcium release (Figure 45, bottom panel). N/OFQ displayed high potency (pEC$_{50}$ 9.39) and maximal effects (237 $\pm$ 15% over the basal values). PWT derivatives of N/OFQ mimicked the peptide stimulatory effects showing similar maximal effects but slightly lower potency (pEC$_{50}$ 8.75 $-$ 9.16) (Figure 45, bottom panel). Inhibition response experiments were performed by testing increasing concentrations (10 pM $-$ 10 μM) of the standard NOP antagonist SB-612111 against a fixed concentration of agonist approximately corresponding to its EC$_{80}$ (10 nM for N/OFQ and 30 nM for all PWT derivatives). SB-612111 concentration dependently inhibited the stimulatory effect of N/OFQ, displaying a pK$_B$ value of 8.01. Similar results were obtained challenging the antagonist against the stimulatory effect of PWT1-N/OFQ, PWT2-N/OFQ and PWT3-N/OFQ. pK$_B$ values of SB-612111 vs PWT compounds were in the range 7.82 $-$ 8.23.
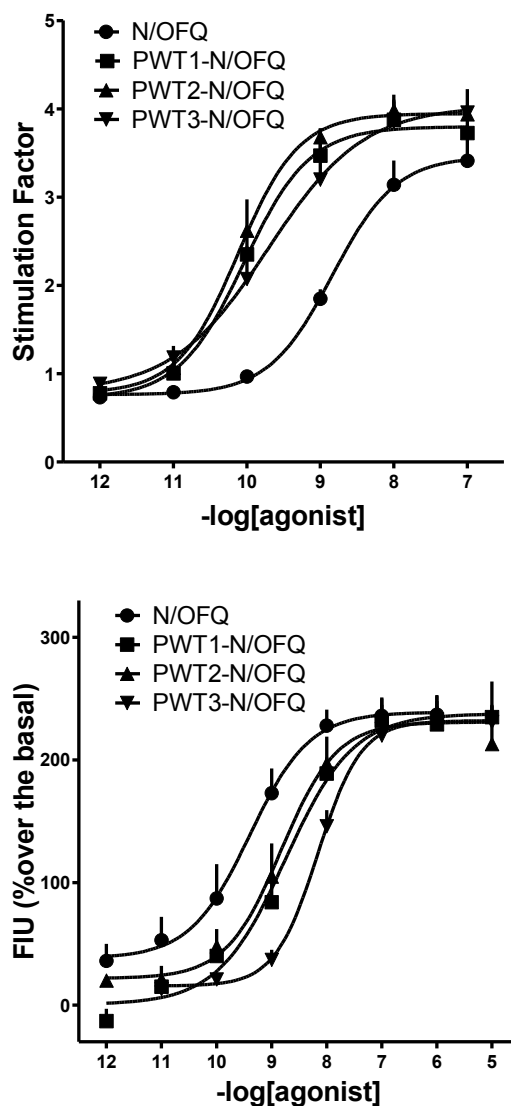
Figure 45 - Concentration response curves to N/OFQ and its PWT derivatives in [^{35}S]GTPγS binding experiments performed in CHO$_{NOP}$ cell membranes (top panel) and in calcium mobilization experiments performed on CHO cells coexpressing the NOP receptor and the Gα$_{qi5}$ chimeric protein (bottom panel). Data are mean ± sem of 4 experiments performed in duplicate.

In order to assess the selectivity of action of PWT derivatives of N/OFQ, calcium mobilization experiments were also performed in cells expressing chimeric G protein and the classical opioid receptors MOP, DOP and KOP. In this series of experiments dermorphin, DPDPE and dynorphin A were used as standard agonists for MOP, DOP and KOP, respectively. Opioid ligands were all

inactive up to 1 µM in CHO_{NOP} cells (Table 23). In cells expressing the MOP receptor dermorphin evoked concentration dependent stimulatory effects with pEC_{50} of 9.29 and maximal effects of 135 ± 21 %. The stimulatory effects of dermorphin were mimicked by dynorphin A that was however approx. 300 fold less potent. In these cells DPDPE, N/OFQ and its PWT derivatives, were found inactive up to 1 µM. In cells expressing the DOP receptor DPDPE evoked concentration dependent stimulatory effects with pEC_{50} of 9.57 and maximal effects of 86 ± 14 %. Dynorphin A was also able to elicit calcium mobilization in these cells producing similar maximal effects but being approximately 100 fold less potent. All the other agonists were inactive up to 1 µM. Finally, in KOP cells dynorphin A stimulated calcium release in a concentration dependent manner with very high potency (pEC_{50} of 10.04) and maximal effects of 225 ± 10 %. All other agonists were inactive in these cells.

Table 23 - Calcium mobilization studies. Potencies of N/OFQ, its PWT derivatives, and standard opioid agonists in CHO cells expressing the human NOP or classical opioid receptors and chimeric proteins.

	NOP	MOP	DOP	KOP
	pEC_{50} ($CL_{95\%}$)	pEC_{50} ($CL_{95\%}$)	pEC_{50} ($CL_{95\%}$)	pEC_{50} ($CL_{95\%}$)
N/OFQ	9.39 (9.23 - 9.57)	< 6	< 6	< 6
PWT1-N/OFQ	8.75 (8.35 - 9.15)	< 6	< 6	< 6
PWT2-N/OFQ	8.83 (8.47 - 9.18)	< 6	< 6	< 6
PWT3-N/OFQ	9.16 (9.08 - 9.24)	< 6	< 6	< 6
Dermorphin	< 6	9.29 (9.19 - 9.38)	< 6	< 6
DPDPE	< 6	< 6	9.57 (9.03 - 10.11)	< 6
Dynorphin A	< 6	6.76 (6.50 - 7.02)	7.63 (7.38 – 7.88)	10.04 (9.93 – 10.16)

Data are the mean of 3 separate experiments performed in duplicate.

Electrically stimulated isolated tissue experiments - PWT1-N/OFQ mimicked the inhibitory effect of N/OFQ producing similar maximal effects but showing approximately 3 fold higher potency (pEC_{50} 7.85). Similar results were obtained by testing PWT2-N/OFQ and PWT3-N/OFQ: both molecules elicited maximal effects similar to those of N/OFQ being more potent than the natural peptide (Figure 46). Interestingly enough, the inhibitory effect induced by N/OFQ takes place immediately after adding the peptide to the bath and was immediately reversible after washing the tissue (Figure 47). On the contrary, PWT1-N/OFQ induced a slower inhibitory effect which was rather resistant to washing (Figure 47). Superimposable results both in terms of slow kinetic and washing resistant effects were obtained with PWT2-N/OFQ and PWT3-N/OFQ (not shown).
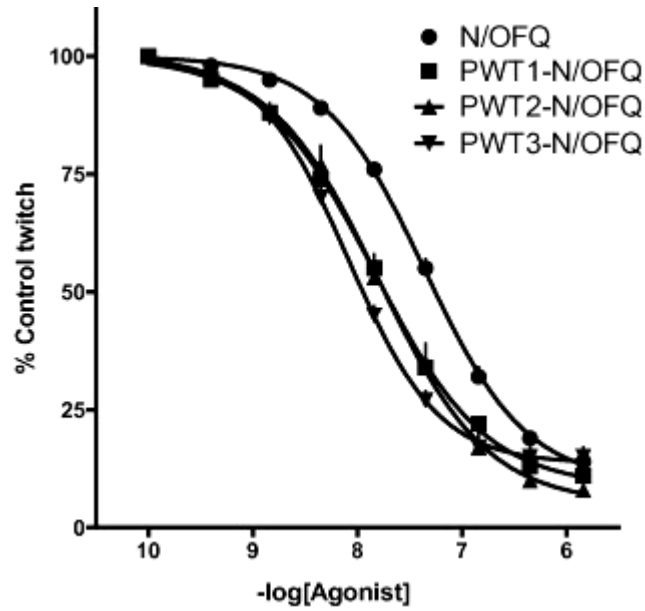
Figure 46. Concentration response curves to N/OFQ, PWT1-N/OFQ, PWT2-N/OFQ and PWT3-N/OFQ in the electrically stimulated mouse vas deferens. The values are means ± SEM of 4 separate experiments
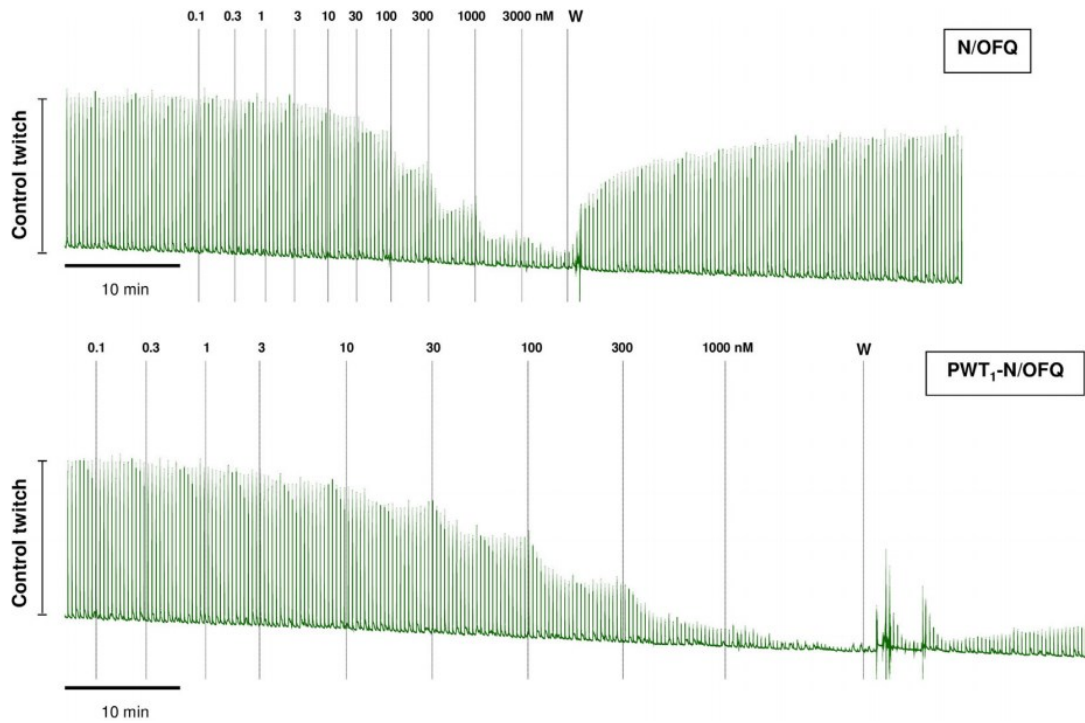
Figure 47. Typical tracings showing concentration response curves to N/OFQ and to PWT1-N/OFQ. Note the slow kinetic of PWT1-N/OFQ action and slow and incomplete reversal after washing

The inhibitory effects elicited by equieffective concentrations of N/OFQ and PWT1-N/OFQ, that is, 30 and 10 nM, respectively was challenged versus the NOP antagonist SB-61211123 using a curative protocol. As shown in Figure 48 SB-612111 1 μM rapidly and fully reversed the inhibitory effect of N/OFQ and PWT1-N/OFQ.
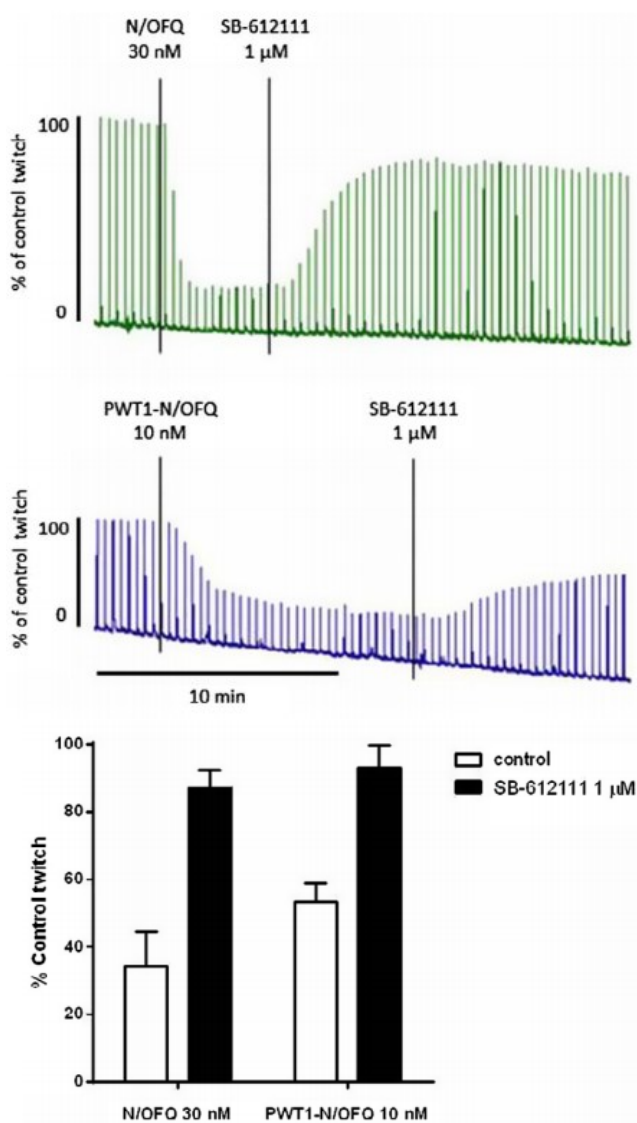
Figure 48. Typical tracings showing the curative effect of SB-612111 1 μM vs. the inhibitory action of equieffective concentrations of N/OFQ and to PWT1-N/OFQ. The bar graph summarizes the results obtained in 5 separate experiments.

In a separate series of experiments, concentration response curves to N/OFQ, PWT1-N/OFQ, PWT2-N/OFQ, and PWT3-N/OFQ were performed in the absence and presence of SB-612111. SB-612111 100 nM did not modify per se the control twitches but produced a rightward shift of the concentration response curve to N/OFQ without modifying the maximal effect induced by the agonist (Figure 49, top left panel). A pK_B value of 8.48 was derived from these data. Similar findings were obtained by challenging SB-612111 versus PWT compounds. Of note the pK_B value obtained for SB-612111 against PWT1-N/OFQ (8.02) was slightly lower than those obtained against N/OFQ or the other PWT compounds (Figure 49 and Table 24).
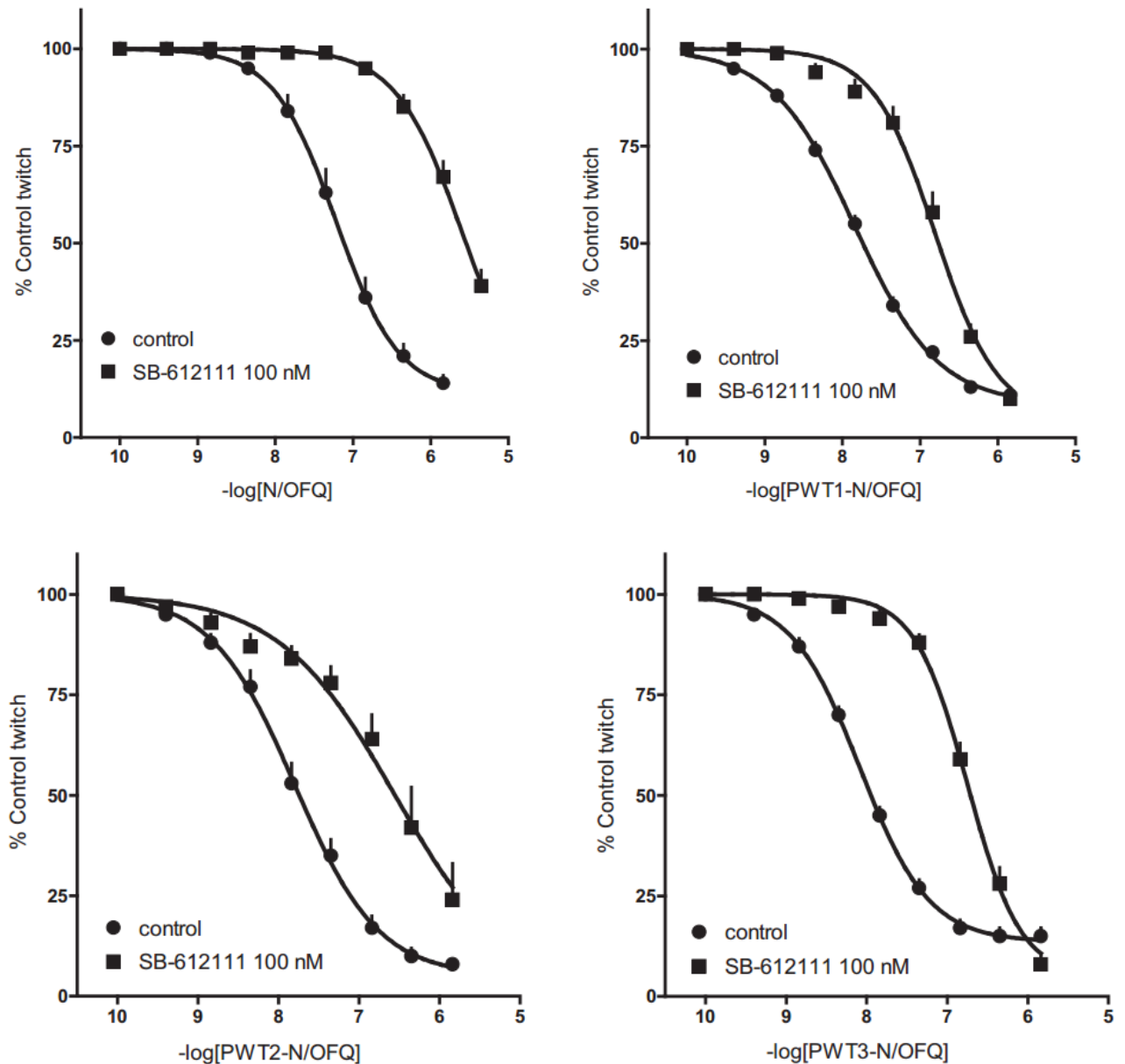
Figure 49. Concentration-response curve to N/OFQ (top left panel), PWT1-N/OFQ (top right panel), PWT2-N/OFQ (bottom left panel) and PWT3-N/OFQ (bottom right panel) obtained in the absence (control) and in the presence of SB-612111 (100 nM) in the electrically stimulated mouse vas deferens. The values are means ± SEM of at least 4 separate experiments.

Table 24. Agonist effects of N/OFQ and its PWT derivatives and antagonist potency of SB-612111 in the electrically stimulated mouse vas deferens.

	$E_{max} \pm$ sem	pEC_{50} ($CL_{95\%}$)	pK_B ($CL_{95\%}$) SB-612111
N/OFQ	88±1	7.37 (7.29-7.45)	8.48 (8.19-8.77)
PWT1-N/OFQ	89±1	7.85 (7.73-7.97)	8.02 (7.84-8.20)
PWT2-N/OFQ	93±2	7.78 (7.57-7.99)	8.22 (7.61-8.83)
PWT3-N/OFQ	85±2	8.08 (7.99-8.17)	8.33 (8.17-8.49)

Data are mean of at least 4 separate experiments.

In tissues taken from NOP(-/-) the inhibitory effects elicited by the natural peptide N/OFQ were no longer evident (Figure 50). In contrast the three PWT derivatives of N/OFQ maintained the ability to inhibit the electrically induced contractions in NOP(-/-) tissues showing however reduced potency by more than 10 fold for PWT1-N/OFQ and approximately 100 fold for PWT2-N/OFQ and PWT3-N/OFQ (Figure 50). The selective DOP receptor agonist DPDPE produced similar inhibitory effects in NOP(+/+) and NOP(-/-) tissues showing high potency ($pEC_{50} \approx 8.5$) and maximal effects (≈ 95 %) (data not shown).
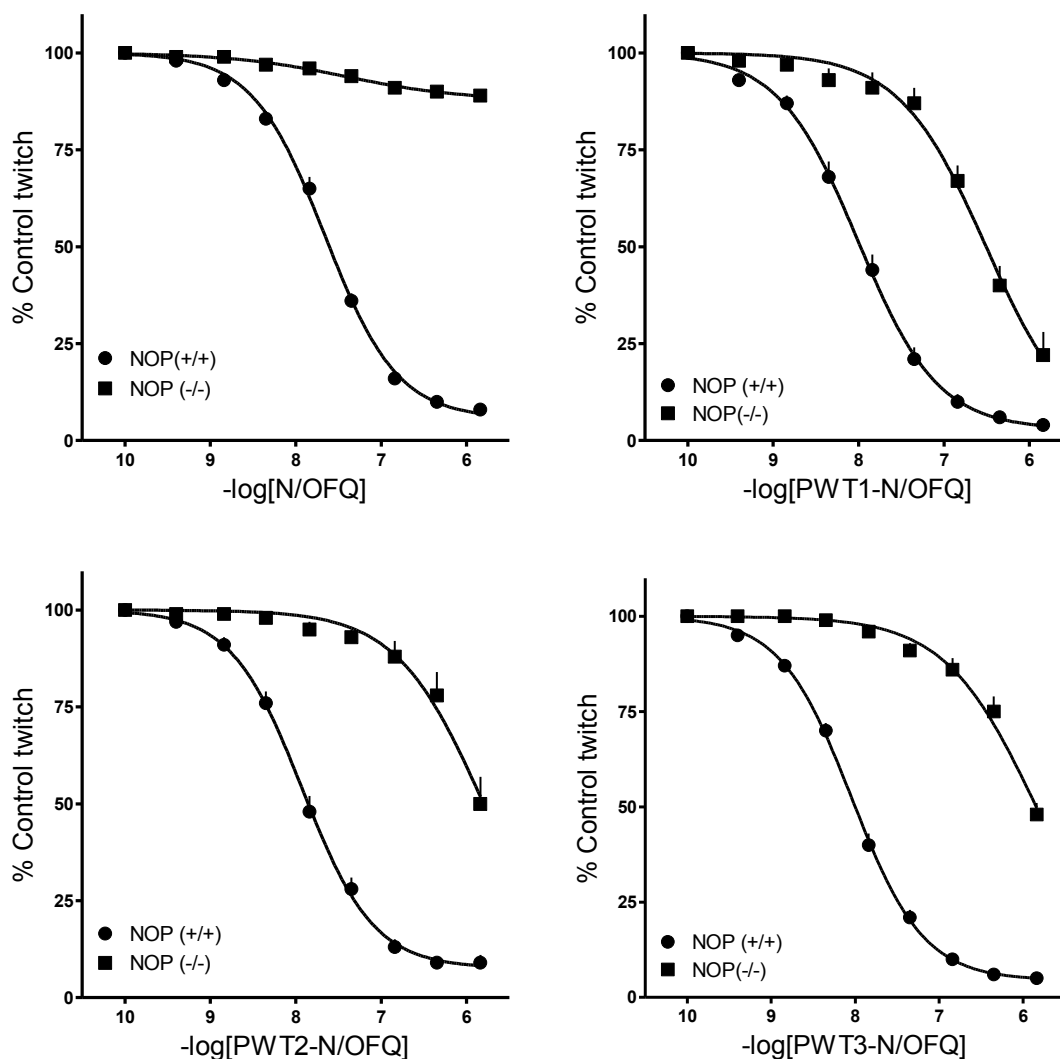
Figure 50. Concentration response curve to N/OFQ and its PWT derivatives in electrically stimulated mouse vas deferens taken from NOP(+/+) and NOP(-/-) animals. Data are mean ± sem of 4 experiments.

The in vivo effects of PWT derivatives of N/OFQ have been evaluated on spontaneous locomotor activity and in food intake studies in mice (Guerrini *et al.*, 2014; Rizzi *et al.*, 2014). Without going into details, PWT derivatives showed, compared to N/OFQ, an increase in terms of potency in inhibiting the mice locomotor activity and in the orexigenic effects, and exhibited a prolonged duration of action, i.e. PWT2-N/OFQ showed a significant inhibitory effects after 24 hours of i.c.v. injection while N/OFQ was no more active.

Collectively, in this study we investigated the pharmacological profile of tetrabranched derivatives of N/OFQ generated using the PWT technology. In vitro experiments demonstrated that PWT compounds bound the NOP receptor with high affinity and behaved as full agonists both at human recombinant and animal native receptors. While NOP selectivity over classical opioid receptors was not affected, knockout studies in isolated tissues documented, compared to N/OFQ, a decline in selectivity of the PWT compounds, which was modest or moderate depending on the type of core. In vivo studies have confirmed the ability of PWT compounds to mimic the effects of N/OFQ and their higher potency. In addition the in vivo duration of action of PWT derivatives is far longer than that of N/OFQ. The results obtained in the present study, together with those published, demonstrated that the PWT technology can be successfully applied to the N/OFQ peptide sequence to generate novel NOP ligands that display compared to the natural peptide similar biological activity but extremely prolonged duration of action.

In receptor binding studies performed on membranes obtained from cells stably expressing the human NOP receptor N/OFQ displayed subnanomolar affinity (pK_i 9.42) in line with previous studies (9.62, (Camarda *et al.*, 2009), 9.68, (Spagnolo *et al.*, 2007)). PWT derivatives of N/OFQ concentration dependently displaced [^{3}H]N/OFQ binding displaying higher affinity than N/OFQ by 3 to 10 fold. This result is in line with previous findings that showed that N/OFQ dendrimers displaced [^{3}H]N/OFQ binding from rat brain membranes with 4.5 fold higher affinity than N/OFQ (Bracci *et al.*, 2003). Similar results were also reported with multibranched derivatives of other peptide sequences including Leu-enkephalin (9 fold), Met-enkephalin (4 fold), and neurotensin(8-13) (12 fold) (Bracci *et al.*, 2003). Even larger increases in affinity of multibranched peptides compared to the native peptide sequence, from 20 to 350 fold depending on the linker unit used, was reported in the case of melanocyte stimulating hormone (Brabez *et al.*, 2011). However no differences were found when the full sequence of neurotensin was used (Bracci *et al.*, 2003). Thus an increase in binding affinity of multibranched peptides compared to the natural sequences seems to be a rather general rule even if there are significant differences depending on the specific peptide sequence and the linker used.

In functional assays performed on the human recombinant NOP receptor ([^{35}S]GTPγS binding and calcium mobilization) and at native NOP receptors expressed in the mouse vas deferens PWT compounds mimicked the actions of N/OFQ producing similar maximal effects. Thus PWT compounds always behave as NOP receptor full agonists. This applies to PWT1-N/OFQ, PWT2-N/OFQ and PWT3-N/OFQ and therefore we can suggest that the different cores used for

generating these compounds have negligible if any impact on the ability of the peptide sequence to adopt the biologically active conformation responsible for full agonist pharmacological activity.

As far as potency is concerned the following rank order of potency has been measured in the $[^{35}S]GTP\gamma S$ binding assay and mouse vas deferens assay PWT1-N/OFQ = PWT2-N/OFQ = PWT3-N/OFQ > N/OFQ. These results are in line with the increased affinity displayed by PWT compounds in binding studies. However an opposite result has been obtained in calcium mobilization studies where N/OFQ displayed a value of potency higher than those of PWT compounds. Since the rank order of agonist potency is considered the receptor fingerprint this discrepant result deserves attention. The calcium mobilization assay is based on the aberrant signaling generated by the chimeric $G\alpha_{qi5}$ protein that forces the NOP receptor to signal via the calcium pathway. Therefore it is possible that the aberrant signaling may cause modifications of the pharmacological profile of the receptor. However the following considerations argue against this proposal. In a previous systematic study a large panel of NOP ligands, including full and partial agonists as well as antagonists, has been evaluated in the calcium assay and the results we obtained were superimposable to those of classical G_i based assays and tissues studies (Camarda *et al.*, 2009). Moreover it is reasonable to assume that N/OFQ and PWT compounds interact with the binding pocket of the NOP receptor (whose 3D structure is now available (Thompson *et al.*, 2012)) with the same chemical structures i.e. the N/OFQ N-terminal tetrapeptide FGGF (Calo & Guerrini, 2013). Thus other reasons may account for the discrepant result. As mentioned in the results section, PWT compounds displayed in the mouse vas deferens slow kinetic of action compared to N/OFQ. Camarda and colleagues showed that the calcium mobilization assay tends to underestimate the potency of agonists characterized by a slow interaction with the NOP receptor (Camarda *et al.*, 2009) such the peptides UFP-112 (Rizzi *et al.*, 2007), UFP-113 (Arduin *et al.*, 2007) and ZP120 (Rizzi *et al.*, 2002) and the non peptide Ro 64-6198 (Rizzi *et al.*, 2001). This phenomenon may derive from the non equilibrium conditions which characterize the calcium assay. In fact the relatively long time needed to obtain the full activation of the NOP receptor by slowly equilibrating agonists is not compatible with the rapid and transient nature of the calcium response. This may likely explain the underestimation of the potency of N/OFQ PWT derivatives in this assay. Interestingly Charlton and Vauquelin made simulations in two different experimental systems modeled to mimic the $[^{35}S]GTP\gamma S$ binding and the calcium assay with two

133

different agonists: a high affinity slowly associating ligand (L1) and a lower affinity fast onset ligand (L2). The simulation displayed an opposite rank order of potency of agonists in the two assays with L1 > L2 in the system mimicking the [^{35}S]GTPγS assay and L2 > L1 in the system mimicking the calcium assay (see for details Figure 4 of (Charlton & Vauquelin, 2010)). Thus the results of this simulation perfectly match our experimental data obtained with N/OFQ and its PWT derivatives; this suggests that the reversal of the rank order of agonist potency measured in the calcium assay may likely derive from kinetic artifacts.

As far as receptor selectivity is concerned receptor binding and calcium mobilization studies demonstrated that the high selectivity of N/OFQ over classical opioid receptors is maintained by PWT derivatives. The molecular basis for the selectivity of action of NOP ligands over classical opioid receptors have been recently documented comparing the 3D crystal structure of these receptors (Filizola & Devi, 2013). In the NOP receptor binding pocket the N-terminal tetrapeptide of the N/OFQ related peptide UFP-101 (Nphe-Gly-Gly-Phe) make the same hydrophobic interactions as the aromatic rings of C-24 (the ligand used to generate the NOP crystal), and the N-terminal amino group forms a salt bridge with Asp 130 thus supporting a close similarity in the binding poses between small molecules and peptides (Thompson *et al.*, 2012). Although this information is relative to the inactive form of these receptors (i.e. in complex with antagonists) most likely similar mechanisms regulate the interaction of N/OFQ with the NOP receptor and its selectivity over classical opioid receptor as discussed in detail in (Calo & Guerrini, 2013). These same molecular mechanisms are not affected by applying the PWT technology to the N/OFQ sequence since tetra branched derivatives of N/OFQ displayed similar selectivity over classical opioid receptor as N/OFQ itself.

SB-612111 counteracted the inhibitory effect exerted by N/OFQ in the electrically stimulated vas deferens producing a rightward shift of the concentration response curve to N/OFQ without modifying its maximal effects and showing a pK$_B$ value of 8.48; this value of antagonist potency is superimposable to that previously reported in literature (8.50 (Spagnolo *et al.*, 2007)). Similar results were obtained by challenging SB-612111 against PWT-N/OFQ compounds both in terms of competitive interaction and antagonist potency. This result demonstrated that the action of PWT-N/OFQ compounds derives from their ability to bind and activate the NOP receptor. In other words, these findings suggest that PWT-N/OFQ compounds do not lose the high selectivity of action of the natural peptide N/OFQ. Of note the potency of SB-612111 against PWT1-N/OFQ was slightly lower. This may suggest that the NOP selectivity of this derivative is lower than that

of N/OFQ and the other PWT compounds. Thus PWT2 and PWT3 seem to be better than PWT1 in terms of maintaining the high selectivity of action of the natural peptide sequence.

For further clarifying the selectivity of action of PWT compounds, N/OFQ and its PWT derivatives were tested in tissues taken from NOP(+/+) and NOP(-/-) mice. The inhibitory effect exerted by N/OFQ in the electrically stimulated vas deferens of NOP(+/+) mice was no longer evident in tissues taken from NOP(-/-) animals. This is in line with findings previously obtained in NOP(-/-) mice (Carra *et al.*, 2005; Rizzi *et al.*, 2007) and in NOP(-/-) rats (Rizzi *et al.*, 2011). In parallel experiments PWT derivatives of N/OFQ were still active in NOP(-/-) tissues although showing reduced potency from 20 (PWT1-N/OFQ) to more than 100 fold (PWT2-N/OFQ and PWT3-N/OFQ). These findings, together with the antagonism results, indicate that the absolute selectivity of N/OFQ seems to be affected by the application of the PWT technology and tetrabranched derivatives of N/OFQ are able to interact in this preparation at relatively high concentrations with an undefined receptor to inhibit the twitch response. Interestingly the loss of selectivity of tetrabranched peptides is moderate for PWT1-N/OFQ and modest for PWT2-N/OFQ and PWT3-N/OFQ; thus it seems that the PWT2 and PWT3 cores are superior to PWT1 in maintaining the selectivity of action of the natural sequence. Further studies are needed to investigate if this is a general phenomenon of if it depends on the specific peptide sequence used to generate the PWT derivatives. However the partial loss of selectivity displayed by PWT derivatives in the mouse vas deferens should not be overemphasized. In fact in this assay off target effects were reported for different non peptide NOP agonists. For instance Ro 64-6198 (Jenck *et al.*, 2000), the most extensively published non peptide NOP agonist (Shoblock, 2007), mimicked N/OFQ inhibitory effect in the mouse vas deferens. However in this preparation the effects of Ro 64-6198 could not be antagonized by selective NOP antagonists ([Nphe[1]]N/OFQ(1-13)-NH$_2$, J-113397) even in the presence of naloxone (Rizzi *et al.*, 2001). Other molecules such as Ro 65-6570 (Wichmann *et al.*, 2000) or SCH 221510 (Varty *et al.*, 2008) were also able to inhibit the twitch response of the mouse vas deferens however their effects were not sensitive to the NOP antagonist J-113397 and their concentration response curves in NOP(+/+) and in NOP(-/-) tissues were superimposable (Molinari *et al.*, 2012).

For evaluating the in vivo pharmacological activities of PWT derivatives of N/OFQ, the mouse locomotor activity (LA) assay was used in our laboratories. In the original article reporting its identification, N/OFQ was shown to inhibit LA after supraspinal administration (Reinscheid *et*

al., 1995). This was later confirmed in mice and rats in different laboratories (Lambert, 2008). However, some studies have reported biphasic effects of N/OFQ on LA with low doses producing stimulation and high doses producing inhibition (Florin *et al.*, 1996). The exclusive involvement of the NOP receptor in this action of N/OFQ has been firmly demonstrated in both receptor antagonism and knockout studies (Calo and Guerrini, 2013). In the present study, in the first series of experiments we performed dose–response curves to N/OFQ and to its PWT derivatives by measuring the animal behaviour for 120 min. N/OFQ produced biphasic effects depending upon the dose and time. In particular, relatively low doses of peptide produced stimulatory effects, whereas high doses produced robust inhibitory effects during the first hour after administration and stimulatory effects during the second hour. A similar pattern of effects was measured in response to the supraspinal administration of PWT derivatives of N/OFQ, with the following major differences: agonist potency and onset and duration of action. The biphasic effect of N/OFQ on LA associated with the very different onset and duration of action of the natural peptide versus PWT derivatives makes the comparison of the dose–response curves and the calculation of agonist potency quite difficult. However, the profound inhibition of locomotor behavior obtained immediately after the injection of 10 nmol of N/OFQ and after 2 h (PWT2-N/OFQ) or more (PWT1-N/OFQ and PWT3-N/OFQ) from the injection of PWT compounds suggests an approximate dose-ratio of 40. This increase in agonist potency is larger than that observed in *in vitro* studies. This may possibly derive from the lower susceptibility to peptidase action reported for multibranched peptides compared with the free peptide sequence. In fact, Bracci *et al.* (2003) demonstrated that N/OFQ was degraded within 2 h of incubation with serum or rat brain membranes, whereas a tetrabranched derivative of N/OFQ was still detectable after 24 h. Interestingly, a structure-based hypothesis of branched peptide resistance to proteolysis has been proposed previously (Falciani *et al.*, 2007b). Since peptide metabolism is likely to be more relevant *in vivo* than *in vitro*, it is reasonable to assume that the lower susceptibility to peptidase action contributes to the increased agonist potency displayed by these compounds *in vivo*. Another major difference between N/OFQ and PWT-N/OFQ action is the kinetic of action. The onset of PWT-N/OFQ action is delayed compared with that of N/OFQ and the duration of action seems to be longer. In fact, the inhibitory effects exerted by PWT compounds at the higher dose tested were more pronounced during the second than the first hour after injection. Interestingly, these *in vivo* differences parallel the kinetic of action of these compounds *in vitro* in the mVD where they mimicked N/OFQ actions but showed slower kinetic and wash-resistant effects. To

further investigate the duration of action of PWT derivatives of N/OFQ, an overnight experiment was performed where the effects of equieffective doses of N/OFQ and PWT derivatives were compared. The results of this experiment clearly demonstrate that N/OFQ produces short lasting effects, whereas those elicited by PWT derivatives lasted for the whole period of observation. To further investigate possible differences in the duration of action of PWT derivatives, animals were injected with the same doses and their LA was measured 24 h after injection. Mice treated with N/OFQ and PWT1-N/OFQ displayed a locomotor behaviour similar to that of saline treated animal, whereas mice treated with PWT3-N/OFQ displayed reduced LA, although the differences did not reach a statistical level of significance. In contrast, even after 24 h from the injection, mice treated with PWT2-N/OFQ displayed a statistically significant reduction in the horizontal and vertical activities and increase in immobility time. Collectively, these *in vivo* studies demonstrated that PWT compounds mimic the effects of N/OFQ on LA, but with higher potency and much longer duration of action. In particular, PWT2-N/OFQ was found to be the PWT derivative showing the longest duration of action. Thus, the PWT2 seems to be the best core in terms both of retaining the selectivity of action of the native peptide sequence and of increasing, by several fold, the *in vivo* duration of action. To investigate the involvement of the NOP receptor in the *in vivo* action of PWT2-N/OFQ, the effect of this compound on LA was assessed in NOP(+/+) and NOP(−/−) mice. PWT2-N/OFQ 250 pmol induced a robust inhibitory effect on LA of NOP(+/+) mice while being completely inactive in NOP(−/−) animals. This result clearly demonstrates that the action of PWT2-N/OFQ on LA, similar to what has previously been reported for N/OFQ (Nishi *et al*., 1997; Carra *et al*., 2005), is exclusively due to stimulation of NOP receptors. Collectively, the results from the *in vitro* and *in vivo* studies demonstrate that PWT2-N/OFQ is a full agonist of the NOP receptor characterized by high potency, good selectivity and remarkable *in vivo* duration of action. Among available ligands, the most potent and selective agonist for the NOP receptor is the peptide UFP-112, which was designed using a combination of several chemical modifications that increase NOP receptor affinity/potency and/or reduce susceptibility to enzymatic degradation (Rizzi *et al*., 2007; Calo *et al*., 2011). Compared with UFP-112, PWT2-N/OFQ displays slightly lower potency and selectivity of action. However, the duration of action of PWT2-N/OFQ is longer than that of UFP-112. In fact, the inhibitory effects of UFP-112 on LA lasted for about 6 h (Rizzi *et al*., 2007), whereas those elicited by PWT2-N/OFQ were still evident after 24 h from injection. In conclusion, the present study showed that the PWT can be successfully applied to the peptide sequence of N/OFQ to

generate tetrabranched derivatives characterized by a pharmacological profile similar to the native peptide, but associated with a higher potency and a marked prolongation of action *in vivo*. The compound PWT2-N/OFQ displayed good selectivity and the longest duration of action *in vivo*. This NOP receptor ligand is therefore proposed as a novel research tool particularly to investigate those conditions in which a prolonged activation of the NOP receptor may evoke beneficial effects. More generally, the PWT strategy may be easily used to generate innovative and interesting ligands for peptide GPCRs. Using the PWT2 core, we are planning to generate and study several PWT derivatives obtained with different peptide sequences characterized by diverse pharmacological activity (antagonist, partial and full agonists). The information coming from these studies will allow us to firmly establish the value of the PWT strategy for the generation of innovative ligands for peptide receptors.

In conclusion, the in vitro studies demonstrated that PWT derivatives of N/OFQ behave as potent full agonists at human recombinant and animal native NOP receptors and display a profile of NOP selectivity which is inferior to that of N/OFQ but clearly superior to that of the available non peptide NOP agonists. In vivo results demonstrated confirmed high NOP selectivity and demonstrated high potency associated to extremely prolonged duration of action. In summary this study provide evidence that the PWT technology can be successfully applied to the peptide sequence of N/OFQ to generate tetrabranched derivatives characterized by a pharmacological profile similar to the native peptide associated with an higher potency and a marked prolongation of action in vivo. The compound PWT2-N/OFQ displayed good selectivity and the longest duration of action in vivo. PWT2-N/OFQ is therefore proposed as a novel research tool particularly to investigate those conditions in which a prolonged activation of the NOP receptor may evoke beneficial effects.

4. General conclusions

This thesis summarized an intensive work aimed to a twofold aim: pharmacologically characterize novel ligands and set-up and validate innovative in vitro assays for investigating NOP and classical opioid receptors.

In the frame of these studies both peptide and non peptide ligands have been investigated. Innovative ligands of peptide nature for targeting NOP and classical opioid receptors are certainly useful because of the well known pharmacodynamic advantages of peptides such as high potency associated to extraordinary selectivity of action. On the other hand peptides have poor pharmacokinetic properties due to their high molecular weight and low metabolic resistance. Thus, these compounds are extremely useful pharmacological tools but, at least in most of the cases, poor candidates as drug prototypes. Opposite considerations can be done for small molecules. In fact non peptide compounds display in general good pharmacokinetic properties such as capability to cross biological membranes including the blood brain barrier, high metabolic stability, good bioavalability, etc. On the other hand in most of the cases is difficult with small molecules to get high potency associated with high selectivity and this is often the reason underling off target side effects. However small molecules have been and still are the standard source for generating drug candidates.

The calcium mobilization assay performed on cells expressing chimeric G proteins was used for investigating the pharmacological profile of several molecules acting as NOP or classical opioid receptor ligands. As far as opiates molecules are concerned, an intensive SAR work has been performed on morphine and oxymorphone, targeting position 17 and position 6 of morphine. These SAR studies led to the discovery of a novel and interesting MOP selective ligand (i.e. 14-methoxy-6-cyanomorphine) and contributed to increase the knowledge of morphine SAR within the three classical opioid receptors. Another SAR study has been conducted on endomorphin-2 related cyclic pentapeptides. This study let to the identification of interesting mixed opioid receptor ligands based on the structure p-MePhe[4] substituted cyclic EM-2 that displayed remarkable antinociceptive activity after supraspinal administration. As far as NOP ligands are concerned, it has been demonstrated that the non peptide compound NiK-21273 behaves as a highly potent, competitive, and selective NOP receptor antagonist. In addition this compound has

been used to confirm and extend evidence that NOP antagonist have therapeutic potential as novel drug for treating Parkinson disease. Always in the field non peptide NOP ligands three SAR studies were performed on spiroxatrine derivatives. These studies identified the role of different substituents in different positions for NOP receptor binding and activation. Some of these compounds displayed moderate potency acting as NOP receptor agonists. SAR studies were also performed on N/OFQ related peptides. In this field a systematic study of position Thr[5] was performed by substituting this residue with natural and unnatural aminoacids. The results of this study suggest that position 5 does not play a pivotal role in receptor activation; the secondary alcoholic function of Thr is not important for receptor binding; side chain size, lipo/hydrophilic balance as well as hydrogen bond capability are also not crucial for receptor binding; an aliphatic amino function positively charged with at least 3 carbon atom distance from the peptide backbone has a huge disrupting effect on receptor binding. In conclusion this study demonstrated that a simple ethyl side chain is sufficient in N/OFQ position 5 for maintaining bioactivity. Always in the field of novel peptide ligands for the NOP receptor, in the present thesis we deeply investigated three tetrabranched derivatives of N/OFQ synthesized with an innovative chemical approach named PWT. PWT1-N/OFQ, PWT2-N/OFQ, and PWT3-N/OFQ are very interesting NOP ligands that maintain in vitro the same pharmacological profile of the natural peptide. Interestingly enough PWT derivatives mimicked the in vivo effects of N/OFQ on locomotor activity being more potent and displaying an extraordinary long lasting duration of action. Similar results were recently obtained by testing PWT2-N/OFQ as spinal analgesic in mice and non human primates (Rizzi et al., personal communication). A similar in vitro pharmacology associated with an increased in vivo potency and particularly duration of action seems to be a general feature of PTW derivative of peptide ligands. This is suggested by results obtained applying the PWT modification to different peptide sequences including natural tachykinins (substance P, neurokinin A and B) REF and neuropeptide S REF. Studies are under way to investigate the in vitro and in vivo pharmacology of PWT derivatives of other biologically active peptides including the DOP preferring agonist Leu-enkephalin, the MOP selective agonist dermorphin, the NOP selective antagonist UFP-101, and the universal opioid receptor agonist [Dmt[1]]N/OFQ(1-13)NH$_2$. When the results of these ongoing studies will be available we may draw well grounded conclusions on the general value of PWT derivatives as innovative ligands for peptidergic receptors.

A parallel aim of the present thesis was to extend and validate the use of calcium mobilization assay performed on cells expressing chimeric G proteins for studying the classical opioid receptors. Cells expressing either MOP or KOP receptors and the $G\alpha_{qi5}$ chimeric G protein, displayed satisfactory signal to noise ratios, while cells expressing the DOP receptor and the $G\alpha_{qi5}$ have been put aside for cells expressing the most efficient $G\alpha_{qG66Di5}$ chimeric protein. A quite large panel of standard opioid ligands including full agonists and pure antagonists have been pharmacologically characterized in calcium mobilization experiments. Despite few cases where artifacts have been recognized (i.e. underestimation of the potency of slow interacting agonists and unsurmountable behavior of slow dissociating competitive antagonists), the data obtained are robust and perfectly in line with literature results. This corroborate the validity of the calcium mobilization assay as primary screening test. The usefulness and convenience of the calcium mobilization assay applied to the field of NOP and classical opioid receptor pharmacology is convincingly demonstrated by the large list of compounds of different chemical nature evaluated in the present thesis and by the good match obtained by comparing the results of the calcium assay with those obtained with classical methods for investigating G_i coupled receptors.

A BRET based assay was setup for investigating the ability of a panel of NOP receptor ligands of different pharmacological activity to promote or block NOP/G protein and NOP/arrestin interaction. NOP/G protein interaction studied in cell membranes allows a precise estimation of ligand potency and efficacy with values highly consistent with the known pharmacological profile of this receptor as determined with classical biochemical assays for Gi coupled receptors as well as with bioassay studies on animal tissues. The same panel of ligands displayed marked differences in the ability to promote NOP/β-arrestin 2 interactions. Full agonists displayed in general lower potency and some of them an inverted rank order of potency. This reversal in agonist order of potency strongly suggest biased agonism. Compounds acting as partial agonist at NOP/G-protein behaved as competitive antagonists at NOP/β-arrestin 2 and similar values of potency in the two assays. Antagonists displayed similar values of potency for NOP/$G\beta_1$ and NOP/β-arrestin 2 interaction and perfectly the same rank order. Thus this study represents the first attempt to investigate NOP receptor functional selectivity. Accumulating evidence in the field of GPCR including opioids suggests that functional selectivity and biased agonists might be a completely innovative strategy to dissociate the biological actions elicited by a selective ligand.

In other words biased agonists by maximizing beneficial effects and/or reducing side effects can be proposed as entirely novel class of more effective / safer drugs. N/OFQ via selective stimulation of the NOP receptor exerts multiple biological actions and several therapeutic indications has been proposed for NOP selective agonists (i.e. spinal analgesia, anxiolysis, cough, urinary incontinence) and antagonists (i.e. depression, Parkinson, sepsis). Clearly such a large panel of biological functions controlled by the N/OFQ/NOP receptor system may represents and important drawback in terms of drug development. Thus the identification of G protein and arrestin NOP receptor biased agonists together with the knowledge of which biological functions depend on NOP/G protein or NOP/arresting signaling may allow the scientific community to activate rational programs for the development of NOP biased agonist as innovative drugs. In this perspective our laboratory is going to activate SAR studies aimed at identify arresting biased agonists and to investigate the phenotype and the response to N/OFQ of β-arrestin 2 knockout mice in several behavioral assays.

In summary the studies performed in the frame of my PhD project extend our knowledge on the pharmacological profile of NOP and classical opioid receptors, provided to the scientific community novel compounds, pharmacologically characterized in detail, to be used as research tools and possibly as drug prototypes, and made available novel pharmacological assays useful for selecting fully innovative drugs such as NOP receptor biased agonists.

References

Alexander SP, Benson HE, Faccenda E, Pawson AJ, Sharman JL, Spedding M, Peters JA, Harmar AJ, Collaborators C (2013). The Concise Guide to PHARMACOLOGY 2013/14: G protein-coupled receptors. *British journal of pharmacology* **170**(8)**:** 1459-1581.

Amodeo P, Guerrini R, Picone D, Salvadori S, Spadaccini R, Tancredi T, Temussi PA (2002). Solution structure of nociceptin peptides. *J Pept Sci* **8**(9)**:** 497-509.

Arduin M, Spagnolo B, Calo G, Guerrini R, Carra G, Fischetti C, Trapella C, Marzola E, McDonald J, Lambert DG, Regoli D, Salvadori S (2007). Synthesis and biological activity of nociceptin/orphanin FQ analogues substituted in position 7 or 11 with Calpha,alpha-dialkylated amino acids. *Bioorganic & medicinal chemistry* **15**(13)**:** 4434-4443.

Auld DS, Southall NT, Jadhav A, Johnson RL, Diller DJ, Simeonov A, Austin CP, Inglese J (2008). Characterization of chemical libraries for luciferase inhibitory activity. *Journal of medicinal chemistry* **51**(8)**:** 2372-2386.

Ayoub MA, Trinquet E, Pfleger KD, Pin JP (2010). Differential association modes of the thrombin receptor PAR1 with Galphai1, Galpha12, and beta-arrestin 1. *FASEB journal : official publication of the Federation of American Societies for Experimental Biology* **24**(9)**:** 3522-3535.

Battisti UM, Corrado S, Sorbi C, Cornia A, Tait A, Malfacini D, Cerlesi MC, Calo G, Brasili L (2014). Synthesis, enantiomeric separation and docking studies of spiropiperidine analogues as ligands of the nociceptin/orphanin FQ receptor. *MedChemComm* **5**(7)**:** 973-983.

Beckett AH, Casy AF (1954). Synthetic analgesics: stereochemical considerations. *The Journal of pharmacy and pharmacology* **6**(12)**:** 986-1001.

Ben Haddou T, Beni S, Hosztafi S, Malfacini D, Calo G, Schmidhammer H, Spetea M (2014a). Pharmacological investigations of N-substituent variation in morphine and oxymorphone: opioid receptor binding, signaling and antinociceptive activity. *PloS one* **9**(6)**:** e99231.

Ben Haddou T, Malfacini D, Calo G, Aceto MD, Harris LS, Traynor JR, Coop A, Schmidhammer H, Spetea M (2014b). Exploring pharmacological activities and signaling of morphinans substituted in position 6 as potent agonists interacting with the mu opioid receptor. *Molecular pain* **10:** 48.

Bertorelli R, Corradini L, Rafiq K, Tupper J, Calo G, Ongini E (1999). Nociceptin and the ORL-1 ligand [Phe1psi (CH2-NH)Gly2]nociceptin(1-13)NH2 exert anti-opioid effects in the Freund's adjuvant-induced arthritic rat model of chronic pain. *British journal of pharmacology* **128**(6)**:** 1252-1258.

Black JW, Leff P (1983). Operational models of pharmacological agonism. *Proceedings of the Royal Society of London. Series B, Containing papers of a Biological character. Royal Society* **220**(1219)**:** 141-162.

Bohn LM, Lefkowitz RJ, Caron MG (2002). Differential mechanisms of morphine antinociceptive tolerance revealed in (beta)arrestin-2 knock-out mice. *The Journal of neuroscience : the official journal of the Society for Neuroscience* **22**(23)**:** 10494-10500.

Bohn LM, Lefkowitz RJ, Gainetdinov RR, Peppel K, Caron MG, Lin FT (1999). Enhanced morphine analgesia in mice lacking beta-arrestin 2. *Science* **286**(5449)**:** 2495-2498.

Brabez N, Lynch RM, Xu L, Gillies RJ, Chassaing G, Lavielle S, Hruby VJ (2011). Design, synthesis, and biological studies of efficient multivalent melanotropin ligands: tools toward melanoma diagnosis and treatment. *Journal of medicinal chemistry* **54**(20)**:** 7375-7384.

Bracci L, Falciani C, Lelli B, Lozzi L, Runci Y, Pini A, De Montis MG, Tagliamonte A, Neri P (2003). Synthetic peptides in the form of dendrimers become resistant to protease activity. *J Biol Chem* **278**(47)**:** 46590-46595.

Brunton LL, Chabner B, Knollman BrC, Goodman LSPbot (2011). *Goodman & Gilman's The pharmacological basis of therapeutics*. 12th ed. / editor, Laurence L. Brunton ; associate editors, Bruce A. Chabner, Bjorn C. Knollmann. edn. McGraw-Hill: New York, N.Y. ; London.

Calo' G, Guerrini R (2013). Medicinal Chemistry, Pharmacology, and Biological Actions of Peptide Ligands Selective for the Nociceptin/Orphanin FQ Receptor. In: (ed)^(eds). *Research and Development of Opioid-Related Ligands*, edn, Vol. 1131: American Chemical Society. p^pp 275-325.

Calo G, Bigoni R, Rizzi A, Guerrini R, Salvadori S, Regoli D (2000a). Nociceptin/orphanin FQ receptor ligands. *Peptides* **21**(7)**:** 935-947.

Calo G, Guerrini R (2013). Medicinal Chemistry, Pharmacology, and Biological Actions of Peptide Ligands Selective for the Nociceptin/Orphanin FQ Receptor. In: (ed)^(eds). *Research and Development of Opioid-Related Ligands*, edn, Vol. 1131: American Chemical Society. p^pp 275-325.

Calo G, Guerrini R, Bigoni R, Rizzi A, Marzola G, Okawa H, Bianchi C, Lambert DG, Salvadori S, Regoli D (2000b). Characterization of [Nphe(1)]nociceptin(1-13)NH(2), a new selective nociceptin receptor antagonist. *British journal of pharmacology* **129**(6)**:** 1183-1193.

Calo G, Guerrini R, Rizzi A, Salvadori S, Burmeister M, Kapusta DR, Lambert DG, Regoli D (2005). UFP-101, a peptide antagonist selective for the nociceptin/orphanin FQ receptor. *CNS drug reviews* **11**(2)**:** 97-112.

Calo G, Guerrini R, Rizzi A, Salvadori S, Regoli D (2000c). Pharmacology of nociceptin and its receptor: a novel therapeutic target. *British journal of pharmacology* **129**(7)**:** 1261-1283.

Calo G, Rizzi A, Bodin M, Neugebauer W, Salvadori S, Guerrini R, Bianchi C, Regoli D (1997). Pharmacological characterization of nociceptin receptor: an in vitro study. *Canadian journal of physiology and pharmacology* **75**(6)**:** 713-718.

Calo G, Rizzi A, Bogoni G, Neugebauer V, Salvadori S, Guerrini R, Bianchi C, Regoli D (1996). The mouse vas deferens: a pharmacological preparation sensitive to nociceptin. *European journal of pharmacology* **311**(1)**:** R3-5.

Calo G, Rizzi A, Marzola G, Guerrini R, Salvadori S, Beani L, Regoli D, Bianchi C (1998). Pharmacological characterization of the nociceptin receptor mediating hyperalgesia in the mouse tail withdrawal assay. *British journal of pharmacology* **125**(2)**:** 373-378.

Calo G, Rizzi A, Rizzi D, Bigoni R, Guerrini R, Marzola G, Marti M, McDonald J, Morari M, Lambert DG, Salvadori S, Regoli D (2002). [Nphe1,Arg14,Lys15]nociceptin-NH2, a novel potent and selective antagonist of the nociceptin/orphanin FQ receptor. *British journal of pharmacology* **136**(2)**:** 303-311.

Camarda V, Calo G (2013). Chimeric G proteins in fluorimetric calcium assays: experience with opioid receptors. *Methods in molecular biology* **937:** 293-306.

Camarda V, Fischetti C, Anzellotti N, Molinari P, Ambrosio C, Kostenis E, Regoli D, Trapella C, Guerrini R, Salvadori S, Calo G (2009). Pharmacological profile of NOP receptors coupled with calcium signaling via the chimeric protein $G\alpha_{qi5}$. *Naunyn-Schmiedeberg's archives of pharmacology* **379:** 599-607.

Carra G, Rizzi A, Guerrini R, Barnes TA, McDonald J, Hebbes CP, Mela F, Kenigs VA, Marzola G, Rizzi D, Gavioli E, Zucchini S, Regoli D, Morari M, Salvadori S, Rowbotham DJ, Lambert DG, Kapusta DR, Calo G (2005). [(pF)Phe4,Arg14,Lys15]N/OFQ-NH2 (UFP-102), a highly potent and selective agonist of the nociceptin/orphanin FQ receptor. *J Pharmacol Exp Ther* **312**(3)**:** 1114-1123.

Casella I, Ambrosio C, Gro MC, Molinari P, Costa T (2011). Divergent agonist selectivity in activating beta1- and beta2-adrenoceptors for G-protein and arrestin coupling. *The Biochemical journal* **438**(1)**:** 191-202.

Charlton SJ, Vauquelin G (2010). Elusive equilibrium: the challenge of interpreting receptor pharmacology using calcium assays. *British journal of pharmacology* **161**(6)**:** 1250-1265.

Cheng ZJ, Fan GH, Zhao J, Zhang Z, Wu YL, Jiang LZ, Zhu Y, Pei G, Ma L (1997). Endogenous opioid receptor-like receptor in human neuroblastoma SK-N-SH cells: activation of inhibitory G protein and homologous desensitization. *Neuroreport* **8**(8)**:** 1913-1918.

Ciccocioppo R, Angeletti S, Sanna PP, Weiss F, Massi M (2000). Effect of nociceptin/orphanin FQ on the rewarding properties of morphine. *European journal of pharmacology* **404**(1-2)**:** 153-159.

Ciruela F, Jacobson KA, Fernandez-Duenas V (2014). Portraying G protein-coupled receptors with fluorescent ligands. *ACS chemical biology* **9**(9)**:** 1918-1928.

Conklin BR, Farfel Z, Lustig KD, Julius D, Bourne HR (1993). Substitution of three amino acids switches receptor specificity of Gq alpha to that of Gi alpha. *Nature* **363**(6426)**:** 274-276.

Corbani M, Gonindard C, Meunier JC (2004). Ligand-regulated internalization of the opioid receptor-like 1: a confocal study. *Endocrinology* **145**(6)**:** 2876-2885.

DeLean A, Munson PJ, Rodbard D (1978). Simultaneous analysis of families of sigmoidal curves: application to bioassay, radioligand assay, and physiological dose-response curves. *The American journal of physiology* **235**(2)**:** E97-102.

DeWire SM, Yamashita DS, Rominger DH, Liu G, Cowan CL, Graczyk TM, Chen XT, Pitis PM, Gotchev D, Yuan C, Koblish M, Lark MW, Violin JD (2013). A G protein-biased ligand at the mu-opioid receptor is potently analgesic with reduced gastrointestinal and respiratory dysfunction compared with morphine. *J Pharmacol Exp Ther* **344**(3)**:** 708-717.

Dietis N, McDonald J, Molinari S, Calo G, Guerrini R, Rowbotham DJ, Lambert DG (2012). Pharmacological characterization of the bifunctional opioid ligand H-Dmt-Tic-Gly-NH-Bzl (UFP-505). *British journal of anaesthesia* **108**(2)**:** 262-270.

Dooley CT, Houghten RA (1996). Orphanin FQ: receptor binding and analog structure activity relationships in rat brain. *Life sciences* **59**(1)**:** PL23-29.

Dooley CT, Spaeth CG, Berzetei-Gurske IP, Craymer K, Adapa ID, Brandt SR, Houghten RA, Toll L (1997). Binding and in vitro activities of peptides with high affinity for the nociceptin/orphanin FQ receptor, ORL1. *J Pharmacol Exp Ther* **283**(2)**:** 735-741.

Emami-Nemini A, Roux T, Leblay M, Bourrier E, Lamarque L, Trinquet E, Lohse MJ (2013). Time-resolved fluorescence ligand binding for G protein-coupled receptors. *Nature protocols* **8**(7)**:** 1307-1320.

Evans CJ, Keith DE, Jr., Morrison H, Magendzo K, Edwards RH (1992). Cloning of a delta opioid receptor by functional expression. *Science* **258**(5090)**:** 1952-1955.

Fenalti G, Giguere PM, Katritch V, Huang XP, Thompson AA, Cherezov V, Roth BL, Stevens RC (2014). Molecular control of delta-opioid receptor signalling. *Nature* **506**(7487)**:** 191-196.

Ferrari SL, Pierroz DD, Glatt V, Goddard DS, Bianchi EN, Lin FT, Manen D, Bouxsein ML (2005). Bone response to intermittent parathyroid hormone is altered in mice null for {beta}-Arrestin2. *Endocrinology* **146**(4)**:** 1854-1862.

Fichna J, Janecka A, Costentin J, Do Rego JC (2007). The endomorphin system and its evolving neurophysiological role. *Pharmacol Rev* **59**(1)**:** 88-123.

Fichna J, Perlikowska R, Wyrebska A, Gach K, Piekielna J, do-Rego JC, Toth G, Kluczyk A, Janecki T, Janecka A (2011). Effect of 2',6'-dimethyl-L-tyrosine (Dmt) on pharmacological activity of cyclic endomorphin-2 and morphiceptin analogs. *Bioorganic & medicinal chemistry* **19**(23)**:** 6977-6981.

Filizola M, Devi LA (2013). Grand opening of structure-guided design for novel opioids. *Trends in pharmacological sciences* **34**(1)**:** 6-12.

Fischetti C, Camarda V, Rizzi A, Pela M, Trapella C, Guerrini R, McDonald J, Lambert DG, Salvadori S, Regoli D, Calo G (2009). Pharmacological characterization

of the nociceptin/orphanin FQ receptor non peptide antagonist Compound 24. *European journal of pharmacology* **614**(1-3)**:** 50-57.

Fleming FF, Yao L, Ravikumar PC, Funk L, Shook BC (2010). Nitrile-containing pharmaceuticals: efficacious roles of the nitrile pharmacophore. *Journal of medicinal chemistry* **53**(22)**:** 7902-7917.

Fredriksson R, Lagerstrom MC, Lundin LG, Schioth HB (2003). The G-protein-coupled receptors in the human genome form five main families. Phylogenetic analysis, paralogon groups, and fingerprints. *Molecular pharmacology* **63**(6)**:** 1256-1272.

Furchgott RF (1966). The use of beta-haloaklylamines in the differentiation of the receptors and in the determination of dissociation constants of receptor–agonist complexes. *N.J. Harper, A.B. Simmonds (Eds.) Advances in Drug Research. Academic Press*.

Furst S, Hosztafi S (2008). The chemical and pharmacological importance of morphine analogues. *Acta physiologica Hungarica* **95**(1)**:** 3-44.

Gavioli EC, Calo G (2013). Nociceptin/orphanin FQ receptor antagonists as innovative antidepressant drugs. *Pharmacology & therapeutics* **140**(1)**:** 10-25.

Ge X, Qiu Y, Loh HH, Law PY (2009). GRIN1 regulates micro-opioid receptor activities by tethering the receptor and G protein in the lipid raft. *J Biol Chem* **284**(52)**:** 36521-36534.

Goto Y, Arai-Otsuki S, Tachibana Y, Ichikawa D, Ozaki S, Takahashi H, Iwasawa Y, Okamoto O, Okuda S, Ohta H, Sagara T (2006). Identification of a novel spiropiperidine opioid receptor-like 1 antagonist class by a focused library approach featuring 3D-pharmacophore similarity. *Journal of medicinal chemistry* **49**(3)**:** 847-849.

Greedy BM, Bradbury F, Thomas MP, Grivas K, Cami-Kobeci G, Archambeau A, Bosse K, Clark MJ, Aceto M, Lewis JW, Traynor JR, Husbands SM (2013). Orvinols with mixed kappa/mu opioid receptor agonist activity. *Journal of medicinal chemistry* **56**(8)**:** 3207-3216.

Greiner E, Schottenberger H, Wurst K, Schmidhammer H (2001). Novel class of morphinans with acrylonitrile incorporated substructures as key intermediates for non-oxygen-bridged opioid ligands. *Journal of the American Chemical Society* **123**(16)**:** 3840-3841.

Griffin MT, Figueroa KW, Liller S, Ehlert FJ (2007). Estimation of agonist activity at G protein-coupled receptors: analysis of M2 muscarinic receptor signaling through Gi/o,Gs, and G15. *J Pharmacol Exp Ther* **321**(3)**:** 1193-1207.

Grisel JE, Mogil JS, Belknap JK, Grandy DK (1996). Orphanin FQ acts as a supraspinal, but not a spinal, anti-opioid peptide. *Neuroreport* **7**(13)**:** 2125-2129.

Grundmann M, Kostenis E (2015). Label-Free Biosensor Assays in GPCR Screening. *Methods in molecular biology* **1272:** 199-213.

Guerrini R, Calo G, Rizzi A, Bianchi C, Lazarus LH, Salvadori S, Temussi PA, Regoli D (1997). Address and message sequences for the nociceptin receptor: a structure-activity study of nociceptin-(1-13)-peptide amide. *Journal of medicinal chemistry* **40**(12)**:** 1789-1793.

Guerrini R, Calo G, Rizzi A, Bigoni R, Bianchi C, Salvadori S, Regoli D (1998). A new selective antagonist of the nociceptin receptor. *British journal of pharmacology* **123**(2)**:** 163-165.

Guerrini R, Marzola E, Trapella C, Pela M, Molinari S, Cerlesi MC, Malfacini D, Rizzi A, Salvadori S, Calo G (2014). A novel and facile synthesis of tetra branched derivatives of nociceptin/orphanin FQ. *Bioorganic & medicinal chemistry* **22**(14)**:** 3703-3712.

Hackler L, Zadina JE, Ge LJ, Kastin AJ (1997). Isolation of relatively large amounts of endomorphin-1 and endomorphin-2 from human brain cortex. *Peptides* **18**(10)**:** 1635-1639.

Hansen DW, Jr., Stapelfeld A, Savage MA, Reichman M, Hammond DL, Haaseth RC, Mosberg HI (1992). Systemic analgesic activity and delta-opioid selectivity in [2,6-dimethyl-Tyr1,D-Pen2,D-Pen5]enkephalin. *Journal of medicinal chemistry* **35**(4)**:** 684-687.

Hu E, Calo G, Guerrini R, Ko MC (2010). Long-lasting antinociceptive spinal effects in primates of the novel nociceptin/orphanin FQ receptor agonist UFP-112. *Pain* **148**(1)**:** 107-113.

Hughes J, Kosterlitz HW, Leslie FM (1975). Effect of morphine on adrenergic transmission in the mouse vas deferens. Assessment of agonist and antagonist potencies of narcotic analgesics. *Br J Pharmacol.* **53**(3)**:** 371-381.

Janecka A, Staniszewska R, Fichna J (2007). Endomorphin analogs. *Current medicinal chemistry* **14**(30)**:** 3201-3208.

Jenck F, Wichmann J, Dautzenberg FM, Moreau JL, Ouagazzal AM, Martin JR, Lundstrom K, Cesura AM, Poli SM, Roever S, Kolczewski S, Adam G, Kilpatrick G (2000). A synthetic agonist at the orphanin FQ/nociceptin receptor ORL1: anxiolytic profile in the rat. *Proceedings of the National Academy of Sciences of the United States of America* **97**(9)**:** 4938-4943.

Kam KW, New DC, Wong YH (2002). Constitutive activation of the opioid receptor-like (ORL1) receptor by mutation of Asn133 to tryptophan in the third transmembrane region. *Journal of neurochemistry* **83**(6)**:** 1461-1470.

Katritch V, Cherezov V, Stevens RC (2012). Diversity and modularity of G protein-coupled receptor structures. *Trends in pharmacological sciences* **33**(1)**:** 17-27.

Katritch V, Fenalti G, Abola EE, Roth BL, Cherezov V, Stevens RC (2014). Allosteric sodium in class A GPCR signaling. *Trends in biochemical sciences* **39**(5)**:** 233-244.

Kawamoto H, Ozaki S, Itoh Y, Miyaji M, Arai S, Nakashima H, Kato T, Ohta H, Iwasawa Y (1999). Discovery of the first potent and selective small molecule opioid

receptor-like (ORL1) antagonist: 1-[(3R,4R)-1-cyclooctylmethyl-3- hydroxymethyl-4-piperidyl]-3-ethyl-1, 3-dihydro-2H-benzimidazol-2-one (J-113397). *Journal of medicinal chemistry* **42**(25)**:** 5061-5063.

Ke N, Nguyen K, Irelan J, Abassi YA (2015). Multidimensional GPCR Profiling and Screening Using Impedance-Based Label-Free and Real-Time Assay. *Methods in molecular biology* **1272:** 215-226.

Kelly E (2013). Efficacy and ligand bias at the mu-opioid receptor. *British journal of pharmacology* **169**(7)**:** 1430-1446.

Kenakin TP (2014). Chapter 6 - Orthosteric Drug Antagonism. In: Kenakin TP (ed)^(eds). *A Pharmacology Primer (Fourth Edition)*, edn. San Diego: Academic Press. p^pp 119-154.

Kenakin TP, Beek D (1982). In vitro studies on the cardiac activity of prenalterol with reference to use in congestive heart failure. *J Pharmacol Exp Ther* **220**(1)**:** 77-85.

Keresztes A, Borics A, Toth G (2010). Recent advances in endomorphin engineering. *ChemMedChem* **5**(8)**:** 1176-1196.

Kieffer BL (1995). Recent advances in molecular recognition and signal transduction of active peptides: receptors for opioid peptides. *Cellular and molecular neurobiology* **15**(6)**:** 615-635.

Kieffer BL, Befort K, Gaveriaux-Ruff C, Hirth CG (1992). The delta-opioid receptor: isolation of a cDNA by expression cloning and pharmacological characterization. *Proceedings of the National Academy of Sciences of the United States of America* **89**(24)**:** 12048-12052.

King M, Chang A, Pasternak GW (1998). Functional blockade of opioid analgesia by orphanin FQ/nociceptin. *Biochem Pharmacol* **55**(9)**:** 1537-1540.

Knapman A, Connor M (2015). Fluorescence-based, high-throughput assays for mu-opioid receptor activation using a membrane potential-sensitive dye. *Methods in molecular biology* **1230:** 177-185.

Kostenis E, Martini L, Ellis J, Waldhoer M, Heydorn A, Rosenkilde MM, Norregaard PK, Jorgensen R, Whistler JL, Milligan G (2005a). A highly conserved glycine within linker I and the extreme C terminus of G protein alpha subunits interact cooperatively in switching G protein-coupled receptor-to-effector specificity. *J Pharmacol Exp Ther* **313**(1)**:** 78-87.

Kostenis E, Waelbroeck M, Milligan G (2005b). Techniques: promiscuous Galpha proteins in basic research and drug discovery. *Trends in pharmacological sciences* **26**(11)**:** 595-602.

Lambert DG (2008). The nociceptin/orphanin FQ receptor: a target with broad therapeutic potential. *Nature reviews. Drug discovery* **7**(8)**:** 694-710.

Lapalu S, Moisand C, Mazarguil H, Cambois G, Mollereau C, Meunier JC (1997). Comparison of the structure-activity relationships of nociceptin and dynorphin A using chimeric peptides. *FEBS Lett* **417**(3)**:** 333-336.

Largent-Milnes TM, Vanderah TW (2010). Recently patented and promising ORL-1 ligands: where have we been and where are we going? *Expert opinion on therapeutic patents* **20**(3)**:** 291-305.

Larhammar D, Sundström G, Dores RM (2013). Chapter 213 - Evolution of the Opioid System. In: Kastin AJ (ed)^(eds). *Handbook of Biologically Active Peptides (Second Edition)*, edn. Boston: Academic Press. p^pp 1562-1569.

Le Bars D, Gozariu M, Cadden SW (2001). Animal models of nociception. *Pharmacol Rev* **53**(4)**:** 597-652.

Lefkowitz RJ, Shenoy SK (2005). Transduction of receptor signals by beta-arrestins. *Science* **308**(5721)**:** 512-517.

Levitt ES, Clark MJ, Jenkins PM, Martens JR, Traynor JR (2009). Differential effect of membrane cholesterol removal on mu- and delta-opioid receptors: a parallel comparison of acute and chronic signaling to adenylyl cyclase. *J Biol Chem* **284**(33)**:** 22108-22122.

Li T, Fujita Y, Tsuda Y, Miyazaki A, Ambo A, Sasaki Y, Jinsmaa Y, Bryant SD, Lazarus LH, Okada Y (2005). Development of potent mu-opioid receptor ligands using unique tyrosine analogues of endomorphin-2. *Journal of medicinal chemistry* **48**(2)**:** 586-592.

Li T, Jinsmaa Y, Nedachi M, Miyazaki A, Tsuda Y, Ambo A, Sasaki Y, Bryant SD, Marczak E, Li Q, Swartzwelder HS, Lazarus LH, Okada Y (2007). Transformation of mu-opioid receptor agonists into biologically potent mu-opioid receptor antagonists. *Bioorganic & medicinal chemistry* **15**(3)**:** 1237-1251.

Linz K, Christoph T, Tzschentke TM, Koch T, Schiene K, Gautrois M, Schroder W, Kogel BY, Beier H, Englberger W, Schunk S, De Vry J, Jahnel U, Frosch S (2014). Cebranopadol: a novel potent analgesic nociceptin/orphanin FQ peptide and opioid receptor agonist. *J Pharmacol Exp Ther* **349**(3)**:** 535-548.

Liu WX, Wang R (2012). Endomorphins: potential roles and therapeutic indications in the development of opioid peptide analgesic drugs. *Medicinal research reviews* **32**(3)**:** 536-580.

Loew GH, Berkowitz DS (1978). Quantum chemical studies of N-substituent variation in the oxymorphone series of opiate narcotics. *Journal of medicinal chemistry* **21**(1)**:** 101-106.

Lord JA, Waterfield AA, Hughes J, Kosterlitz HW (1977). Endogenous opioid peptides: multiple agonists and receptors. *Nature* **267**(5611)**:** 495-499.

Lutfy K, Sharza SA, Maidment NT (1999). Tolerance develops to the inhibitory effect of orphanin FQ on morphine-induced antinociception in the rat. *Neuroreport* **10**(1)**:** 103-106.

Mahmoud S, Margas W, Trapella C, Calo G, Ruiz-Velasco V (2010). Modulation of silent and constitutively active nociceptin/orphanin FQ receptors by potent receptor antagonists and Na+ ions in rat sympathetic neurons. *Molecular pharmacology* **77**(5)**:** 804-817.

Manabe T, Noda Y, Mamiya T, Katagiri H, Houtani T, Nishi M, Noda T, Takahashi T, Sugimoto T, Nabeshima T, Takeshima H (1998). Facilitation of long-term potentiation and memory in mice lacking nociceptin receptors. *Nature* **394**(6693)**:** 577-581.

Manglik A, Kruse AC, Kobilka TS, Thian FS, Mathiesen JM, Sunahara RK, Pardo L, Weis WI, Kobilka BK, Granier S (2012). Crystal structure of the micro-opioid receptor bound to a morphinan antagonist. *Nature* **485**(7398)**:** 321-326.

Margas W, Sedeek K, Ruiz-Velasco V (2008). Coupling specificity of NOP opioid receptors to pertussis-toxin-sensitive Galpha proteins in adult rat stellate ganglion neurons using small interference RNA. *Journal of neurophysiology* **100**(3)**:** 1420-1432.

Marti M, Mela F, Budri M, Volta M, Malfacini D, Molinari S, Zaveri NT, Ronzoni S, Petrillo P, Calo G, Morari M (2013). Acute and chronic antiparkinsonian effects of the novel nociceptin/orphanin FQ receptor antagonist NiK-21273 in comparison with SB-612111. *British journal of pharmacology* **168**(4)**:** 863-879.

Marti M, Mela F, Veronesi C, Guerrini R, Salvadori S, Federici M, Mercuri NB, Rizzi A, Franchi G, Beani L, Bianchi C, Morari M (2004). Blockade of nociceptin/orphanin FQ receptor signaling in rat substantia nigra pars reticulata stimulates nigrostriatal dopaminergic transmission and motor behavior. *The Journal of neuroscience : the official journal of the Society for Neuroscience* **24**(30)**:** 6659-6666.

Martin WR, Eades CG, Thompson JA, Huppler RE, Gilbert PE (1976). The effects of morphine- and nalorphine- like drugs in the nondependent and morphine-dependent chronic spinal dog. *J Pharmacol Exp Ther* **197**(3)**:** 517-532.

Mathiesen JM, Vedel L, Brauner-Osborne H (2013). cAMP biosensors applied in molecular pharmacological studies of G protein-coupled receptors. *Methods in enzymology* **522:** 191-207.

McDonald J, Barnes TA, Okawa H, Williams J, Calo G, Rowbotham DJ, Lambert DG (2003). Partial agonist behaviour depends upon the level of nociceptin/orphanin FQ receptor expression: studies using the ecdysone-inducible mammalian expression system. *British journal of pharmacology* **140**(1)**:** 61-70.

Meng F, Xie GX, Thompson RC, Mansour A, Goldstein A, Watson SJ, Akil H (1993). Cloning and pharmacological characterization of a rat kappa opioid receptor. *Proceedings of the National Academy of Sciences of the United States of America* **90**(21)**:** 9954-9958.

Meunier JC, Mollereau C, Toll L, Suaudeau C, Moisand C, Alvinerie P, Butour JL, Guillemot JC, Ferrara P, Monserrat B, Mazarguil H, Vassart G, Parmentier M, Costentin J (1995). Isolation and structure of the endogenous agonist of opioid receptor-like ORL1 receptor. *Nature* **377:** 532-535.

Mogil JS, Pasternak GW (2001). The molecular and behavioral pharmacology of the orphanin FQ/nociceptin peptide and receptor family. *Pharmacol Rev* **53**(3)**:** 381-415.

Molinari P, Casella I, Costa T (2008). Functional complementation of high-efficiency resonance energy transfer: a new tool for the study of protein binding interactions in living cells. *The Biochemical journal* **409**(1)**:** 251-261.

Molinari P, Vezzi V, Sbraccia M, Gro C, Riitano D, Ambrosio C, Casella I, Costa T (2010). Morphine-like opiates selectively antagonize receptor-arrestin interactions. *J Biol Chem* **285**(17)**:** 12522-12535.

Molinari S, Camarda V, Rizzi A, Marzola G, Salvadori S, Marzola E, Molinari P, McDonald J, Ko MC, Lambert DG, Calo G, Guerrini R (2012). [Dmt(1)]N/OFQ(1-13)-NH(2) , a potent nociceptin/orphanin FQ and opioid receptor universal agonist. *British journal of pharmacology*.

Mollereau C, Simons MJ, Soularue P, Liners F, Vassart G, Meunier JC, Parmentier M (1996). Structure, tissue distribution, and chromosomal localization of the prepronociceptin gene. *Proceedings of the National Academy of Sciences of the United States of America* **93**(16)**:** 8666-8670.

Murphy NP, Ly HT, Maidment NT (1996). Intracerebroventricular orphanin FQ/nociceptin suppresses dopamine release in the nucleus accumbens of anaesthetized rats. *Neuroscience* **75**(1)**:** 1-4.

Mustazza C, Bastanzio G (2011). Development of nociceptin receptor (NOP) agonists and antagonists. *Medicinal research reviews* **31**(4)**:** 605-648.

Norskov-Lauritsen L, Thomsen AR, Brauner-Osborne H (2014). G protein-coupled receptor signaling analysis using homogenous time-resolved Forster resonance energy transfer (HTRF(R)) technology. *International journal of molecular sciences* **15**(2)**:** 2554-2572.

Okada K, Sujaku T, Chuman Y, Nakashima R, Nose T, Costa T, Yamada Y, Yokoyama M, Nagahisa A, Shimohigashi Y (2000). Highly potent nociceptin analog containing the Arg-Lys triple repeat. *Biochemical and biophysical research communications* **278**(2)**:** 493-498.

Onaran HO, Rajagopal S, Costa T (2014). What is biased efficacy? Defining the relationship between intrinsic efficacy and free energy coupling. *Trends in pharmacological sciences* **35**(12)**:** 639-647.

Pasternak GW, Pan YX (2013). Mu opioids and their receptors: evolution of a concept. *Pharmacol Rev* **65**(4)**:** 1257-1317.

Peckham EM, Traynor JR (2006). Comparison of the antinociceptive response to morphine and morphine-like compounds in male and female Sprague-Dawley rats. *J Pharmacol Exp Ther* **316**(3)**:** 1195-1201.

Perlikowska R, Malfacini D, Cerlesi MC, Calo G, Piekielna J, Floriot L, Henry T, do-Rego JC, Tomboly C, Kluczyk A, Janecka A (2014). Pharmacological characterization of endomorphin-2-based cyclic pentapeptides with methylated phenylalanine residues. *Peptides* **55:** 145-150.

Pfleger KD, Eidne KA (2006). Illuminating insights into protein-protein interactions using bioluminescence resonance energy transfer (BRET). *Nature methods* **3**(3)**:** 165-174.

Piekielna J, Perlikowska R, Gach K, Janecka A (2013). Cyclization in opioid peptides. *Current drug targets* **14**(7)**:** 798-816.

Portoghese PS (1965). A new concept on the mode of interaction of narcotic analgesics with receptors. *Journal of medicinal chemistry* **8**(5)**:** 609-616.

Pradhan AA, Smith ML, Kieffer BL, Evans CJ (2012). Ligand-directed signalling within the opioid receptor family. *British journal of pharmacology* **167**(5)**:** 960-969.

Raehal KM, Bohn LM (2014). beta-arrestins: regulatory role and therapeutic potential in opioid and cannabinoid receptor-mediated analgesia. *Handbook of experimental pharmacology* **219:** 427-443.

Raehal KM, Schmid CL, Groer CE, Bohn LM (2011). Functional selectivity at the mu-opioid receptor: implications for understanding opioid analgesia and tolerance. *Pharmacol Rev* **63**(4)**:** 1001-1019.

Rajagopal S, Rajagopal K, Lefkowitz RJ (2010). Teaching old receptors new tricks: biasing seven-transmembrane receptors. *Nature reviews. Drug discovery* **9**(5)**:** 373-386.

Raynor K, Kong H, Chen Y, Yasuda K, Yu L, Bell GI, Reisine T (1994). Pharmacological characterization of the cloned kappa-, delta-, and mu-opioid receptors. *Molecular pharmacology* **45**(2)**:** 330-334.

Redrobe JP, Calo G, Regoli D, Quirion R (2002). Nociceptin receptor antagonists display antidepressant-like properties in the mouse forced swimming test. *Naunyn-Schmiedeberg's archives of pharmacology* **365**(2)**:** 164-167.

Reinscheid RK, Ardati A, Monsma FJ, Jr., Civelli O (1996). Structure-activity relationship studies on the novel neuropeptide orphanin FQ. *J Biol Chem* **271**(24)**:** 14163-14168.

Reinscheid RK, Nothacker HP, Bourson A, Ardati A, Henningsen RA, Bunzow JR, Grandy DK, Langen H, Monsma FJ, Jr., Civelli O (1995). Orphanin FQ: a neuropeptide that activates an opioidlike G protein-coupled receptor. *Science* **270**(5237)**:** 792-794.

Rizzi A, Malfacini D, Cerlesi MC, Ruzza C, Marzola E, Bird MF, Rowbotham DJ, Salvadori S, Guerrini R, Lambert DG, Calo G (2014). In vitro and in vivo pharmacological characterization of nociceptin/orphanin FQ tetrabranched derivatives. *British journal of pharmacology* **171**(17)**:** 4138-4153.

Rizzi A, Molinari S, Marti M, Marzola G, Calo G (2011). Nociceptin/orphanin FQ receptor knockout rats: in vitro and in vivo studies. *Neuropharmacology* **60**(4)**:** 572-579.

Rizzi A, Spagnolo B, Wainford RD, Fischetti C, Guerrini R, Marzola G, Baldisserotto A, Salvadori S, Regoli D, Kapusta DR, Calo G (2007). In vitro and in

vivo studies on UFP-112, a novel potent and long lasting agonist selective for the nociceptin/orphanin FQ receptor. *Peptides* **28**(6)**:** 1240-1251.

Rizzi D, Bigoni R, Rizzi A, Jenck F, Wichmann J, Guerrini R, Regoli D, Calo G (2001). Effects of Ro 64-6198 in nociceptin/orphanin FQ-sensitive isolated tissues. *Naunyn-Schmiedeberg's archives of pharmacology* **363**(5)**:** 551-555.

Rizzi D, Rizzi A, Bigoni R, Camarda V, Marzola G, Guerrini R, De Risi C, Regoli D, Calo G (2002). [Arg14,Lys15]nociceptin, a highly potent agonist of the nociceptin/orphanin FQ receptor: in vitro and in vivo studies. *J Pharmacol Exp Ther* **300:** 57-63.

Roelse M, de Ruijter NC, Vrouwe EX, Jongsma MA (2013). A generic microfluidic biosensor of G protein-coupled receptor activation-monitoring cytoplasmic [Ca(2+)] changes in human HEK293 cells. *Biosensors & bioelectronics* **47:** 436-444.

Salahpour A, Espinoza S, Masri B, Lam V, Barak LS, Gainetdinov RR (2012). BRET biosensors to study GPCR biology, pharmacology, and signal transduction. *Frontiers in endocrinology* **3:** 105.

Sasaki Y, Sasaki A, Niizuma H, Goto H, Ambo A (2003). Endomorphin 2 analogues containing Dmp residue as an aromatic amino acid surrogate with high mu-opioid receptor affinity and selectivity. *Bioorganic & medicinal chemistry* **11**(5)**:** 675-678.

Satoh M, Minami M (1995). Molecular pharmacology of the opioid receptors. *Pharmacology & therapeutics* **68**(3)**:** 343-364.

Schiller PW (2010). Bi- or multifunctional opioid peptide drugs. *Life sciences* **86**(15-16)**:** 598-603.

Schmidhammer H, Spetea M, Windisch P, Schutz J, Riba P, Al-Khrasani M, Furst S (2013). Functionalization of the carbonyl group in position 6 of morphinan-6-ones. Development of novel 6-amino and 6-guanidino substituted 14-alkoxymorphinans. *Current pharmaceutical design* **19**(42)**:** 7391-7399.

Schroder W, Lambert DG, Ko MC, Koch T (2014). Functional plasticity of the N/OFQ-NOP receptor system determines analgesic properties of NOP receptor agonists. *British journal of pharmacology* **171**(16)**:** 3777-3800.

Schunk S, Linz K, Hinze C, Frormann S, Oberborsch S, Sundermann B, Zemolka S, Englberger W, Germann T, Christoph T, Kogel BY, Schroder W, Harlfinger S, Saunders D, Kless A, Schick H, Sonnenschein H (2014). Discovery of a Potent Analgesic NOP and Opioid Receptor Agonist: Cebranopadol. *ACS medicinal chemistry letters* **5**(8)**:** 857-862.

Schutz J, Spetea M, Koch M, Aceto MD, Harris LS, Coop A, Schmidhammer H (2003). Synthesis and biological evaluation of 14-alkoxymorphinans. 20. 14-phenylpropoxymetopon: an extremely powerful analgesic. *Journal of medicinal chemistry* **46**(19)**:** 4182-4187.

Schutz J, Windisch P, Kristeva E, Wurst K, Ongania KH, Horvath UE, Schottenberger H, Laus G, Schmidhammer H (2005). Mechanistic diversity of the van Leusen reaction applied to 6-ketomorphinans and synthetic potential of the resulting acrylonitrile substructures. *The Journal of organic chemistry* **70**(13)**:** 5323-5326.

Shoblock JR (2007). The pharmacology of Ro 64-6198, a systemically active, nonpeptide NOP receptor (opiate receptor-like 1, ORL-1) agonist with diverse preclinical therapeutic activity. *CNS Drug Rev.* **13**(1)**:** 107-136.

Simon EJ, Hiller JM, Edelman I (1973). Stereospecific binding of the potent narcotic analgesic (3H) Etorphine to rat-brain homogenate. *Proceedings of the National Academy of Sciences of the United States of America* **70**(7)**:** 1947-1949.

Soergel DG, Subach RA, Burnham N, Lark MW, James IE, Sadler BM, Skobieranda F, Violin JD, Webster LR (2014). Biased agonism of the mu-opioid receptor by TRV130 increases analgesia and reduces on-target adverse effects versus morphine: A randomized, double-blind, placebo-controlled, crossover study in healthy volunteers. *Pain* **155**(9)**:** 1829-1835.

Spagnolo B, Carra G, Fantin M, Fischetti C, Hebbes C, McDonald J, Barnes TA, Rizzi A, Trapella C, Fanton G, Morari M, Lambert DG, Regoli D, Calo G (2007b). Pharmacological Characterization of the Nociceptin/Orphanin FQ Receptor Antagonist SB-612111   [(-)-cis-1-Methyl-7-[[4-(2,6-dichlorophenyl)piperidin-1-yl]methyl]-6,7,8,9 -tetrahydro-5H-benzocyclohepten-5-ol]: In Vitro Studies. *J Pharmacol Exp Ther.* **321**(3)**:** 961-967.

Spampinato S, Baiula M, Calienni M (2007). Agonist-regulated internalization and desensitization of the human nociceptin receptor expressed in CHO cells. *Current drug targets* **8**(1)**:** 137-146.

Spetea M, Asim MF, Wolber G, Schmidhammer H (2013). The micro opioid receptor and ligands acting at the micro opioid receptor, as therapeutics and potential therapeutics. *Current pharmaceutical design* **19**(42)**:** 7415-7434.

Spetea M, Bohotin CR, Asim MF, Stubegger K, Schmidhammer H (2010). In vitro and in vivo pharmacological profile of the 5-benzyl analogue of 14-methoxymetopon, a novel mu opioid analgesic with reduced propensity to alter motor function. *European journal of pharmaceutical sciences : official journal of the European Federation for Pharmaceutical Sciences* **41**(1)**:** 125-135.

Spetea M, Greiner E, Aceto MD, Harris LS, Coop A, Schmidhammer H (2005). Effect of a 6-cyano substituent in 14-oxygenated N-methylmorphinans on opioid receptor binding and antinociceptive potency. *Journal of medicinal chemistry* **48**(15)**:** 5052-5055.

Spetea M, Schmidhammer H (2012). Recent advances in the development of 14-alkoxy substituted morphinans as potent and safer opioid analgesics. *Current medicinal chemistry* **19**(15)**:** 2442-2457.

Standifer KM, Pasternak GW (1997). G proteins and opioid receptor-mediated signalling. *Cellular signalling* **9**(3-4)**:** 237-248.

Stevens RC, Cherezov V, Katritch V, Abagyan R, Kuhn P, Rosen H, Wuthrich K (2013). The GPCR Network: a large-scale collaboration to determine human GPCR structure and function. *Nature reviews. Drug discovery* **12**(1)**:** 25-34.

Pert CB, Snyder SH (1973). Opiate receptor: demonstration in nervous tissue. *Science* **179**(4077)**:** 1011-1014.

Tallarida RJ, Robinson MJ, Porreca F, Cowan A (1982). Estimation of the dissociation constant of naloxone in the naive and morphine-tolerant guinea-pig isolated ileum: analysis by the constrained Schild plot. *Life sciences* **31**(16-17)**:** 1691-1694.

Terenius L (1973). Characteristics of the "receptor" for narcotic analgesics in synaptic plasma membrane fraction from rat brain. *Acta pharmacologica et toxicologica* **33**(5)**:** 377-384.

Testa B, Mayer JM (2006). The Hydrolysis of Carboxylic Acid Ester Prodrugs. In: (ed)^(eds). *Hydrolysis in Drug and Prodrug Metabolism*, edn: Verlag Helvetica Chimica Acta. p^pp 419-534.

Thompson AA, Liu W, Chun E, Katritch V, Wu H, Vardy E, Huang XP, Trapella C, Guerrini R, Calo G, Roth BL, Cherezov V, Stevens RC (2012). Structure of the nociceptin/orphanin FQ receptor in complex with a peptide mimetic. *Nature* **485**(7398)**:** 395-399.

Thompson CM, Wojno H, Greiner E, May EL, Rice KC, Selley DE (2004). Activation of G-proteins by morphine and codeine congeners: insights to the relevance of O- and N-demethylated metabolites at mu- and delta-opioid receptors. *J Pharmacol Exp Ther* **308**(2)**:** 547-554.

Tian JH, Xu W, Fang Y, Han JS (1997). [Antagonistic effect of orphanin FQ on morphine analgesia in rat brain]. *Sheng Li Xue Bao* **49**(3)**:** 333-338.

Toll L, Berzetei-Gurske IP, Polgar WE, Brandt SR, Adapa ID, Rodriguez L, Schwartz RW, Haggart D, O'Brien A, White A, Kennedy JM, Craymer K, Farrington L, Auh JS (1998). Standard binding and functional assays related to medications development division testing for potential cocaine and opiate narcotic treatment medications. *NIDA research monograph* **178:** 440-466.

Trapella C, Fischetti C, Pela M, Lazzari I, Guerrini R, Calo G, Rizzi A, Camarda V, Lambert DG, McDonald J, Regoli D, Salvadori S (2009). Structure-activity studies on the nociceptin/orphanin FQ receptor antagonist 1-benzyl-N-{3-[spiroisobenzofuran-1(3H),4'-piperidin-1-yl]propyl} pyrrolidine-2-carboxamide. *Bioorganic & medicinal chemistry* **17**(14)**:** 5080-5095.

Vachon L, Costa T, Herz A (1987). Opioid receptor desensitization in NG 108-15 cells. Differential effects of a full and a partial agonist on the opioid-dependent GTPase. *Biochem Pharmacol* **36**(18)**:** 2889-2897.

Varty GB, Lu SX, Morgan CA, Cohen-Williams ME, Hodgson RA, Smith-Torhan A, Zhang H, Fawzi AB, Graziano MP, Ho GD, Matasi J, Tulshian D, Coffin VL, Carey GJ (2008a). The anxiolytic-like effects of the novel, orally active nociceptin

opioid receptor agonist 8-[bis(2-methylphenyl)methyl]-3-phenyl-8-azabicyclo[3.2.1]octan-3-ol (SCH 221510). *J Pharmacol Exp Ther* **326**(2)**:** 672-682.

Vezzi V, Onaran HO, Molinari P, Guerrini R, Balboni G, Calo G, Costa T (2013). Ligands raise the constraint that limits constitutive activation in G protein-coupled opioid receptors. *J Biol Chem* **288**(33)**:** 23964-23978.

Violin JD, Crombie AL, Soergel DG, Lark MW (2014). Biased ligands at G-protein-coupled receptors: promise and progress. *Trends in pharmacological sciences* **35**(7)**:** 308-316.

Violin JD, DeWire SM, Yamashita D, Rominger DH, Nguyen L, Schiller K, Whalen EJ, Gowen M, Lark MW (2010). Selectively engaging beta-arrestins at the angiotensin II type 1 receptor reduces blood pressure and increases cardiac performance. *J Pharmacol Exp Ther* **335**(3)**:** 572-579.

Walters RW, Shukla AK, Kovacs JJ, Violin JD, DeWire SM, Lam CM, Chen JR, Muehlbauer MJ, Whalen EJ, Lefkowitz RJ (2009). beta-Arrestin1 mediates nicotinic acid-induced flushing, but not its antilipolytic effect, in mice. *The Journal of clinical investigation* **119**(5)**:** 1312-1321.

Wichmann J, Adam G, Rover S, Cesura AM, Dautzenberg FM, Jenck F (1999). 8-acenaphthen-1-yl-1-phenyl-1,3,8-triaza-spiro[4.5]decan-4-one derivatives as orphanin FQ receptor agonists. *Bioorganic & medicinal chemistry letters* **9**(16)**:** 2343-2348.

Wichmann J, Adam G, Rover S, Hennig M, Scalone M, Cesura AM, Dautzenberg FM, Jenck F (2000). Synthesis of (1S,3aS)-8-(2,3,3a,4,5, 6-hexahydro-1H-phenalen-1-yl)-1-phenyl-1,3,8-triaza-spiro[4. 5]decan-4-one, a potent and selective orphanin FQ (OFQ) receptor agonist with anxiolytic-like properties. *Eur J Med Chem* **35**(9)**:** 839-851.

Winter CA, Orahovats PD, Lehman EG (1957). Analgesic activity and morphine antagonism of compounds related to nalorphine. *Archives internationales de pharmacodynamie et de therapie* **110**(2-3)**:** 186-202.

Wise A, Gearing K, Rees S (2002). Target validation of G-protein coupled receptors. *Drug discovery today* **7**(4)**:** 235-246.

Wu G (2010). *Assay development : fundamentals and practices*. edn. Wiley: Hoboken, N.J.

Yu TP, Fein J, Phan T, Evans CJ, Xie CW (1997). Orphanin FQ inhibits synaptic transmission and long-term potentiation in rat hippocampus. *Hippocampus* **7**(1)**:** 88-94.

Zadina JE, Hackler L, Ge LJ, Kastin AJ (1997). A potent and selective endogenous agonist for the mu-opiate receptor. *Nature* **386**(6624)**:** 499-502.

Zaratin PF, Petrone G, Sbacchi M, Garnier M, Fossati C, Petrillo P, Ronzoni S, Giardina GA, Scheideler MA (2004). Modification of nociception and morphine tolerance by the selective opiate receptor-like orphan receptor antagonist (-)-cis-1-

methyl-7-[[4-(2,6-dichlorophenyl)piperidin-1-yl]methyl]-6,7,8,9-tetrahy dro-5H-benzocyclohepten-5-ol (SB-612111). *J Pharmacol Exp Ther* **308**(2)**:** 454-461.

Zaveri N, Polgar WE, Olsen CM, Kelson AB, Grundt P, Lewis JW, Toll L (2001). Characterization of opiates, neuroleptics, and synthetic analogs at ORL1 and opioid receptors. *European journal of pharmacology* **428**(1)**:** 29-36.

Zaveri NT (2011). The Nociceptin/Orphanin FQ Receptor (NOP) as a Target for Drug Abuse Medications. *Curr Top Med Chem* **11**(9)**:** 1151-1156.

Zeilhofer HU, Calo G (2003). Nociceptin/orphanin FQ and its receptor--potential targets for pain therapy? *J Pharmacol Exp Ther* **306**(2)**:** 423-429.

Zhang J, Ferguson SS, Barak LS, Menard L, Caron MG (1996). Dynamin and beta-arrestin reveal distinct mechanisms for G protein-coupled receptor internalization. *J Biol Chem* **271**(31)**:** 18302-18305.

Zhang Y, Wang Z, Cox DP, Civelli O (2012). Study on the activation of the opioid receptors by a set of morphine derivatives in a well-defined assay system. *Neurochemical research* **37**(2)**:** 410-416.

Zheng H, Chu J, Qiu Y, Loh HH, Law PY (2008). Agonist-selective signaling is determined by the receptor location within the membrane domains. *Proceedings of the National Academy of Sciences of the United States of America* **105**(27)**:** 9421-9426.

Zhu CB, Cao XD, Xu SF, Wu GC (1997). Orphanin FQ potentiates formalin-induced pain behavior and antagonizes morphine analgesia in rats. *Neurosci Lett* **235**(1-2)**:** 37-40.

Publications list

Papers in preparation

Ruzza C, Rizzi A, Malfacini D, Cerlesi MC, Ferrari F, Marzola E, Guerrini R, Zaveri NT and Calo' G. In vitro pharmacological characterization of novel nociceptin/orphanin FQ receptor partial agonists. (in preparation).

Submitted Papers

Malfacini D, Ambrosio C, Gro' MC, Sbraccia M, Trapella C, Guerrini R, Broide R, Francis J, Bonora M, Pinton P, Costa T, and Calo' G (submitted) Pharmacological profile of nociceptin/orphanin FQ receptors interacting with G-proteins and β-arrestins 2. *PloS one*.

Published Papers

Battisti UM, Corrado S, Sorbi C, Cornia A, Tait A, Malfacini D, Cerlesi MC, Calo G and Brasili L (2014) Synthesis, enantiomeric separation and docking studies of spiropiperidine analogues as ligands of the nociceptin/orphanin FQ receptor. *MedChemComm* **5**:973-983.

Ben Haddou T, Beni S, Hosztafi S, Malfacini D, Calo G, Schmidhammer H and Spetea M (2014a) Pharmacological investigations of N-substituent variation in morphine and oxymorphone: opioid receptor binding, signaling and antinociceptive activity. *PloS one* **9**:e99231.

Ben Haddou T, Malfacini D, Calo G, Aceto MD, Harris LS, Traynor JR, Coop A, Schmidhammer H and Spetea M (2014b) Exploring pharmacological activities and signaling of morphinans substituted in position 6 as potent agonists interacting with the mu opioid receptor. *Molecular pain* **10**:48.

Corrado S, Battisti UM, Sorbi C, Tait A, Malfacini D, Camarda V, Calo G and Brasili L (2014) Synthesis and Structure-Activity Relationships of Triazaspirodecanone Derivatives as Nociceptin/Orphanin FQ Receptor Ligands. *Chem Biol Drug Des*.

Guerrini R, Marzola E, Trapella C, Molinari S, Cerlesi MC, Malfacini D, Rizzi A and Salvadori S (2014) A novel and facile synthesis of tetra branched derivatives of nociceptin/orphanin FQ. *Bioorganic & medicinal chemistry* **22**:3703-3712.

Guerrini R, Marzola E, Trapella C, Pacifico S, Cerlesi MC, Malfacini D, Ferrari F, Bird MF, Lambert DG, Salvadori S and Calo G (2015) Structure activity studies of nociceptin/orphanin FQ(1-13)-NH2 derivatives modified in position 5. *Bioorg Med Chem*.

Marti M, Mela F, Budri M, Volta M, Malfacini D, Molinari S, Zaveri NT, Ronzoni S, Petrillo P, Calo G and Morari M (2013) Acute and chronic antiparkinsonian effects of the novel nociceptin/orphanin FQ receptor antagonist NiK-21273 in comparison with SB-612111. *Br J Pharmacol* **168**:863-879.

Perlikowska R, Malfacini D, Cerlesi MC, Piekielna J, Floriot L, Henry T, do-Rego JC, Tömböly C, Kluczyk A and Janecka A (2014) Pharmacological characterization of endomorphin-2-based cyclic pentapeptides with methylated phenylalanine residues. *Peptides* **55**:145-150.

Rizzi A, Malfacini D, Cerlesi MC, Ruzza C, Marzola E, Bird MF, Rowbotham DJ, Salvadori S, Guerrini R, Lambert DG and Calo G (2014) In vitro and in vivo pharmacological characterization of nociceptin/orphanin FQ tetrabranched derivatives. *Br J Pharmacol* **171**:4138-4153.

Ruzza C, Rizzi A, Malfacini D, Cerlesi MC, Ferrari F, Marzola E, Ambrosio C, Gro C, Severo S, Costa T, Calo G and Guerrini R (2014) Pharmacological characterization of tachykinin tetrabranched derivatives. *Br J Pharmacol* **171**:4125-4137.

Ruzza C, Rizzi A, Malfacini D, Pulga A, Pacifico S, Salvadori S, Trapella C, Reinscheid RK, Calo G and Guerrini R (2015) In vitro and in vivo pharmacological characterization of a neuropeptide S tetrabranched derivative. *Pharmacol Res Perspect* **3**:e00108.